

MFN 08-016

Enclosure 2

**Licensing Topical Report NEDO-33083-A,
Supplement 1, Revision 1,
"TRACG Application for ESBWR Stability Analysis,"
January 2008**

Non-Proprietary Version



HITACHI

GE Hitachi Nuclear Energy

3901 Castle Hayne Road, Wilmington, NC 28401

NEDO-33083-A
Supplement 1
Revision 1
eDRF-0000-0030-1246
Class I
January 2008

Licensing Topical Report

**TRACG Application for ESBWR
Stability Analysis**

NON-PROPRIETARY INFORMATION NOTICE

This is a non-proprietary version of the document NEDE-33083P-A, Supplement 1, Revision 1, which has the proprietary information removed. Portions of the document that have been removed are indicated by open and closed double brackets as shown here [[]].

IMPORTANT NOTICE REGARDING CONTENTS OF THIS REPORT

PLEASE READ CAREFULLY

The information contained in this document is furnished as reference to the NRC Staff for the purpose of obtaining NRC approval of the ESBWR Certification and implementation. The only undertakings of GE Hitachi Nuclear Energy (GEH) with respect to information in this document are contained in contracts between GEH and participating utilities, and nothing contained in this document shall be construed as changing those contracts. The use of this information by anyone other than those participating entities and for any purposes other than those for which it is intended is not authorized; and with respect to any unauthorized use, GEH makes no representation or warranty, and assumes no liability as to the completeness, accuracy, or usefulness of the information contained in this document.

Enclosures 1 and 2 Contain Sensitive Proprietary Information

August 29, 2007

MFN-07-542

Received electronically
on 10/12/07

Mr. Robert E. Brown
Senior Vice President, Regulatory Affairs
GE-Hitachi Nuclear Energy Americas LLC
3901 Castle Hayne Rd MC A-45
Wilmington NC 28401

SUBJECT: REISSUANCE OF SAFETY EVALUATION REGARDING THE APPLICATION OF THE GE-HITACHI NUCLEAR ENERGY AMERICAS LLC (GEH) LICENSING TOPICAL REPORT "TRACG APPLICATION FOR ESBWR STABILITY ANALYSIS," NEDE-33083P, SUPPLEMENT 1

Dear Mr. Brown:

By letter dated April 18, 2002, GEH requested a pre-application review of the economic simplified boiling water reactor (ESBWR) advanced passive reactor design. On December 22, 2004, GEH submitted licensing topical report (TR) "TRACG Application for ESBWR Stability Analysis," NEDE-33083P, Supplement 1, for staff review as part of the pre-application review. Subsequently, on August 24, 2005, GEH submitted the ESBWR design certification application.

By letter dated May 23, 2006, the Nuclear Regulatory Commission (NRC) staff issued a safety evaluation (SE) regarding the application for ESBWR Stability Analysis. The letter requested that you review the SE for proprietary information. By letter dated June 23, 2006, from David H. Hinds, GEH identified this information line by line pursuant to the criteria of Title 10 of the *Code of Federal Regulations* (10 CFR) Section 2.390. The proprietary information contained in the SE (Enclosure 1) and associated Technical Evaluation report (TER) (Enclosure 2) is indicated by brackets, red font and underlined text. We have prepared a non-proprietary version of the SE (Enclosure 3) and TER (Enclosure 4) that do not contain proprietary information. The staff made a few minor editorial changes after the first issuance that were based on GEH's comments on factual accuracy—these minor changes did not impact the conclusions.

The enclosed SE is limited to the application of TRACG to ESBWR stability analysis. The staff concludes that TRACG, including the application methodology, is an acceptable evaluation model for ESBWR stability analysis. The staff finds "TRACG Application for ESBWR Stability Analysis," NEDE-33083P, Supplement 1, acceptable for referencing during the ESBWR design certification review to the extent specified and under the limitations delineated in the licensing TR and in the associated NRC SE. The SE, which is enclosed, defines the basis for acceptance of the licensing TR.

The staff requests that GEH publish the revised version of the TR listed above within 3 months of receipt of this letter. The accepted version of NEDE-33083P, Supplement 1, shall incorporate this letter and the enclosed SE and all requests for additional information and their

Enclosures 1 and 2 Contain Sensitive Proprietary Information

Enclosures 1 and 2 Contain Sensitive Proprietary Information

responses between the title page and the abstract, and add an "-A" (designating accepted) following the report identification number (i.e., NEDE-33083P-A, Supplement 1).

If NRC's criteria or regulations change so that its conclusion that the once acceptable TR is invalidated, GEH and/or the applicant referencing the TR will be expected to revise and resubmit its respective documentation, or submit justification for the continued applicability of the TR without revision of the respective documentation.

The subject TR and supporting documentation has been reviewed by the Advisory Committee on Reactor Safeguards, which has agreed with the staff recommendation for approval by their letter of April 21, 2006.

If you have any further questions regarding this review, please contact Amy E. Cubbage (301-415-2875).

Sincerely,

/RA/

David B. Matthews, Director
Division of New Reactor Licensing
Office of New Reactors

Docket No. 52-010

Enclosures: 1. Safety Evaluation (Proprietary)
2. Technical Evaluation Report (Proprietary)
3. Safety Evaluation (Non-Proprietary)
4. Technical Evaluation Report (Non-Proprietary)

cc: See next page (w/o Enclosures 1 and 2)

Enclosures 1 and 2 Contain Sensitive Proprietary Information

Enclosures 1 and 2 Contain Sensitive Proprietary Information

responses between the title page and the abstract, and add an "-A" (designating accepted) following the report identification number (i.e., NEDE-33083P-A, Supplement 1).

If NRC's criteria or regulations change so that its conclusion that the once acceptable TR is invalidated, GEH and/or the applicant referencing the TR will be expected to revise and resubmit its respective documentation, or submit justification for the continued applicability of the TR without revision of the respective documentation.

The subject TR and supporting documentation has been reviewed by the Advisory Committee on Reactor Safeguards, which has agreed with the staff recommendation for approval by their letter of April 21, 2006.

If you have any further questions regarding this review, please contact Amy E. Cubbage (301-415-2875).

Sincerely,

/RA/

David B. Matthews, Director
Division of New Reactor Licensing
Office of New Reactors

Docket No. 52-010

Enclosures: 1. Safety Evaluation (Proprietary)
2. Technical Evaluation Report (Proprietary)
3. Safety Evaluation (Non-Proprietary)
4. Technical Evaluation Report (Non-Proprietary)

cc: See next page (w/o Enclosures 1 and 2)

Hard Copy

NGE1 R/F
BBavol
ACubbage
MShuaibi

E-Mail

Distribution:

Public /Non-Public
RidsNroSGreen
RidsNroBBavol
RidsNroSnpb
RidsNroSrsb
RidsOgcMailCenter
RidsAcrsAcnwMailCenter
RidsRgn2MailCenter
ADAMS ACCESSION NO. ML072270192-Letter

OFFICE	PM:NGE1	PM:NGE1	BC:SNPB
NAME	BBavol	ACubbage	AMendiola
DATE	08/15/07	08/16/07	08/21/07
OFFICE	BC:SRSB	BC: NGE1	D:DNRL/NRO
NAME	JDonoghue	MShuaibi	DMatthews
DATE	08/21/07	08/23/07	08/29/07

OFFICIAL RECORD COPY

Enclosures 1 and 2 Contain Sensitive Proprietary Information

DC GE - ESBWR Mailing List

List #24

cc:

Ms. Michele Boyd
Legislative Director
Energy Program
Public Citizens Critical Mass Energy
and Environmental Program
215 Pennsylvania Avenue, SE
Washington, DC 20003

Mr. Marvin Fertel
Senior Vice President
and Chief Nuclear Officer
Nuclear Energy Institute
1776 I Street, NW
Suite 400
Washington, DC 20006-3708

Mr. Ray Ganthner
AREVA, Framatome ANP, Inc.
3315 Old Forest Road
P.O. Box 10935
Lynchburg, VA 24506-0935

Dr. Gail H. Marcus
U.S. Department of Energy
Room 5A-143
1000 Independence Avenue, SW
Washington, DC 20585

Email

APH@NEI.org (Adrian Heymer)
awc@nei.org (Anne W. Cottingham)
bennettS2@bv.com (Steve A. Bennett)
bob.brown@ge.com (Robert E. Brown)
BrinkmCB@westinghouse.com (Charles Brinkman)
chris.maslak@ge.com (Chris Maslak)
CumminWE@Westinghouse.com (Edward W. Cummins)
cwaltman@roe.com (C. Waltman)
dan1.williamson@ge.com (Dan Williamson)
david.hinds@ge.com (David Hinds)
david.lewis@pillsburylaw.com (David Lewis)
David.piepmeyer@ge.com (David Piepmeyer)
dlochbaum@UCSUSA.org (David Lochbaum)
don.lewis@ge.com (Don Lewis)
erg-xl@cox.net (Eddie R. Grant)
frankq@hursttech.com (Frank Quinn)
Frostie.white@ge.com (Frostie White)
gcesare@enercon.com (Guy Cesare)
george.honma@ge.com (George Honma)
george.stramback@gene.ge.com (George Stramback)
george.wadkins@ge.com (George Wadkins)
GovePA@BV.com (Patrick Gove)
greshaja@westinghouse.com (James Gresham)
gzinke@entergy.com (George Alan Zinke)
hickste@earthlink.net (Thomas Hicks)
james.beard@gene.ge.com (James Beard)
jcurtiss@winston.com (Jim Curtiss)
jgutierrez@morganlewis.com (Jay M. Gutierrez)
jim.kinsey@ge.com (James Kinsey)
jim.riccio@wdc.greenpeace.org (James Riccio)
JINesrsta@cpsenergy.com (James J. Nesrsta)
joel.Friday@ge.com (Joel Friday)
john.o'neil@pillsburylaw.com (John O'Neil)
john.sorensen@ge.com (John Sorensen)
Joseph.savage@ge.com (Joseph Savage)
Joseph_Hegner@dom.com (Joseph Hegner)
junichi_uchiyama@mhi.co.jp (Junichi Uchiyama)
kathy.sedney@ge.com (Kathy Sedney)
kenneth.ainger@exeloncorp.com (Kenneth Ainger)
KSutton@morganlewis.com (Kathryn M. Sutton)
kurt.schaefer@ge.com (Kurt Schaefer)
kwaugh@impact-net.org (Kenneth O. Waugh)
lou.lanese@ge.com (Lou Lanese)
lynchs@gao.gov (Sarah Lynch - Meeting Notices Only)
MaddenG@BV.com (George Madden)
maria.webb@pillsburylaw.com (Maria Webb)
mark.beaumont@wsms.com (Mark Beaumont)
Marvin_Smith@dom.com (Marvin L. Smith)

matias.travieso-diaz@pillsburylaw.com (Matias Travieso-Diaz)
media@nei.org (Scott Peterson)
mgiles@entergy.com (M. Giles)
mike_moran@fpl.com (Mike Moran)
mwetterhahn@winston.com (M. Wetterhahn)
nirsnet@nirs.org (Michael Mariotte)
pareez.golub@ge.com (Pareez Golub)
patriciaL.campbell@ge.com (Patricia L. Campbell)
paul@beyondnuclear.org (Paul Gunter)
paul.gaukler@pillsburylaw.com (Paul Gaukler)
peter.jordan@ge.com (Peter Jordan)
Petrovb@westinghouse.com (Bojan Petrovic)
phinnen@entergy.com (Paul Hinnenkamp)
pshastings@duke-energy.com (Peter Hastings)
RJB@NEI.org (Russell Bell)
RKTemple@cpsenergy.com (R.K. Temple)
roberta.swain@ge.com (Roberta Swain)
ronald.hagen@eia.doe.gov (Ronald Hagen)
sandra.sloan@areva.com (Sandra Sloan)
SauerB@BV.com (Robert C. Sauer)
sharon.lyons@ge.com (Sharon Lyons)
sfrantz@morganlewis.com (Stephen P. Frantz)
steven.hucik@ge.com (Steven Hucik)
steven.stark@ge.com (Steven Stark)
tom.miller@hq.doe.gov (Tom Miller)
trsmith@winston.com (Tyson Smith)
waraksre@westinghouse.com (Rosemarie E. Waraks)
wayne.marquino@ge.com (Wayne Marquino)
whorin@winston.com (W. Horin)

SAFETY EVALUATION BY THE OFFICE OF NUCLEAR REACTOR REGULATION
APPLICATION OF THE TRACG COMPUTER CODE TO STABILITY ANALYSIS FOR THE
ESBWR DESIGN NEDE—33083P, SUPPLEMENT 1

1.0 INTRODUCTION

General Electric Company (GE) submitted NEDE-33083P, Supplement 1, "TRACG Application for ESBWR Stability Analysis," for staff review as part of the pre-application review activities for the economic simplified boiling water reactor (ESBWR) advanced passive design (Reference 1). The description of the models in the code is provided by Reference 2. TRACG was submitted for ESBWR pre-application review for analysis of the loss-of-coolant (LOCA) scenario in Reference 3. TRACG has been reviewed and approved for application to anticipated operational occurrences (AOOs) in operating BWRs (Reference 4) for prediction of the initial pressure peak in anticipated transients without scram (ATWS) in operating BWRs (Reference 5) and for application to LOCAs in the ESBWR (Reference 6).

The NRC has reviewed and approved "ODYSY Application for Stability Licensing Calculations," NEDC-32992-P, for operating boiling water reactors (BWRs) (References 14 and 15). ODYSY is a frequency domain code used to determine the core open loop transfer function and from that function infer the decay ratio. The TRACG stability methodology is fundamentally different from that of ODYSY. TRACG directly calculates the time domain response to a flow perturbation and the decay ratio is calculated based on the transient behavior predicted.

GE is seeking NRC approval to use the prescribed methodologies in Reference 1 to predict the margin to instability for the ESBWR under normal operating conditions and anticipated transients. GE also seeks NRC approval for predicting the ESBWR startup trajectory using TRACG.

2.0 REGULATORY BASIS

General Design Criterion (GDC) 12 requires that unstable oscillations either be prevented or detected and suppressed before fuel design limits are exceeded. GDC 12 states:

The reactor core and associated coolant, control, and protection systems shall be designed to assure that power oscillations which can result in conditions exceeding specified acceptable fuel design limits are not possible or can be reliably and readily detected and suppressed.

GE submitted a methodology to demonstrate instabilities are highly unlikely.

GDC 10 requires that the reactor protection system must be capable of terminating any anticipated transients, including unstable power oscillations, prior to exceeding fuel design limits. GDC 10 states:

The reactor core and associated coolant, control, and protection systems shall be designed with appropriate margin to assure that specified acceptable fuel design limits are not exceeded during any condition of normal operation, including the effects of anticipated operational occurrences.

By satisfying GDC 12 through analysis that demonstrates power oscillations are highly unlikely, GE proposes to then rely on a detect and suppress system within the reactor protection system as a backup to eliminate power oscillations from consideration under GDC 10. Thus, only AOOs must be considered. This safety evaluation (SE) is limited to the capability of TRACG and the prescribed methodology to analyze the likelihood of power oscillations in the ESBWR design.

3.0 TECHNICAL EVALUATION

The requirements of a realistic methodology are somewhat different from those of a prescriptive methodology in that more realistic models can be used and a measure of the uncertainty in the code must be determined. Various means of achieving an estimate of uncertainty are available in the realm of statistical analysis. GE has chosen to follow the basic code, scaling, applicability, and uncertainty (CSAU) approach outlined in NUREG/CR-5249 (Reference 7). While the CSAU approach defines the process by which uncertainty analysis is performed, it leaves room for GE to determine the exact statistical methodology to be applied. In both the AOO application of TRACG and the ATWS application, GE chose to apply a normal distribution one-sided upper limit statistical methodology. The staff discussed this approach in References 4 and 5. The approach taken for application of TRACG to the ESBWR stability event is again the normal distribution one-sided upper limit statistical methodology. A description of the methodology will be found in Section 3.13 of this SE.

Basics of Boiling Water Reactor Stability

Oscillations due to changes in flow regime (bi-modal) can occur during startup. As the power increases the flow will transition into different flow regimes, i.e., slug flow to annular to churn-turbulent. Under some conditions the flow may oscillate back and forth between flow regimes. This will occur for each channel separately such that the core will not be oscillating as a whole. This results in increased noise in the core flow. Since the flow regime is well defined for steady-state full-power operations, this type of instability is not expected at full-power conditions.

Control system instabilities are caused by some external controller rather than power/flow mismatch. This may be due to a control system algorithm that causes a pump or valve to oscillate under certain conditions or to spurious control blade motion. Control system instabilities are not a part of the application of TRACG since they are not neutronic/thermal-hydraulic driven instabilities.

Loop oscillations (also called Type 1 oscillations) are often seen in a heated channel with a chimney riser in natural circulation. A packet of steam with a higher void fraction flowing up the chimney causes an increase in buoyancy and an increase in flow in the channel. This increase in flow causes a decrease in void production in the heated channel, which causes the buoyancy to decrease and the flow to decrease. The decrease in flow causes an increase in void production and the oscillation cycle starts over again. This would not occur in a critical nuclear reactor since the average core void fraction must remain constant due to strong void reactivity feedback.

Density wave oscillations are the main focus in BWR stability analysis. There have been numerous instability events in BWRs world-wide, most arising from density wave oscillations. A few of the events that have occurred in U.S. operating BWRs, each of which had a 2-3 second period, are:

- LaSalle 2 on March 9, 1988—power oscillation of 25-60 percent
- WPPS WNP 2 on August 15, 1992—power oscillation of 23-43 percent
- Nine Mile Point 2 on July 24, 2003—power oscillation and OPRM SCRAM
- Perry on December 23, 2004—power oscillation and OPRM SCRAM

The dynamic aspects of nuclear reactors have been studied and described in general for decades (Reference 18). The dynamics of the BWR have been studied in extensive detail due to the concern for neutronic thermal-hydraulic stability resulting from operation in the presence of moderator voids (References 19 to 24). Most of the more than two dozen instability events that have occurred world-wide in BWRs are the result of special stability tests. However, some have occurred during normal operation, resulting in reactor shutdown. The basic cause of this type of instability is a change in reactivity caused by void fraction fluctuations.

Three modes of density wave oscillation are considered for analysis using the TRACG thermal-hydraulic computer code: core-wide (or in-phase) mode, regional (out-of-phase) mode, and channel mode. In the case of the core-wide instability mode, the power and flow of the entire core oscillate in phase. On the other hand, in the case of the regional instability, the power and flow in one half of the core oscillate out of phase with the power and flow in the other half of the core. In the case of the channel instability, the flow oscillates in one channel independently of the remainder of the core.

Extensive discussion has been provided in Reference 24 regarding the complex nature of BWR dynamics. To summarize that discussion, the oscillatory response of the BWR depends on the movement of density waves through the core coupled with neutronic feedback. The density wave causes a delay in the local pressure drop due to a change in inlet flow. The sum of all local pressure drops may then result in a local drop that is out of phase with the inlet flow.

The neutronic feedback is a function of the neutron dynamics, the fuel dynamics, the local thermal-hydraulics, and the reactivity feedback dynamics.

Prediction of power-flow oscillation, or instability, thus necessitates the ability to accurately characterize the thermal-hydraulic dynamics, especially voiding and two-phase flow, along with an accurate characterization of the neutronic dynamics. Previous staff SEs (References 4 and 6) have provided detailed results of reviews of the neutronic dynamic and two-phase flow

capabilities, respectively, of TRACG. The present review must bring the two together and determine the adequacy of TRACG to predict the stability of the ESBWR design.

GE has previously employed the ODYSY code to perform stability analyses for operating BWRs. The ODYSY code is a frequency domain code with a one-dimensional kinetics model that was approved for use in operating plant analyses (Reference 15).

The ODYSY code is based on the ODYN thermal-hydraulic transient methodology coupled with the kinetics model. These models form the basis for determining the forward and feedback transfer functions of excitation to the system on the system response. The product of these two transfer functions is referred to as the open loop transfer function (OLTF) (Reference 14).

In a case where a system is truly unstable, the OLTF is able to propagate the excitation via feedback mechanisms once the initial perturbation is removed. According to the Nyquist theorem, in a frequency domain, the response of the OLTF can be used to determine if a system is unstable by observing if this response passes through or encircles the negative unity point on the real axis (Reference 30).

In essence the OLTF is a characteristic function of the reactor system given its configuration and conditions. As the point of interest is the negative unity point on the real axis, the actual mechanism of the perturbation to the system is moot since the system will self-sustain an excitation at this point. Typically the OLTFs analyzed by the ODYSY code are the flow/pressure drop OLTF for the channel stability analysis and the core power/feedback power OLTF for the core-wide stability (Reference 14). In either case, the instabilities are driven by density wave propagation, with neutronic feedback being a consideration in the latter analysis.

In many cases the OLTF response for a real reactor system will not pass through the negative unity point for its operating conditions. The decay ratio is then used as a measure of the damping of oscillations for situations where oscillations are not self-excited by the system. The decay ratio is calculated by determining the distance in the frequency domain between the negative unity point on the real axis and the nearest point on the OLTF response locus, thereby allowing one to establish a margin to the onset of instability.

The decay ratio, therefore, is a parameter that characterizes the system given its conditions and is a measure of the system's margin to instability.

In the time domain a decay ratio of unity indicates an oscillatory mode that is exactly self-excited, and the oscillation would continue without an external mechanism driving it. A limit cycle oscillation of this type is the oscillation for a given system that, once excited, will return to the same oscillation if additional higher modes are excited and allowed to decay. A limit cycle oscillation with a decay ratio of unity would therefore be sinusoidal after sufficient time has passed for higher order damped modes to decay.

Decay ratios less than unity indicate that the reactor system is stable as responses to a perturbation in these cases self-dissipate or dampen. While an initial perturbation may excite several different modes of oscillation, the primary interest is the mode nearest to the limit cycle oscillation, as the others will decay after the external driving mechanism is removed. The decay ratio is most easily inferred from the transient response by taking the ratio of a peak in the oscillatory response to a previous peak.

GE proposes to use the TRACG time domain code to perform stability analyses. In the time domain the OLTF is not calculated directly. Instead an artificial perturbation (i.e., an external driving mechanism) is applied to the system. In these cases the flow or pressure is varied by changing boundary conditions in the model. The external driving force is then removed and the code predicts the transient behavior of the system.

The decay ratio is then inferred by observing the transient response. While this means of determining the decay ratio is less direct than calculating the OLTF in the frequency domain, and in many ways more computationally expensive, the decay ratio remains a characteristic parameter of the core for its given conditions. The decay ratio is determined based on the ratio of subsequent positive peaks in the transient response trace. Given that the response is not a perfect analytical solution, this ratio should be calculated while the positive peaks are relatively large to prevent masking from numerical noise.

The larger peaks tend to occur early in the transient before significant damping has occurred. However, in the very earliest stages of the transient, higher order modes of oscillation (many points on the OLTF locus) may be excited. However, these rapidly decay compared to the fundamental mode—which is nearest to the limit cycle. Therefore, a balance in each calculation must be preserved to ensure that the selected peaks in the transient response are not too early or too late in the transient. GE consistently selects the same pair of transient response peaks in order to determine the decay ratio for any given initial perturbation.

Scope of Review

The scope of the staff's review is limited to the capability of the TRACG code to perform stability analyses for the ESBWR and does not address the acceptability of the ESBWR design. The validity and applicability of the TRACG code inputs must be assessed for the specific design. The inputs that impact the stability of a specific design, though noncritical in a review of the methodology, include:

- the dynamic gap conductance input
- heat transfer/critical power correlations for the fuel bundles
- cross section data input for the kinetics model

For the current purpose, these inputs are assumed to be representative in order to perform an assessment of the methods used for predicting decay ratios, though the staff notes a review of these inputs will be performed during the ESBWR design certification review.

While the scope of this review does include best-estimate predictions of core behavior during startup, the determination of the decay ratio is based on artificial external perturbations. The decay ratio is a measure of the margin between the system's feedback response where an arbitrary density wave oscillation becomes self-excited.

CSAU-Based Technical Evaluation

The CSAU methodology consists of 14 steps contained within 3 elements. The first element includes Steps 1 through 6 and determines the requirements and code capabilities. The scenario-modeling requirements are identified and compared against code capabilities to

determine the applicability of the code to the specific plant and accident scenario. Code limitations are noted during Element 1.

The second element in the methodology includes Steps 7 through 10 and assesses the capabilities of the code by comparison of calculations against experimental data to determine code accuracy and scaleup capability and to determine appropriate ranges over which parameter variations must be considered in sensitivity studies.

The third element in the methodology consists of Steps 11 through 14 and individual contributors to uncertainty, such as plant input parameters, state, and sensitivities, are calculated, collected, and combined with biases and uncertainties into a total uncertainty.

Element 1 - Requirements and Code Capability

3.1 Step 1 - Scenario Selection

The processes and phenomena that can occur during an accident or transient vary considerably depending on the specific event being analyzed. GE has identified power-flow stability as the event to which the methodology under review will be applied. Application of the methodology to other transients and accidents has not been considered in this review.

GE is consistent with this step in the CSAU approach.

3.2 Step 2 - Nuclear Power Plant (NPP) Selection

The dominant phenomena and timing for an event can vary significantly from one nuclear power plant design to another. GE has specified the nuclear power plant applicability for the methodology under review to be the ESBWR natural circulation, passive design.

GE is consistent with this step in the CSAU approach.

3.3 Step 3 - Phenomena Identification and Ranking

The behavior of a nuclear power plant undergoing an accident or transient is not influenced in an equal manner by all phenomena that occur during the event. A determination must be made to establish those phenomena that are important for each event and various phases within an event. Development of a phenomena identification and ranking table (PIRT) establishes those phases and phenomena that are significant to the progress of the event being evaluated.

Important phenomena for stability in the ESBWR have been identified in a PIRT. The PIRT for stability includes all the high-ranked and medium-ranked phenomena. Phenomena associated with the prediction of dryout and film boiling, cladding deformation, etc., are considered to be of low importance on the PIRT because TRACG simulations of ESBWR instabilities indicate a relatively large critical power ratio (CPR) margin. The staff is reviewing GE's application of its critical heat flux (CHF) correlation to ESBWR as part of design certification. Should the CPR margins be reduced significantly relative to what was originally predicted as part of this stability topical report review, the staff expects GE to update its stability PIRT accordingly.

A full discussion of the GE stability PIRT can be found in the enclosed technical evaluation report (TER) review of Reference 1, Section 3.

The PIRT is comprehensive and gives the appropriate rating to important stability phenomena.

GE is consistent with this step in the CSAU approach.

3.4 Step 4 - Frozen Code Version Selection

The version of a code, or codes, reviewed for acceptance must be "frozen" to insure that after an evaluation has been completed, changes to the code do not impact the conclusions and that changes occur in an auditable and traceable manner. GE has specified that the TRACG04 code, which is under configuration control, was used for the ESBWR stability application.

GE is consistent with this step in the CSAU approach.

3.5 Step 5 - Provision of Complete Code Documentation

This step is to provide documentation on the frozen code version such that evaluation of the code's applicability to postulated transient or accident scenarios for a specific plant design can be performed through a traceable record. GE has provided the necessary documentation through submittal of ESBWR stability-specific documentation and reference to code documentation in the possession of the staff from the previous reviews of the TRACG code reported in References 4, 5, and 6.

GE is consistent with this step in the CSAU approach.

3.6 Step 6 - Determination of Code Applicability

A discussion is provided in the enclosed TER regarding the rationale of GE in moving from use of the "dog-bite" stability map of the operating BWR fleet to an ESBWR-specific three-dimensional calculated stability map using the TRACG code. TRACG is a two-fluid code capable of one-dimensional and three-dimensional thermal-hydraulic representation along with three-dimensional neutronic representation. A two-fluid model coupled with a three-dimensional kinetics model is necessary to perform time domain BWR stability analyses (Reference 28).

The key phenomena identified in the ESBWR stability PIRT can be simulated with the TRACG code. Since TRACG is capable of directly calculating the limiting event, regional decay ratio, ESBWR stability criteria will be based on calculated results rather than the "dog-bite" approximation, which was based on operating reactor experience. The staff agrees with this approach, with the provisions summarized in the enclosed TER, which are reiterated in the conditions and conclusions of this SE, Sections 4 and 5.

Specifically, the criteria are based on:

- limiting channel decay ratio <0.8,
- core decay ratio <0.8, and
- regional decay ratio <0.8,

which take into account an uncertainty of 0.2 in the calculated decay ratio.

The evaluations will be made at 95-percent probability and 95-percent confidence. The values are acceptable if they are within the 0.8 maximum acceptance criterion. Additionally, GE has established a design goal of maintaining the mean, or nominal, values of each decay ratio less than 0.4 for the ESBWR design.

GE is consistent with this step in the CSAU approach.

The staff finds each step in Element 1 to be consistent with the CSAU approach and therefore acceptable.

Element 2 - Assessment and Ranging of Parameters

3.7 Step 7 - Establish Assessment Matrix

The capability of TRACG to predict the important thermal-hydraulic phenomena for natural circulation and flow instabilities has been assessed through comparisons with separate effects tests, integral systems tests, and full-scale plant data. These assessments include tests performed in the FRIGG, CRIEPI, SIRIUS, and PANDA facilities, along with Dodewaard (natural circulation startup), Ontario Hydro, and the Peach Bottom Unit 2 (stability) data.

The tests performed at the SIRIUS facility at the Central Research Institute of the Electric Power Industry (CRIEPI) in Japan are of interest in assessing TRACG for instabilities, particularly for loop oscillations that may occur in low-pressure startup conditions.

SIRIUS tests were performed in a facility consisting of a heated core simulator a little more than half the height of the ESBWR core with a chimney that is half the height of the ESBWR chimney. Tests were performed at both low and high system pressure. The tests were designed to simulate thermal-hydraulic instabilities in natural circulation BWRs. Data from the CRIEPI low-pressure oscillation tests address the highly ranked PIRT phenomena for the ESBWR. Further description of the facility is found in References 25 and 26. The ability of TRACG to represent the test facility and predict the results is within reasonable uncertainty limits. A discussion of the code biases and standard deviations is found in the enclosed TER.

The TER discusses the concern that the period of oscillations in the SIRIUS facility is almost a factor of 10 larger than that anticipated in the ESBWR. This time-scaling difference is not significant since the test is used strictly to assess the ability of TRACG to predict the density wave propagation and not the response of the ESBWR design. The staff agrees with this point.

Assessment of TRACG for natural circulation startup was performed by comparison with the February 1992 startup of the Dodewaard natural circulation BWR. Dodewaard was a commercially operated natural circulation BWR, built in the Netherlands, that operated from 1969 to 1997. Comparisons with the 1992 startup indicate good agreement between TRACG and the plant data. A full description of the startup and data comparisons can be found in Reference 26. TRACG predictions of the Dodewaard startup demonstrate the ability of the code to perform startup trajectory calculations for natural circulation BWRs.

In addition, comparisons were made between TRACG predictions and the Peach Bottom Unit 2 stability tests conducted in 1977. The Peach Bottom tests are of interest not only for demonstrating the ability of TRACG to model density wave phenomena; the Peach Bottom tests also provided a reasonable database for tests conducted at low decay ratios representative of those anticipated for ESBWR. The standard deviation of the TRACG error is less than that proposed by GE for TRACG stability analysis (0.2). Further discussion of the comparison between TRACG and the Peach Bottom Unit 2 stability test can be found in the enclosed TER.

Full discussion of the assessment program is found in the enclosed TER.

GE is consistent with this step in the CSAU approach.

3.8 Step 8 - NPP Nodalization Definition

A fine axial nodalization is used in the core entrance to attempt to maintain a constant Courant number and to provide more detailed modeling of the lower void regions of the core in which void oscillations have the greatest impact on stability. The staff finds the approach described in Reference 13 acceptable first, to determine the error resulting from the numerical damping due to discrete nodalization, and, second, to specify a nodalization scheme that will result in errors in decay ratio from numerical damping not to exceed 10 percent.

As stated before, the time domain methodology is often more computationally expensive and less direct in terms of determining the system decay ratio than a frequency domain approach. The three-dimensional kinetics model in TRACG, as well as the ability to model many channel groups, does, however, offer significant benefits—namely the capability to model regional mode oscillations. Yet it is worth noting that the frequency domain codes such as ODYSY predict exact solutions whereas time domain codes are limited by numerical errors created by imperfect spatial and temporal resolution (i.e., noding, timestepping). In order to apply the TRACG methodology, therefore, procedural controls on the calculation must be imposed to prevent numerical diffusion of the calculated transient response. These controls are manifested both in procedures for nodalizing the model components and in internal calculational controls in terms of the Courant number.

The channel grouping and nodalization is of key importance as it will impact not only neutronic feedback in the core, but also the determination of the relative magnitudes of the single-phase and two-phase pressure drops through various regions of the core, namely by producing an uncertainty in the location of the boiling boundary. The axial nodalization was investigated by GE and, in doing so, GE developed a methodology for evaluating the impact of finite nodalization on the uncertainty in the predicted decay ratio.

As for radial nodalization (or channel grouping), the staff has found that grouping based on power is an appropriate method for several reasons. First, the neutron kinetics equations, regardless of the thermal-hydraulic noding, are solved based on 6-inch-square nodes in the core region. Six inches corresponds to roughly one mean free path for a fast neutron. The nodes, however, share thermal-hydraulic conditions based on the associated channel grouping. As the nodes are grouped by power, the shared thermal-hydraulic conditions will be very similar among these nodes, allowing for an acceptable determination of the neutronic feedback. Additionally, this procedure allows for finer radial nodalization for higher order neutronic harmonic modes, which is critical in determining the channel grouping for regional mode

oscillations. Radial nodalization involves collapsing the fuel bundles into approximately
[[]] thermal-hydraulic channels.

The channel grouping depends on the type of calculation being performed. For core-wide stability analysis, the channel grouping described in Figure 5.2-4 of Reference 1 was examined by GE. The staff has determined that the process described in Section 8.1.2.2 for determining adequate channel grouping ensures that the following spatial variations are modeled adequately for stability analyses:

- Inlet orificing
- Radial power
- Higher order flux harmonics
- Hot channels
- Geometry effects (i.e., super bundles)

The proposed axial and radial nodalizations have been used in the past for TRACG calculations of operating reactor stability and have been found to be adequate for these calculations.

For regional stability analyses, a different channel grouping is required to capture the character of higher flux harmonics. The channel grouping for regional decay ratio calculations is based on the magnitude of [[

]] The channel grouping is depicted in Figure 8.1-18 in Reference 1. There are two important characteristics of an adequate regional channel grouping:

- [[

]]

The staff has reviewed this procedure and determined that it is adequate for modeling regional oscillations.

Artificial numerical damping also arises due to finite spatial and temporal differencing. This damping is minimized by using an explicit first-order finite differencing method and maintaining the Courant number near one. The Courant number is the ratio of the product of the time step and velocity to the node size ($\Delta t V / \Delta Z$). When performing analyses with finite differencing in space and time, there are additional terms in the Taylor expansion that are multiplied by the difference between the Courant number and one. When the Courant number is exactly one, these additional terms go to zero and the wave is propagated without dissipation. The damping is more pronounced when using the implicit first-order finite differencing method (Reference 31). The TRACG methodology described in Reference 1 uses explicit time integration and a Courant multiplier of one for this exact purpose.

The Courant multiplier is used for time step control during TRACG calculations. The time step in the calculation is allowed to vary between maximum and minimum step sizes specified by the user. Within those boundaries, however, TRACG enforces certain limits to determine the maximum allowable time step within the user defined band. The Courant limit is controlled by

the Courant multiplier. In essence the time step is constrained such that the Courant number will not exceed the Courant multiplier, but will increase until meeting this limit if the other criteria are met (namely the outer iteration convergence criterion and the rate-change criterion). If a steady-state solution is converged before applying a perturbation, and if the perturbation is small, the time step will be controlled predominantly by the Courant limit. Therefore, for purposes of calculating thermal-hydraulic instability transient responses, a Courant multiplier of one must be specified as stated in Reference 27, the TRACG User Manual.

The staff independently investigated the capability of TRACG to propagate waves without numerical damping based purely on Courant multiplier time step control. These studies are included in Section 3.15.6.

GE is consistent with this step in the CSAU approach.

3.9 Step 9 - Definition of Code and Experimental Accuracy

Simulation of experiments developed from Step 7 using the NPP nodalization from Step 8 provides checks to determine code accuracy. The differences between the code-calculated results and the test data provide bias and deviation information. Code scaleup capability can also be evaluated from separate effects data, full-scale component tests data, plant test data, and plant operating data where available. Overall code capabilities are assessed from integral systems test data and plant operational data. These assessments were performed as part of the GE qualification of the TRACG methodology documented in References 1, 2, and 3. Evaluation of the code accuracy is discussed in the enclosed TER.

The staff finds the scaling approach utilized by GE in applying test data to the TRACG assessment to be acceptable (Reference 6). Appropriate consideration has been given to the data introduced for assessment of the TRACG code for applicability to stability analysis.

GE is consistent with this step in the CSAU approach.

3.10 Step 10 - Determination of Effect of Scale

Various physical processes may give different results as components or facilities vary in scale from small to full size. The effect of scale must be included in the quantification of bias and deviation to determine the potential for scaleup effects. The key stability parameters and phenomena in the ESBWR do not have significantly different scales than in operating reactors. GE has performed full-scale tests on the channel components.

GE is consistent with this step in the CSAU approach.

The staff finds each step in Element 2 to be consistent with the CSAU approach and therefore acceptable.

Element 3 - Sensitivity and Uncertainty Analysis

3.11 Step 11 - Determination of the Effect of Reactor Input Parameters and State

The purpose of this step is to determine the effect that variations in the plant operating parameters have on the uncertainty analysis. Plant process parameters characterize the state of operation and are controllable by the plant operators to a certain degree. Discussion of the applicability of TRACG to input effects such as ESBWR plant startup is found in the enclosed TER.

The staff reviewed the list of sensitive input parameters based on a PIRT and determined that GE has assessed the appropriate plant parameters affecting stability analyses. GE provided a table in Reference 1 detailing the impact of sensitive thermal-hydraulic parameter uncertainty on predicted decay ratios. However, information provided with respect to the sensitivity of the TRACG code to uncertainties in input physics parameters is not complete.

The staff notes that the uncertainties in the physics parameters will be addressed in the design certification review of the ESBWR. The methods employed for generating cross sections for TRACG were not considered part of the scope of the current review in which the void coefficient is a primary factor in determining core stability. Also, a design-specific fuel review is being conducted as part of the ESBWR design certification review. Physics parameters, cross-sections, and critical heat flux correlations affecting void generation will be addressed as part of the design certification.

GE is consistent with this step in the CSAU approach.

3.12 Step 12 - Performance of NPP Sensitivity Calculations

Sensitivity calculations are performed to evaluate methodology sensitivity to various operating conditions that arise from uncertainties in the reactor state at the initiation of the transient, in addition to sensitivity to plant configuration. Sensitivity studies performed are discussed in the enclosed TER.

While the full transient response is characterized by the magnitude of the initial impulse, the decay ratio, and the frequency, the staff determined that GE's assessment of the sensitivity of only the decay ratio is sufficiently complete. The frequency of the oscillation is driven by the void transit time through the channel from the initiation of two-phase flow (boiling boundary) to the bottom of the chimney region. This transit time is based, therefore, solely on the thermal-hydraulic condition of the core shortly after the initiation of the perturbation. The staff previously reviewed TRACG for this purpose as documented in References 5 and 6, and determined that the code is suited to this purpose.

The magnitude of the impulse is determined by the magnitude of the perturbation imposed. GE has separately addressed the sensitivity of the transient response to the perturbation size in Section 8.1 of Reference 1. The staff agrees with the approach presented.

GE is consistent with this step in the CSAU approach.

3.13 Step 13 - Determination of Combined Bias and Uncertainty

The first few steps in the CSAU methodology identify and rank the physical phenomena important to judging the performance of the safety systems and margins in the design. The phenomena are compared to the modeling capability of the code to assess whether the code has the necessary models to simulate the phenomena. Most important, the range of the identified phenomena covered in experiments or test data is compared to the corresponding range of the intended application to assure that the code has been qualified for the highly ranked phenomena over the appropriate range. The result is then provided in a PIRT. The staff has reviewed the PIRT provided and finds it acceptable and consistent with the staff's experience in judging the important phenomena associated with stability.

Discussion of model biases and uncertainties along with their application is found in the enclosed TER.

The discussion of the uncertainty analysis approach presented in Reference 7 envisioned the use of response surfaces for quantifying uncertainty. The staff recognizes that there are other valid and acceptable means by which the uncertainty can be assessed. Other means include that developed following the work by Wilks (References 10 and 11), referred to as order statistics, and a related method referred to as normal distribution upper one-sided limit. Each has advantages and disadvantages.

Order Statistics:

The Monte Carlo method is used to include the effects of perturbations to all important parameters at once. The sample size is defined to yield the desired statistical confidence. The statistical upper bound is determined from the most limiting perturbation (for the first-order statistics).

The basis for order statistics comes from the work of Wilks (Reference 10), and, was further developed by Gesellschaft für Anlagen und Reactorsicherheit (GRS) (Reference 11). Only a modest number of calculations are required, and the effects of interactions between perturbations of different parameters are automatically included. Monte Carlo trials are used to vary all uncertain model and plant parameters randomly and simultaneously, each according to its uncertainty and assumed probability density function (PDF). Subsequently, a method based on the order statistics of the output values is used to derive upper tolerance bounds (one-sided, upper tolerance limits, OSTULs).

Monte Carlo sampling of each parameter according to its assigned PDF yields the value of that parameter to be used for a particular trial. Given such a trial set of input parameters, the calculation process determines the corresponding output parameter of interest. Therefore, while the void coefficient might be set at a -1.5σ value, interfacial shear might be set to a value of $+2\sigma$, each according to its own probability model. In this manner, the effects of interaction between all model parameters are captured in a single calculation. Once the trials have been completed, the desired output parameter, for example, decay ratio, is extracted from each of the trials and the set of parameter values is then used to construct an OUSTL for that particular parameter.

An OSUTL is a function $U = U(x_1, \dots, x_n)$ of the data x_i (which will be the values of an output parameter of interest in a set of Monte Carlo trials), defined by two numbers, $0 < \alpha, \beta < 1$, so that the proportion of future values of the quantity of interest that will be less than U is 100α percent, with confidence at least 100β percent; this is called an OSUTL with 100α percent content, or probability, and 100β percent confidence level.

The order statistics method produces OSUTLs that are valid irrespective of the PDF of the data, requiring only that they be a sample from a continuous PDF. Given values of α and β , the OSUTL can be defined as the largest of the data values, provided the sample size $N \geq \log(1-\beta)/\log \alpha$. For 95-percent content and 95-percent confidence level, the minimum sufficient sample size is $N = 59$.

If the method is implemented as described, that is, if a sample size (59) is chosen so that the sample maximum is the upper tolerance bound sought, 95/95, then this bound has variability that is typical of the maximum of a sample of that size, which can be substantial. To mitigate that variability, one can choose a suitably larger sample size so that the bound sought, 95/95, is given by the second or third largest sample value. The number of sample sizes necessary to achieve the 95/95 bound is:

Order Statistic	Sample Size
Largest	59
2 nd Largest	93
3 rd Largest	124

Normal Distribution One-Sided Upper Tolerance Limit:

[[

]]

The following table illustrates the advantages and disadvantages of these statistical methods.

Comparison of Statistical Approaches

Statistical Method	Advantages	Disadvantages
Order Statistics	<p>The number of random trials is independent of input parameters considered.</p> <p>The method requires no assumption about the PDF of the output parameter.</p> <p>It is not necessary to perform separate calculations to determine the sensitivity of the response to individual input parameters.</p> <p>It is not necessary to make assumptions about the effect on the output of interactions of input parameters.</p>	Results can be very conservative for a small number of trials, and consistent results may require a larger set of trials.
ND-OUSTL	[[[[]]

As noted above, the staff recognizes that there are various means by which uncertainty in a code calculation can be obtained. While the staff has referred to the response surface approach in References 7 and 9, there are advantages in use of other methods such as normal distribution one-sided upper tolerance limit. Most notably, the methodology can require significantly reduced calculation cases, thus reducing the cost of performing an analysis. But,

there are significant restrictions, such as demonstration of normality of the resulting probability distribution function. There is no one single correct method of determining uncertainty. Each of these methods has been reviewed carefully by the staff in recent years in various submittals.

GE is consistent with this step in the CSAU approach.

3.14 Analysis Methodology

3.14.1 Normal Operation Stability

While several calculations are done to evaluate the stability of the ESBWR using TRACG during normal operation, the general procedure and stability criterion are essentially the same for each calculation. TRACG is used to calculate a steady-state condition for various operational parameters. From the steady-state, a transient is induced by perturbing the core conditions. The transient response is predicted by TRACG.

The transient response is used to determine the decay ratio. The transient response of interest is either the power or the flow rate. In response to a perturbation, the parameter of interest will oscillate about its steady-state value. The decay ratio is the ratio of the [[

]] If the ratio is less than unity, the system is said to be stable, since over time the system will return to its steady-state condition.

To account for uncertainties, GE has identified an acceptance criterion of 0.8 for the decay ratio for the three analyzed modes of instability: channel, regional, and core-wide.

3.14.2 Anticipated Operational Occurrence Stability

Reference 1 contains an example analysis of ESBWR stability margin following two AOOs. The first is the loss of feedwater heating (LOFWH) and the second is a loss of feedwater (LOFW) flow. The staff has previously reviewed TRACG for calculating transient response to AOOs in operating BWRs and has found that code acceptable for this purpose (Reference 4). Under transient conditions, stability margin is analyzed once a steady-state is achieved.

The staff recognizes that these two AOOs lead to more limiting power-flow conditions, and consequently lower stability margin than the steady-state condition. However, the staff notes that this analysis remains essentially unchanged compared to that used for the steady-state. Therefore, the information provided illustrates the applicability of the prescribed methodology to analyze core conditions other than nominal full-power operation.

The staff has reviewed the information contained in Section 8.4 of Reference 1 and found that the TRACG stability methodology is not suitable for evaluating stability margin during the transients listed, but rather once a steady-state condition has been achieved.

This is a limitation inherent in the methodology. TRACG is used to calculate the decay ratio by perturbing a pressure or flow parameter of the system. The oscillatory response predicted by the code is used to infer the decay ratio. If the system is already experiencing a transient, it is

impossible to ascertain a decay ratio, as the transient response is driven by both any applied perturbation and the natural system response to its current transient condition.

The LOFW flow and LOFWH are limiting AOOs in that each result in core conditions that are more susceptible to instability than the normal operating condition. The LOFWH AOO leads to a high thermal power condition (the scram point is at 115 percent of rated power); therefore an analysis of the stability margin is performed by predicting a steady-state condition following a LOFWH that results in a core condition of 116 percent of rated power. From this steady-state condition, a set of perturbations were used to calculate a series of decay ratios in order to assess the likelihood of an instability event.

The LOFW flow leads to a reduced flow condition relative to the normal operating condition. TRACG was used to artificially force a steady-state condition with the downcomer level slightly above the scram set point. This was meant to simulate the lowest flow condition that could result from this AOO. From the calculated steady-state condition, a series of perturbations were performed to assess the core stability.

The margin to instability is reduced for high-power and low-flow conditions. These two AOOs in particular are limiting for this reason. As GE has forced a steady-state condition at the most limiting scenario (in terms of power and flow conditions), the decay ratio methodology is valid and the results are bounding.

The staff agrees with GE's methodology and finds that the approach is valid for predicting the likelihood of a core instability during an AOO.

3.14.3 Anticipated Transients Without Scram Stability

GE has not provided any information on anticipated transients without scram (ATWS). Stability during ATWS was not considered as part of this review. Approval of the TRACG code for stability analysis during startup and normal operation does not imply acceptance of TRACG for ATWS stability analysis.

3.14.4 Plant Startup Stability

Table 2.3-3 in Reference 17 lists phenomena important for modeling the startup transient. These are not all included in the PIRT, Table 3.1-1 in Reference 1. Exclusion of some important phenomena related to the startup transient from the stability PIRT is acceptable to the staff because the staff believes that the code has the necessary models to simulate ESBWR startup and that there is appropriate qualification and assessment of TRACG for this purpose. The staff has also reviewed Sections 9.0-9.3 of Reference 1 as well as the information provided in Reference 16 and determined that TRACG is capable of predicting a startup trajectory for the ESBWR with neutronic feedback.

While TRACG can predict the transient behavior of the reactor, it is not possible using the prescribed methodology to predict the margin to instability during a reactor transient. The methodology is inherently limited to predicting decay ratios by perturbing a steady-state condition. The staff's approval of TRACG for modeling startup transients is not applicable for predicting safety parameters such as decay ratio or CPR margin.

The staff recommends that to demonstrate compliance with GDC 12, the stability margin during startup be evaluated by calculating the heatup rate at which large power oscillations are observed during startup. The margin to instability can thereby be defined as the difference between the power at the nominal heatup rate (~ 30 °C/hr) and the power at the heatup rate at which large power oscillations are observed.

Detailed startup procedures will be developed by GE at a later time. A projected ESBWR startup procedure would progress as follows:

- The control rods are fully inserted. There are 269 control rods arranged in assemblies, and the assemblies are divided into 10 groups.
- Deaeration begins by drawing a vacuum on the main condenser/vessel using mechanical pumps with the steam drain lines open. The steam dome pressure is held at 52 kPa throughout the deaeration process.
- The coolant is heated to about 82 °C using reactor decay heat and the reactor water cleanup/shutdown cooling (RWCU/SDC) system.
- The startup period begins when the main steam isolation valves (MSIVs) are closed. At this point, control rod groups 1, 2, and 3 are withdrawn in 720 seconds. Group 4 is withdrawn next, with the power remaining at ~ 20 MW of decay heat until 1500 seconds. At this point the reactor becomes critical and further heats the coolant. The reactor power reaches 120 MW, but after that the control rods are used to maintain power at or above 85 MW.
- The coolant in the vessel is subcooled throughout the core, chimney, and separators. An essentially single-phase natural circulation loop is established.
- The reactor heatup is limited to 55 °C/hr, but the coolant at the top of the separators eventually becomes saturated and surface boiling occurs. The surface boiling pressurizes the system. The reactor power is kept at 85 MW.
- Throughout the startup period the RWCU/SDC heat exchangers are used to control the flow in the downcomer. The systems are also used to enhance the coolant flow and reduce lower plenum stratification.
- Once the reactor is pressurized to 6.3 MPa and 279 °C, the MSIVs are opened and the feedwater control system is activated. The turbine bypass valves are used to further regulate the system pressure. The reactor power is increased in steps to 210 MW.
- Once these conditions have been met, the reactor begins its power ascension phase.

Prior to the ascension to full-power stage of startup, the steam flow is either entirely drained or entirely bypassed and there are no flow paths that would allow for balance-of-plant (BOP) feedwater heating feedback phenomena. Therefore, the proposed methodology is acceptable during the stages of startup described in Reference 1. The reactor at the nominal heatup rate reaches the ascension to full-power phase approximately 8 hours after the beginning of the procedure.

The current approach for performing stability analyses does not include a BOP model. The feedback from steam flow into the feedwater system would be required to perform best estimate analyses of the transient response to an actual oscillation over long time periods. Experience modeling the LaSalle instability event showed greater agreement between TRACG and plant data once this feedback mechanism was included (Reference 28).

However, the time scale for the feedwater oscillations in the LaSalle event is on the order of 30 seconds (Reference 28), whereas the decay ratios predicted by TRACG are based on perturbations that essentially damp within a few seconds. The event at LaSalle was in part due to a sticking controller, therefore further reducing the validity of this comparison. For the purposes of determining decay ratios, including the slower feedback from the BOP will not have a significant effect.

In general, however, to perform a best-estimate analysis of a transient response during an instability event, the feedback that occurs via the BOP will have an impact on the core inlet subcooling. The inlet subcooling will affect the boiling boundary and in turn have a significant impact on the evolution of the transient over longer time periods. The current methodology is only approved to calculate the decay ratio based on rapidly terminating transient responses to artificial perturbations (core, channel, or regional) or to predict the onset of unstable behavior during the startup of the plant before the turbine control valves are opened.

Furthermore, the assumption of a constant xenon concentration is a valid assumption during decay ratio calculations as those are done by predicting a relatively rapid transient response based on a perturbation to a steady-state condition. Thus, the xenon concentration will not have sufficient time to change appreciably over the course of the predicted transient.

For startup stability calculations, the duration of the xenon transient condition is significantly longer (~8 hours to reach the ascension to full-power phase). Given that the transient duration prior to the ascension to full-power phase is on the same order as the half life of the xenon precursor, sufficient xenon concentration does not develop during the startup of the plant to have a significant impact on the neutronic behavior of the core during this time. Therefore, the constant xenon assumption is valid for the purposes of predicting the power margin to instability using TRACG for startup up to the ascension to full-power phase.

The ascension to full-power phase of startup was not within the scope of the review because GE has included no information in Reference 1 concerning this transient. During this transient, xenon concentration is increasing and has a more pronounced effect on the power distribution in the core. While a xenon transient evolves over a much longer time period than thermal-hydraulic instabilities, such as void production, its impact on neutronic parameters and core power distribution should be included in an analysis of this phase of startup.

The staff is aware that PANACEA has an option for predicting transient xenon and that this option can be invoked for a startup calculation. The staff expects this to be done for the initial startup of the ESBWR to properly predict the margins during the ascension to full-power phase of startup. The startup transient will be the subject of a subsequent review by the staff during design certification.

3.14.5 Xenon Transients

The staff has reviewed the TRACG model description (Reference 2) and has determined that the code is not acceptable for the analysis of xenon-induced transients as the xenon and fission product concentrations in the fuel are held constant.

Xenon transients typically evolve over several hours due to the relatively slow production mechanism, β decay from ^{135}I , which has a half life of 6.72 hours. Therefore, for the purposes of calculating decay ratios based on a steady-state condition, this assumption will not have any significant impact on the results of the calculations.

While the methodology under review is limited to density wave oscillations, the staff notes that the strong negative void reactivity feedback, as is the case in operating BWRs, is sufficient to damp xenon-induced neutronic oscillations. The review of xenon-induced oscillations is not within the scope of the current review of the TRACG methodology to assess density wave oscillations. However, the staff has determined that the xenon distribution in the core has an impact on the power distribution in the core. The power distribution in turn will have an impact on the boiling boundary within channels in the core and, therefore, have an effect on the thermal-hydraulic stability. Therefore, best-estimate analyses of thermal-hydraulic instabilities should account for the presence of xenon, particularly for transient analyses of long duration—such as the ascension to full-power phase of startup or restart transients where there is appreciable xenon in the core.

In terms of anticipated transients, such as LOFW flow and LOFWH, the transients approach a steady-state condition shortly after initiation. Therefore, a constant xenon concentration is valid in predicting the trajectory following these initiating events using TRACG.

Lastly, while the startup transient occurs over a much longer duration than AOOs, the staff recognizes that the initial core configuration is essentially xenon-free and there is not sufficient time between the beginning and the ascension to full-power phase at the nominal heatup rate to allow for significant xenon buildup. Therefore, TRACG is suitable for predicting the ESBWR startup trajectory until the ascension to full-power phase at the nominal heatup rate as well as at higher heatup rates.

The staff finds each step in Element 3 to be consistent with the CSAU approach and therefore acceptable.

3.15 Staff Independent Calculations

3.15.1 Channel Stability

The staff has reviewed GE's procedure for calculating the single-channel stability margin during normal operation. The staff has found that the procedure described in Section 8.1.1 of Reference 1 is acceptable for calculating the channel decay ratio.

It is important to note for channel stability analyses that two conditions must be set in the model. First, the power must be fixed. Transient power calculations will lead to shifting power

from the channel during the transient and contribute to damping of the oscillation. Second, the explicit numerical integration method option should be activated for the channel being analyzed.

The channel decay ratio calculation serves as a means to evaluate if a fluctuation in the boiling boundary will have a lasting effect on the pressure drop above the boundary, such that lagging two-phase pressure oscillations arising from initial changes in the boiling boundary do not result in a perpetually oscillating boiling boundary.

While the above conditions are stated in Reference 1, Section 8.1.1, the staff notes that Reference 1 does not provide a complete description of the process for selecting the limiting channel for stability analysis. The limiting channel is selected by first calculating the steady-state condition using the whole core model. The hot superbundle is identified based on steam flow through the associated chimney. The limiting channel is the single channel within the hot superbundle with the highest radial peaking factor and the most downward-shifted axial power shape. Both criteria must be specified as it is likely that any given superbundle will have a relatively flat radial power profile.

Figure 1 of this SE shows the transient response of inlet mass flow rate to an instantaneous velocity perturbation for four channels in the core. Each channel represents a single channel. Three of the four channels exhibit very similar transient responses to an inlet velocity perturbation.

The channel designated 142 has a higher decay ratio than the other three channels. The higher decay ratio is driven by the high power and bottom-shifted axial power shape in this channel. This combination leads to more vapor generation towards the bottom of the core and, subsequently, the ratio of the single-phase pressure drop to the two-phase pressure drop is reduced. Figure 2 of this SE shows the difference in axial power shape between the four channels analyzed. The figure shows that channel 142 has a significantly downward-shifted power shape compared with the other channels, while the other four channels have substantially similar axial power shapes.

High-power assemblies with downward-biased axial power shapes have boiling boundaries nearest to the bottom of active fuel. With a small boiling boundary, the flow within the channel is predominantly two phase; therefore, the pressure drop within the channel is predominantly driven by the two-phase flow. The channel stability improves as the ratio of the single-phase to two-phase pressure drop increases; therefore, the more downward-biased the axial power shape for a given channel at the same power level, the more susceptible that channel will be to thermal-hydraulic instabilities arising from flow/pressure drop feedback.

A limiting channel stability analysis should first identify the hot superbundle. If the radial peaking factor is similar for all of the channels in the superbundle, the channel stability should be evaluated using the assembly in the hot superbundle with the limiting (i.e., most downward-biased) axial power shape. This selection criterion is not explicitly stated in Reference 1.

3.15.2 Superbundle and Loop Stability

Superbundle stability was analyzed by the staff using a TRACG model provided by GE. The staff calculated the superbundle decay ratio at end of cycle (EOC) using the following procedure:

• [[

]]

Figure 3 of this SE shows the transient response of a single superbundle to an inlet flow perturbation. The figure also shows the individual responses for the single channel and the 15-channel grouping that represents the remainder of the superbundle. The close agreement between the single-channel transient response illustrated and that calculated for the channel decay ratio confirmatory calculation illustrates two phenomena:

- The superbundle decay ratio will also be less than the hot channel decay ratio, as summing the transient response over multiple channels will effectively mask the response in the limiting channel because the other channels in the superbundle may not have a limiting radial peaking factor or power shape.
- The chimney does not have a significant impact on density wave instability. This is due to thermal-hydraulic communication that occurs above the channel components and due to the low-pressure drop in the chimney region.

In much the same manner as the channel stability calculation for the decay ratio, the purpose of the superbundle analysis is to determine the likelihood of thermal-hydraulic density wave instabilities as a result of the flow/pressure drop feedback. However, when taking the entire superbundle as a single unit, the importance of the associated chimney can also be evaluated. Additional consideration of the superbundle is warranted, as the chimney is a unique design feature of the ESBWR relative to operating BWRs.

The important feedback mechanism for this type of analysis is the relationship between the instantaneous boiling boundary and the lagging impact on the two-phase pressure drop for a fixed channel power and distribution. The total two-phase pressure drop consists of several individual components, the acceleration, friction, contraction, and buoyancy terms in the channels themselves, as well as the acceleration, friction, contraction, and buoyancy in the chimney.

For density wave oscillations, the pressure drop across the superbundle and associated chimney remains constant. Therefore, perturbations to the pressure drop in the single-phase region at the core inlet are exactly balanced by the pressure drop in the two-phase region above the boiling boundary as well as the pressure perturbation in the associated chimney.

During normal operation the chimney will reach a steady-state temperature and therefore will not contribute significantly in terms of heat transfer between the structure and the coolant even under oscillatory conditions such as those being considered as part of this methodology. The chimney can be assumed to be adiabatic. Similarly, the very large flow area in the chimney compared with the core region leads to a small friction pressure drop. As the pressure change from gravity at normal operation is ~ 12 kPa, compared with a system pressure of ~ 7000 kPa, there will be little change in the void content from reduced saturation pressure in this region, and the acceleration term can be neglected as well. Therefore, the predominant contributor to the pressure drop, and to the perturbation in this pressure drop for density wave oscillations, is the buoyancy component.

The fuel support structure and inlet orifice on average contribute ~ 60 kPa pressure drop during normal operation of the ESBWR, combined with a pressure drop in the core region of ~ 70 kPa (Reference 29). Approximate values are noted for the purpose of conceptually illustrating the impact of the chimney. Therefore, the pressure drop from the chimney contributes ~ 10 percent of the pressure drop between the flow inlet into the core region and the top of the chimney region.

The purpose of the chimney is to have a very low-pressure drop to allow for a significant gravity head in the downcomer, based on the large density difference between the liquid water in the annulus and the high-void two-phase mixture in the chimney.

As the pressure drop in the chimney is already small compared to the total pressure drop, changes in the void fraction within the chimney do not play a significant role in the density wave flow/feedback effects in the core. The pressure drop perturbation at the core inlet (side entry orifice of the fuel assemblies in the superbundle) will likely be balanced by an out-of-phase two-phase pressure perturbation above the boiling boundary, where friction losses at the fuel spacers and fuel assembly outlet are likely to be much larger than changes in the overall chimney pressure drop.

The feedback of the pressure perturbation in the chimney on the void and boiling boundary within the core is minimal for the following reasons:

- The void fraction in the chimney is already very large (80 percent or higher on average); therefore small changes in the void fraction result in small fractional changes in the buoyancy pressure drop term in the chimney. A large core flow variation is required to produce only a modest perturbation in the void fraction at the core outlet. Calculations
- performed with LAPUR on an average ESBWR super bundle indicate that a flow perturbation as great as 10 percent would only produce a 2 percent perturbation in the void fraction at the core outlet. This discrepancy would be even greater for the high-power assemblies, where the outlet void fraction is even higher.

- The pressure drop itself is already very small; therefore, a small fractional change in the total pressure drop in the chimney results in a significantly smaller fractional change in the total pressure drop through the super bundle and associated chimney. Therefore, it would require a significant change in void fraction within the chimney to produce a pressure drop perturbation to compensate for the pressure perturbation at the core inlet. When compared with the pressure drop due to friction in the core around spacers, it is much more likely that a direct feedback between core flow and local friction pressure drops in the core would produce the compensating pressure perturbation to maintain the pressure drop across the superbundle and chimney cell for a density wave oscillation.
- There is thermal-hydraulic communication between channels in the superbundle at the chimney inlet; therefore low-power channels, which tend to be more stable, contribute to the total flow through the chimney, and thereby damp any oscillations in the inlet flow arising from oscillations in higher power assemblies in that superbundle. Each assembly has a slightly different power and, therefore, a slightly different wave propagation time from the boiling boundary to the chimney inlet. Therefore, it is unlikely for the chimney to be exactly in phase with each of the assemblies in the associated superbundle. This effect is small based on the relatively flat radial power shape, but may lead to minor pressure perturbations at the assembly outlet due to thermal-hydraulic communication based on slightly different natural frequencies for each channel, particularly if axial power shapes for the channels are different based on burnable poison loadings or depletion.
- The chimney is much taller than the core with a lower fluid velocity; therefore, a density wave with a frequency driven by core flow may have several peaks and troughs axially through the chimney at any given instant, resulting in a change in the integrated pressure perturbation buoyancy term that is much smaller than the local perturbation. As there is no neutronic feedback in the chimney, the feedback mechanism is driven by the integrated pressure drop perturbation and not the local variation in void.

While it is clear that the small pressure drop in the chimney at high-void fractions has a small influence on the oscillatory behavior for density wave instability, one must consider a feedback mechanism arising from density changes that may increase or decrease the relative driving density head, and thus influence the total flow. This mechanism is referred to as loop oscillation. The perturbation in the driving head will have an impact on the boiling boundary and influence the propagation of voids in the core region. This perturbation may lead to a sustained out-of-phase perturbation in the driving head.

While loop oscillations are considered in the startup calculation at low pressures for the ESBWR, the staff does not consider the loop oscillation mechanism for potential instabilities to be a concern for the ESBWR at power. While TRACG has the capability to track void transport, neutron kinetic behavior, and pressure drop feedback dynamically, the fact that demonstration calculations do not show loop oscillatory behavior is consistent with the physical phenomena present for the ESBWR during normal operation. Section 3 of Reference 25 describes several comparisons of TRACG models of the SIRIUS facility and experimental data, thus illustrating that TRACG is capable of predicting loop oscillations for electrically heated channels.

For a critical reactor at the 100 percent rod line, a perturbation in the core flow would result in a corresponding perturbation in core power and void production. The strong void reactivity feedback, which is a key factor in density wave instabilities, drives the reactor to a constant

average void fraction. Therefore, while loop oscillations can occur prior to achieving criticality at high pressure and power, the strong neutronic feedback provides a significant damping to loop oscillations at power by preventing a sustained negative perturbation in core outlet void. A strong negative perturbation in the core outlet void is necessary to develop a perturbation in the chimney buoyancy pressure drop of sufficient magnitude and duration to provide a feedback in core flow at the same frequency of the loop. Given the neutronic condition of the core, loop oscillations for the ESBWR are unlikely, and TRACG predictions of core-wide oscillations are consistent with the staff's understanding of the physical interrelationships between the neutronics and pressure drop feedback mechanisms present in the ESBWR.

Overall the staff has determined that the relevant phenomena for both density wave and loop oscillations are modeled in TRACG consistent with the staff's understanding of the physical phenomena that would occur in the chimney and the chimney's impact on channel and core stability.

Perturbations in chimney void profile have an insignificant effect on core stability. First, the mechanisms by which they may influence core boiling boundary, total pressure drop, and reactivity are entirely dwarfed by phenomena occurring in the core region itself for density wave oscillations; and second, the feedback mechanisms are related to the integrated void profile throughout the region; thus oscillations in local void over time tend to cancel themselves out in the chimney region.

Furthermore, as the importance of the chimney in regard to steady-state analysis, as well as stability analysis, is driven predominantly by the integrated profile; the importance of fine nodalization for the purpose of spatial resolution in the void profile is relatively small. A nodal resolution sufficient to avoid numerical instabilities arising from breaching the Courant limit is required.

This general conclusion is evidenced by the close correlation between void propagation time from the boiling boundary to the top of the core and the oscillation frequency, as well as by results of calculations with variations in the chimney friction factor and nodalization.

Independent calculations performed with LAPUR with various chimney friction factors, as discussed briefly in Section 3.15.4 as well as in the enclosed TER (as accepted by the staff), confirm that at very large friction factors, the pressure drop in the chimney begins to become significant; at this point the chimney does have a small impact on the decay ratio, further supporting the general conclusion that the low-pressure drop in the chimney limits the chimney's importance to stability analysis.

Additional analyses performed by the applicant at the request of the staff have shown that the nodalization of the chimney does not have a significant impact on the stability analysis. In order to maintain a constant Courant number, the chimney was modeled using 33 nodes, each 0.2 meters in height, and the numeric integration was set to explicit in this region. The calculation, as described in Reference 32, shows that TRACG predicts the same decay ratio for both the detailed and standard nodalization schemes. Additionally, GE has performed a series of calculations with a channel/chimney simplified model. The height of the chimney was varied between zero and 6.6 m. The results of these parametric analyses indicate that the chimney height does not have a significant impact on the predicted decay ratio (Reference 32). The calculations performed by GE also demonstrate that the channel two-phase pressure drop

perturbation accounts for the vast majority of the initial single-phase pressure perturbation for density wave oscillations.

Finally, regarding loop oscillations, the staff has determined that TRACG has sufficient capabilities to model the phenomena as evidenced by calculations of the ESBWR startup trajectory, as well as calculations in Reference 25. The staff has also determined that the absence of low-frequency loop oscillations for calculations for full power is consistent with the neutron kinetic phenomena that occur for these conditions.

3.15.3 Core Stability

The procedure outlined in Section 8.1.2 of Reference 1 for calculating the core-wide decay ratio was studied using a separate perturbation with the TRACG code. The staff performed a calculation based on an inlet flow perturbation similar to that for the channel and regional decay ratio calculations. The purpose of predicting the transient response to any perturbation in these analyses is to determine the decay ratio for the reactor system. The neutronic and flow feedback mechanisms for any initial perturbation should result in very similar decay ratios given that once the system is excited at any particular location in the transfer function loop, the decay ratio is a measure of the cyclic propagation of that perturbation back through the entire feedback loop. As was stated before, a decay ratio of unity would represent a system whose feedback loop self-perpetuates the excitation to the system.

The purpose of the staff calculations for core stability are meant to verify that the prescribed procedure in Section 8.1.2 of Reference 1 does produce a characteristic response, that is, a response whose decay ratio and frequency can be produced by applying a different perturbation yet exciting the same feedback loop.

Using a TRACG model provided by GE, the staff calculated the core-wide decay ratio at the EOC using the following procedure:

• [[

]]

The transient response is depicted in Figure 4 of this SE. The resultant decay ratio and frequency agree with the results in Section 8.1.2 of Reference 1, in which a pressure perturbation was used. Based on the results of the analysis, the staff concurs with GE's choice of a pressure perturbation to the turbine inlet for calculating the core-wide decay ratio.

The staff also notes that to perform any stability test for the core-wide behavior in a real system, the physical experiment would be conducted by manipulating the pressure in the main steam lines via turbine control and bypass valves. This was the case for the Peach Bottom low decay ratio experiments. Based on the results of the independent analysis performed by the staff, the staff has found that either a flow or pressure perturbation will affect both the void profile and boiling boundary within the core, and hence initiate a density wave. Following the initial impulse, the same feedback mechanisms (namely void reactivity) are being driven by the propagation of density waves in the active core region—thus the decay of subsequent

oscillations is determined by the nature of the system and these interacting mechanisms independent of the initial excitation.

The results of the staff's independent calculations also confirm that the procedures described in Reference 1 are sufficient in detail to reproduce the results presented by GE.

3.15.4 LAPUR Calculations

Calculations were performed (see the enclosed TER) using the LAPUR frequency domain code (Reference 12). As noted in the enclosed TER, the LAPUR analyses support the stability results obtained with the TRACG code for ESBWR at nominal conditions. LAPUR was used to calculate decay ratios for core-wide, regional, and channel density wave instability modes. In all cases the decay ratios were very low, on the order of 0.1.

Further studies were performed to investigate the importance of modeling the ESBWR chimney. The chimney has a large effect on establishing the steady-state core flow. The LAPUR studies found, however, that once the steady-state core flow is established, the chimney has only a minor impact on unstable oscillations. Chimney friction had to be increased by a factor of 100 before a noticeable change in calculated decay ratio was observed, leading to the conclusion that modeling the chimney does not need to be very accurate to calculate the ESBWR stability performance.

3.15.5 Void Fraction Studies

Void fraction studies were performed (see the enclosed TER) by comparing the steady state void fraction profiles predicted by TRACG with a stand alone drift flux program, with RELAP5, and with TRACE. The standalone drift flux program includes the models for the drift flux parameters documented in Reference 2.

Overall the comparison between TRACG, RELAP5, TRACE, and the standalone drift flux model supports the TRACG void fraction profiles. Differences between the drift flux model and TRACG can be attributed to the incompressible two-phase flow assumptions in the drift flux model and the lack of virtual mass terms in the drift flux model.

3.15.6 Courant Number Studies

As described in Section 3.8 of this SE, additional terms in the Taylor series expansion associated with the finite differencing approximations cause numerical dissipation. When the Courant number is exactly one, these additional terms go to zero. The staff created a simple pipe model to investigate the effect of truncation errors in the TRACG solutions. This model was similar to that described in Appendix A of Reference 28. The staff's model consisted of a vertical pipe model with 24 equal mesh cell lengths of 6 in. (15.2 cm). The pipe was filled with water at 500K which flows upward at 6 ft/s (1.82 m/s). Isothermal and subcooled conditions were maintained at a pressure of 7.0 MPa. A sine wave perturbation was introduced to the inlet temperature, with a 25K amplitude change and a 2-second period. The minimum time step was set at a very small value and the maximum was set at a relatively large value such that the difference between the two was large and TRACG had to select a time step based on the value of the Courant multiplier. When the Courant multiplier was set to exactly 1.0, TRACG showed no dissipation, as demonstrated in Figure 5 of this SE. Figures 6 and 7 of this SE show that when the Courant multiplier was set to a value less than 1.0, there was, as expected, dissipation of the wave. The explicit method was used for the calculations shown in these three

figures. Figure 8 of this SE shows the difference when the implicit method is used. There is noticeable dissipation as compared to Figure 6, which has the same Courant multiplier. This demonstrates that use of the explicit method option and GE's process for nodalizing the core and setting the Courant multiplier to 1.0 are appropriate for minimizing numerical dissipation in a time domain code.

4.0 CONDITIONS

NEDE-33083P, Supplement 1, "TRACG Application for ESBWR Stability Analysis," has been approved by the staff with the following specific conditions:

1. The decay ratio methodology is applicable only to steady-state conditions and cannot be applied during a transient.
2. The decay ratio methodology may be applied for off-normal conditions that may occur after an AOO, once a steady-state condition is reached at the end of the transient. The steady-state condition analyzed should be limiting based on the power and flow conditions reached.
3. The channel decay ratio calculation will be performed using a limiting channel, which is specified based on high radial peaking and downward-biased axial power.
4. The startup stability analysis methodology may only be applied for the phase of startup prior to the ascension to full-power phase (nominally ~8 hours in duration).
5. The ascension to full power, as with all other transient xenon conditions, will be analyzed using the PANACEA transient xenon option and reviewed at the design certification stage.
6. The findings of the staff relate only to the acceptability of the TRACG code to perform stability analyses of the ESBWR and do not represent a final evaluation of the design.

The staff has reviewed GE's procedure for calculating the single-channel stability margin during normal operation. The staff has found that the procedure described in Section 8.1.1 of Reference 1 is acceptable for calculating the channel decay ratio. Therefore, a limiting channel stability analysis should first identify the hot superbundle. If the radial peaking factor is similar for all of the channels in the superbundle, the channel stability should be evaluated using the assembly in the hot superbundle with the limiting (i.e., most downward-biased) axial power shape. Reference 1 should be revised to explicitly state this selection criterion.

To ensure that TRACG is applied within its qualification basis for ESBWR stability, these calculations must follow the procedures outlined in Reference 1. These calculations must be reviewed to ensure that the following restrictions are satisfied:

1. The number of TRACG thermal-hydraulic regions (i.e., channel groupings) in the core must be greater than or equal to [[]]. The channel groupings must capture the variations in inlet orificing, radial power and harmonics, hot channels, and geometry effects (i.e., superbundles of 16 bundles associated with a single chimney). The procedures described in Sections 8.1.2.2 and 8.1.3 are adequate for demonstrating acceptable channel groupings.

2. The axial nodalization in the core must follow the scheme described in Section 5.2, "Effects of Nodalization."
3. The calculation of the channel decay ratio must follow the procedure defined in Section 8.1.1, "Channel Stability Results." The limiting channel must be identified based on a radial power peaking factor and a downward-shifted axial power shape.
4. The calculation of the core-wide decay ratio must follow the procedure defined in Section 8.1.2, "Core Wide Stability Results."
5. The calculation of the regional (out-of-phase) decay ratio must follow the procedure defined in Section 8.1.3, "Regional Stability Results."

5.0 CONCLUSIONS

The staff concludes, based on the above discussion, that TRACG, including the application methodology, is an acceptable evaluation model for ESBWR stability analyses as presented in NEDC-33083P, Supplement 1, "TRACG Application for ESBWR Stability Analysis." The staff therefore concludes that TRACG is acceptable for referencing during the design certification review of the ESBWR, provided the conditions specified in this safety evaluation are met.

If NRC's criteria or regulations change so that its conclusions about the acceptability of the report are invalidated, GE or the applicant referencing the report, or both, will be expected to revise and resubmit the respective documentation, or submit justification for the continued effective applicability of the report without revision of the respective documentation.

The staff notes that the uncertainties in the physics parameters will be addressed in the design certification review of the ESBWR. The methods employed for generating cross sections for TRACG were not considered part of the scope of the current review in which the void coefficient is a primary factor in determining core stability. Any potential changes in the uncertainties in nuclear parameters as a result of this subsequent review should be included in decay ratio acceptance criteria.

The staff also notes that GE will be submitting its fuel design for review by the staff as part of design certification. The staff expects GE to justify continued applicability of its methodology for evaluating stability by evaluating input parameters and uncertainties related to the fuel design to ensure that the methodology for evaluating stability is not affected. Should there be an effect such that conclusions about the acceptability of the stability methodology are invalidated, the staff expects GE to revise and resubmit its respective documentation.

The staff also notes that GE demonstrated that there were large CPR margins associated with the conditions used for evaluating stability, and, therefore, phenomena associated with the prediction of dryout and film boiling, cladding deformation, etc., are considered to be of low importance in GE's stability PIRT. GE will be submitting its CPR correlation as part of design certification. At that time, the staff expects GE to reanalyze the CPR margins for this application, and should there be significantly less margin than previously predicted, the staff expects GE to update its PIRT accordingly.

The staff has reviewed the information contained in Section 8.4 of Reference 1 and found that the TRACG stability methodology is suitable for evaluating stability margin once a steady-state condition is achieved but not during the transients listed.

GE has not provided any information on ATWS in support of this application. Therefore, stability during ATWS was not considered as part of this review, and approval of the TRACG code for stability analysis during startup and normal operation does not imply acceptance of TRACG for ATWS stability analysis.

The staff has reviewed Sections 9.0 through 9.3 of Reference 1 as well as the information provided in Reference 16 and determined that TRACG is capable of predicting a startup trajectory for the ESBWR with neutronic feedback. Therefore, the stability margin during startup should be evaluated by calculating the heatup rate at which there is an onset of instability during startup.

Based on the uncertainty analysis provided in Reference 1, the uncertainty of TRACG ESBWR decay ratio calculations is less than or equal to 0.2. Therefore, the following safety criteria are adequate, and they guarantee compliance with GDC 12.

- Core-wide decay ratio <0.8
- Channel decay ratio <0.8
- Regional (out-of-phase) decay ratio <0.8

The proposed TRACG procedures for calculation of ESBWR stability margins are best estimate for the expected conditions during the cycle. The most likely mode of instability is expected to be regional (out-of-phase). Therefore, to ensure compliance with GDC 10, the ESBWR reactor protection system must incorporate an approved detect and suppress function. The review and approval of this function will be the subject of a separate submittal.

The use of TRACG is acceptable to predict the ESBWR trajectory during the initial phases of startup up to the ascension to full-power phase. During this transient, a stability margin can be determined by increasing the heatup rate until the onset of instability. TRACG is not acceptable for predicting the startup transient during the ascension to full-power phase as xenon is not considered and insufficient information is provided in regard to the impact of the balance of plant. The staff is aware that PANACEA has an option for predicting transient xenon and that this option can be invoked for a startup calculation. The staff expects this to be done for the initial startup of the ESBWR to properly predict the margins during the ascension to full-power phase. The ascension to full-power phase of the startup will be the subject of a subsequent review by the staff during design certification.

The staff concludes that the TRACG thermal-hydraulic analysis code is capable of modeling the phenomena important to prediction of power/flow stability in the ESBWR design based on the evidence submitted by GE and the independent evaluations conducted by the staff.

The staff has determined that void formation is of high importance in neutronic stability, making prediction of void formation critical to the ability of a code to predict the behavior of a nuclear reactor.

The code has been shown to be reasonable in representation of void generation and transmission through comparisons between the TRACG void model, the TRACE (staff thermal-hydraulic analysis code) void model, the RELAP5 void model, and an independent drift flux model.

The staff conducted evaluations that show that the behavior of the chimney, an inherent feature of the ESBWR design, has a negligible impact on the neutronic stability of the reactor. The staff

performed independent analyses using the LAPUR frequency domain code to analyze an ESBWR model with and without a chimney. Essentially identical results were obtained with both models, indicating that the chimney does not have a significant effect on the neutronic stability of the ESBWR design.

The influence of the chimney was studied further by both GE and the staff through analyses using the TRACG code with various nodalization schemes for the chimney. Nodalization within appropriate limits found no appreciable influence due to chimney representation. The assumed nodalization must be reasonable and within appropriate guidelines such that instabilities are predicted or not predicted according to the phenomena affecting the design-specific stability and not because of numerical instabilities masquerading as neutronic instabilities. Violations of numerical analysis limits such as the Courant limit (limited by the node with the smallest $\Delta Z/V$) are known to create numerical instabilities. In addition, the nodalization can impact the time step size used in the code calculation, which also can affect numerical stability. While attempting to study the neutronic stability of a reactor design, numerical instabilities can lead to a faulty analytical conclusion.

The staff has further evaluated the numerical scheme used for integration of the differential equations describing the system behavior and found that the numerical solution scheme appropriately permits oscillation to occur and damp while not causing an oscillation to occur or damp. Thus, the damped oscillations observed in the test cases analyzed can be reasonably taken to be realistic representations of the response of the system being analyzed.

The dominant feature of power/flow stability analysis is that the process is a thermal-hydraulic driven neutronic problem. The TRACG code has adequate models to represent the thermal-hydraulic behavior of the system shown in the present as well as previous reviews conducted by the staff. In addition, the code has the necessary neutronic analysis models to represent the response of the nuclear fueled core. Finally, the numeric solutions capability is capable of permitting, while not causing, oscillations to occur and to correctly account for any system damping that may occur.

The Advisory Committee on Reactor Safeguards has reviewed the proposed use of TRACG and the staff's SE and recommends staff approval of TRACG for analysis of the stability of the ESBWR during normal operation, AOOs, and the low-power phase of reactor startup by letter dated April 21, 2006.

6.0 REFERENCES

1. General Electric Nuclear Energy, NEDE-33083P, Supplement 1, "TRACG Application for ESBWR Stability Analysis," December 2004.
2. General Electric Nuclear Energy, NEDE-32176P, Rev. 2, "TRACG Model Description," December 1999.
3. General Electric Nuclear Energy, NEDE-33083P-A, "TRACG Application for ESBWR," March 2005.
4. Safety Evaluation by the Office of Nuclear Reactor Regulation for NEDE-32906P, *TRACG Application for Anticipated Operational Occurrence (AOOs) Transient Analyses*, June 2002.

5. Letter to J. Klapproth, GE, from H. Berkow, NRC, "Review of GE Nuclear Energy Licensing Topical Report NEDE-32906P, Supplement 1, *TRACG Application for Anticipated Transient Without Scram Transient Analyses*, August 2003.
6. Letter to L. Quintana, GE, from W. Beckner, NRC, "Reissuance of Safety Evaluation Report Regarding the Application of General Electric Nuclear Energy's TRACG Code to ESBWR Loss-of-Coolant Accident (LOCA) Analyses," (NEDC-33083P-A, *TRACG Application for ESBWR*), October 28, 2004.
7. U.S. NRC, NUREG/CR-5249, "*Quantifying Reactor Safety Margins: Application of Code Scaling Applicability, and Uncertainty Evaluation Methodology to a Large-Break, Loss-of-Coolant Accident*," December 1989.
8. U.S. NRC, Draft Standard Review Plan, Section 15.0.2, "*Review of Analytical Computer Codes*," December 2000.
9. U.S. NRC, Regulatory Guide 1.157, "*Best-Estimate Calculations of Emergency Core Cooling System Performance*," May 1999.
10. S.S. Wilks, "*Determination of Sample Sizes for Setting Tolerance Limits*," *Ann. Math. Statistics*, Vol. 12, 1941.
11. H. Glaeser and R. Pochard, "*Review on Uncertainty Methods for Thermal Hydraulic Computer Codes*," "International Conference on New Trends in Nuclear System Thermohydraulics Proceedings," Volume I, Pisa, Italy, May 30 and June 2, 1994.
12. U.S. NRC, NUREG/CR-6696, "*LAPUR5.2 Verification and Users Manual*," February 2001.
13. General Electric Nuclear Energy, NEDE-32177P, "*TRACG Qualification*," Rev. 2, March 2000.
14. General Electric Nuclear Energy, NEDC-32992P, "*ODYSY Application for Stability Licensing Calculations*," October 2000.
15. Letter to J. Klapproth, GE, from S. Richards, NRC, "Review of NEDC-32992P 'ODYSY Application for Stability Licensing Calculation,'" April 20, 2001.
16. Letter from George Stramback to the NRC, "GE Responses to NRC Request for Additional Information Related to NEDE-33083P, Supplement 1, 'TRACG Application for ESBWR Stability Analysis,'" June 2, 2005.
17. General Electric Nuclear Energy, NEDC-33079P, Revision 1, "*ESBWR Test and Analysis Program Description*," March 2005.
18. D. L. Hetrick, "*Dynamics of Nuclear Reactors*," University of Chicago Press, Chicago, Illinois, 1971.
19. J. March-Leuba, "*Dynamic Behavior of Boiling Water Reactors*," PhD Dissertation, University of Tennessee, Knoxville, Tennessee, 1984.

20. J. March-Leuba and E. D. Blakeman, "A Study of Out-of-Phase Power Instabilities in Boiling Water Reactors," 1988 International Reactor Physics Conference, Jackson Hole, Wyoming, September 1988.
21. J. March-Leuba, "A Reduced-Order Model of Boiling Water Reactor Linear Dynamics," *Nuclear Technology*, 75, 15-22, October 1986.
22. J. March-Leuba, D.G. Cacuci, and R. B. Perez, "Nonlinear Dynamics and Stability of Boiling Water Reactors: Part 1—Qualitative Analysis," *Nuclear Science and Engineering*, 93, 111-123, 1986.
23. J. March-Leuba, D.G. Cacuci, and R.B. Perez, "Nonlinear Dynamics and Stability of Boiling Water Reactors: Part 2—Quantitative Analysis," *Nuclear Science and Engineering*, 93, 124-136, 1986.
24. U.S. NRC, NUREG/CR-6003, "Density-Wave Instabilities in Boiling Water Reactors," June 1992.
25. General Electric Nuclear Energy, NEDC-33080P, "TRACG Qualification for ESBWR," August 2002.
26. General Electric Nuclear Energy, NEDC-32725P, Revision 1, "TRACG Qualification for SBWR," Volumes 1 and 2, August 2002.
27. General Electric Nuclear Energy, NEDC-32956P, Revision 0, "TRACG User's Manual," February 2000.
28. SCIE-NRC-330-97, "BWR Stability Modeling with NRC Current Generation Thermal Hydraulic System Codes," October 1997.
29. General Electric Nuclear Energy, 26A6642AP, Revision 0, "ESBWR Design Control Document, Tier 2," Chapter 4: "Reactor," August 2005.
30. R. Lahey, F. Moody, "Thermal Hydraulics of a Boiling Water Nuclear Reactor," American Nuclear Society, 1977.
31. J.G.M. Andersen, J.C. Shaug, A.L. Wirth, "TRACG Time Domain Analysis of Thermal Hydraulic Stability Sensitivity to Numerical Method and Comparison to Data," paper presented at the Stability Symposium, Idaho Falls, Idaho, August 10-11, 1989.
32. Letter from David H. Hinds to the NRC, "GE Response to Stability RAI Number 17-ESBWR Chimney Nodalization," March 31, 2006.

This Figure is Proprietary

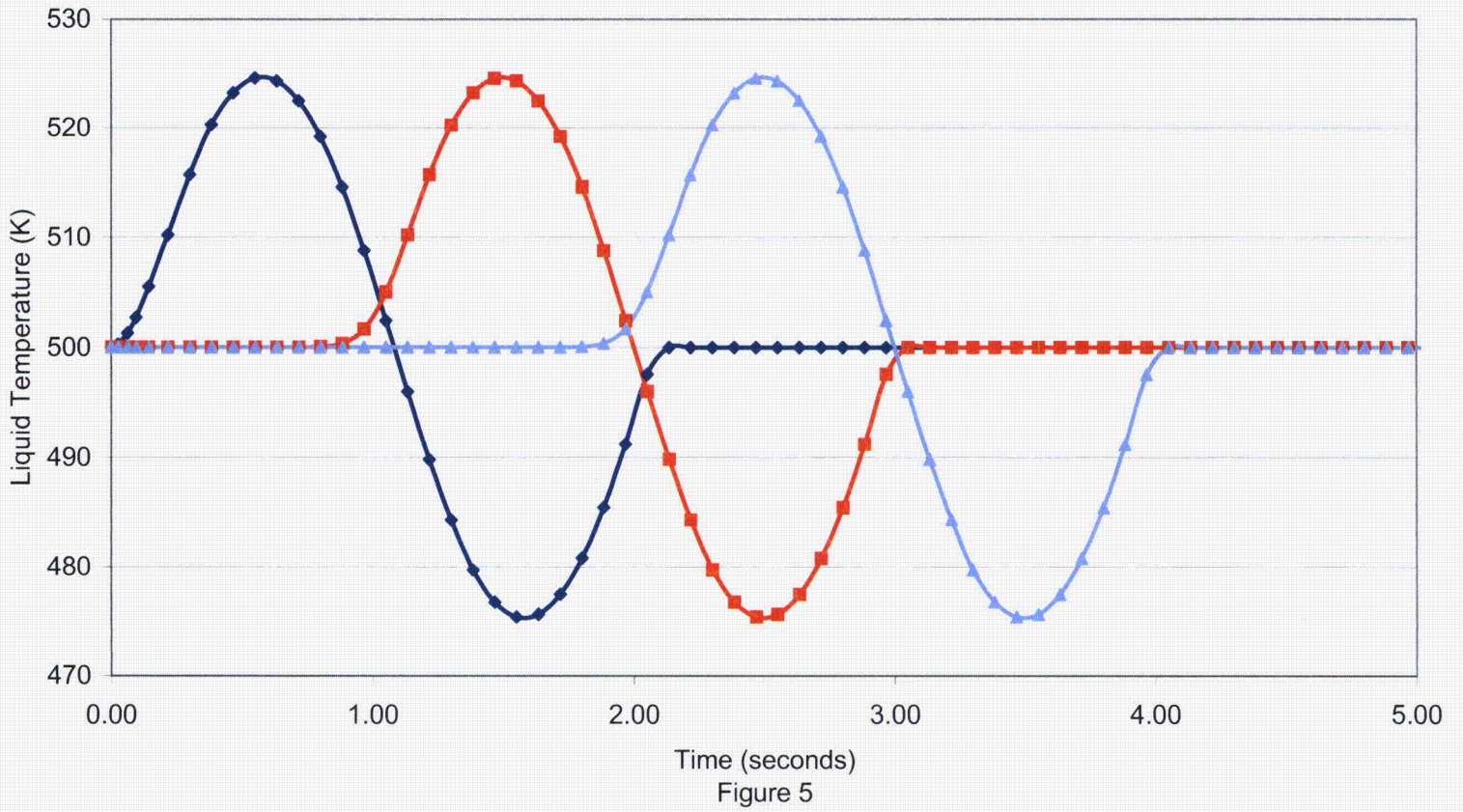
This Figure is Proprietary

This Figure is Proprietary

This Figure is Proprietary

TRACG Sine Wave Propagation
Courant Number 1.0

◆ Inlet ■ Midplane ▲ Outlet



TRACG Sine Wave Propagation
Courant Number 0.75

◆ Inlet ■ Midplane ▲ Outlet

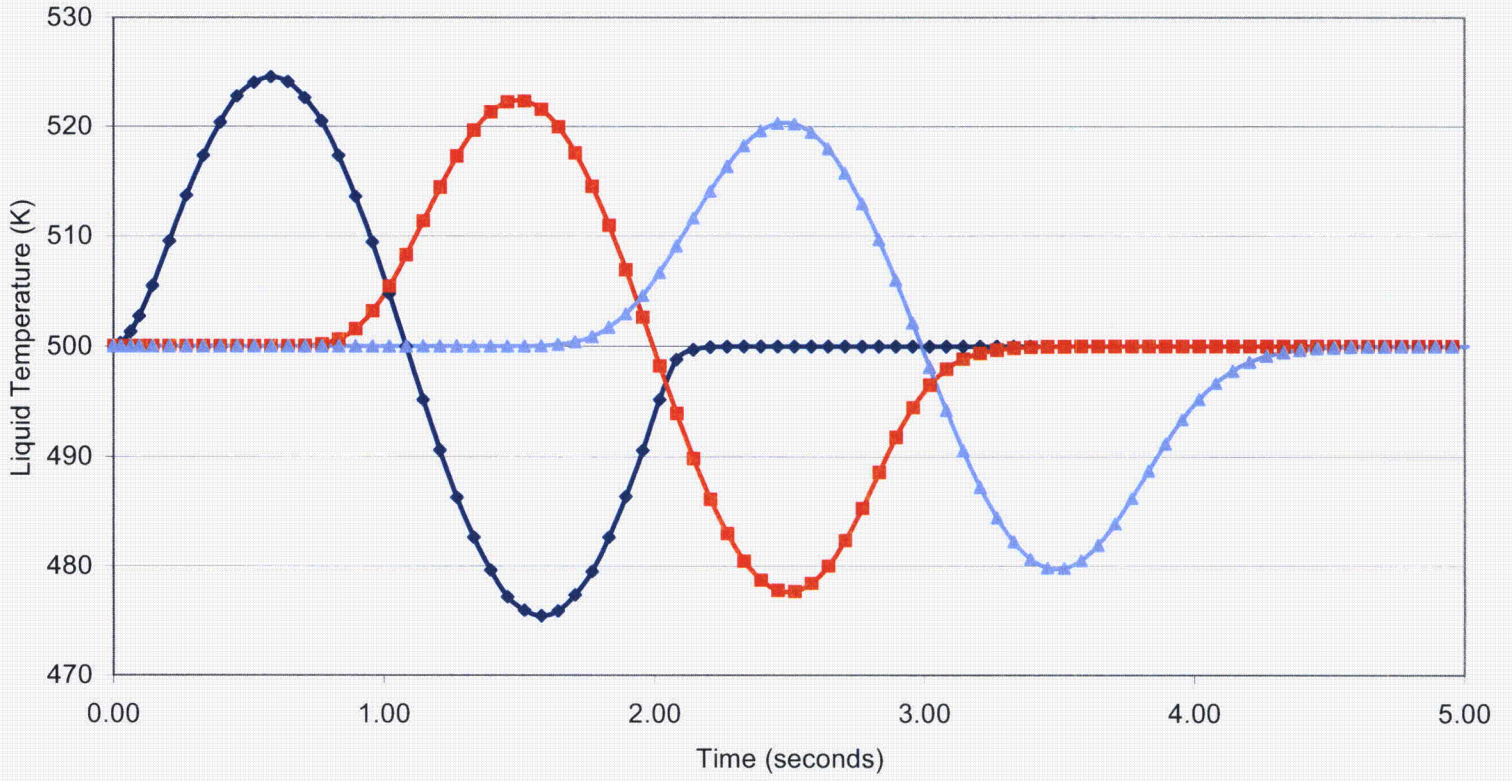
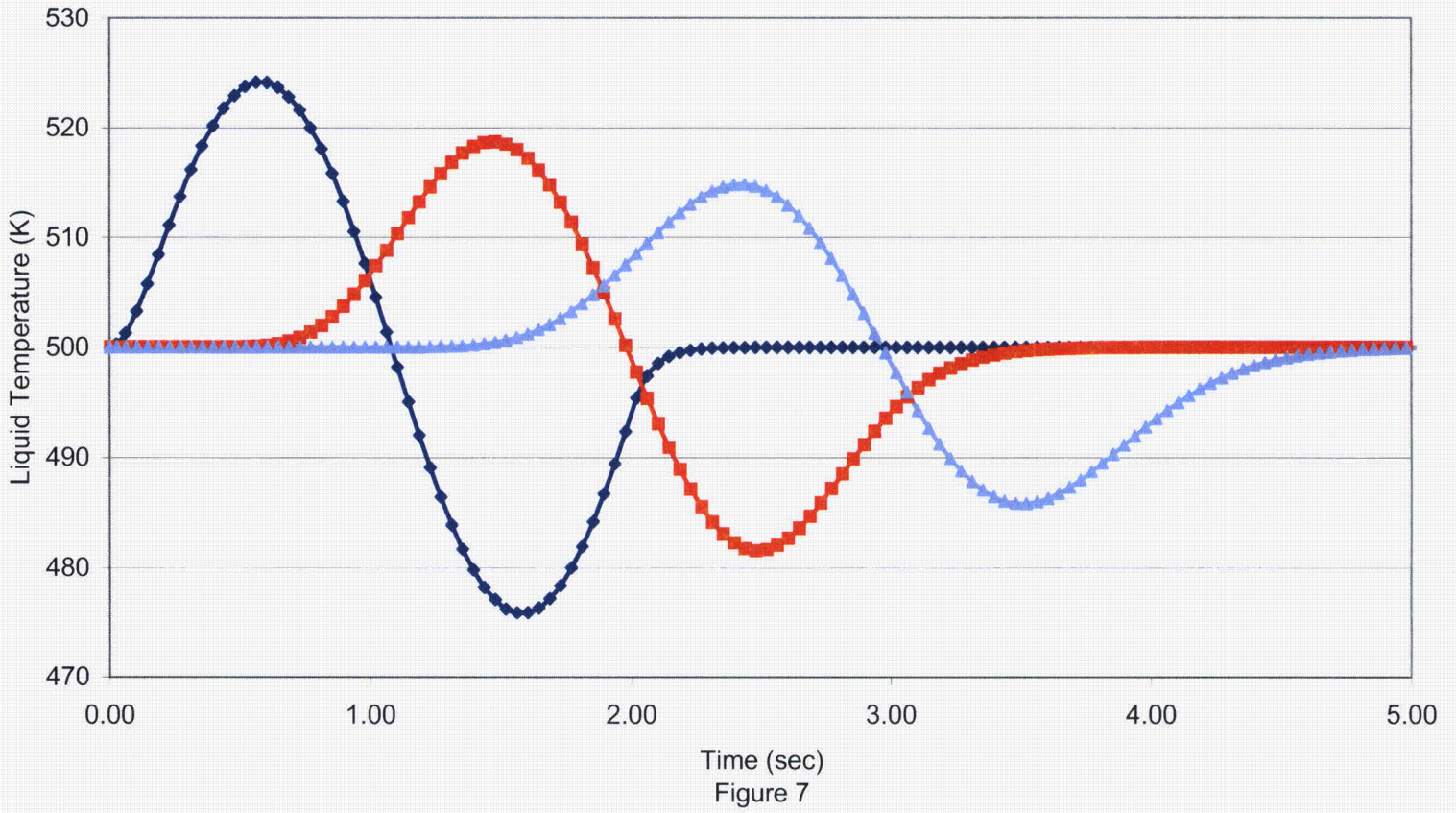


Figure 6

TRACG Sine Wave Propagation
Courant Number 0.25

◆ Inlet ■ Midplane ▲ Outlet



TRACG Sine Wave Propagation - Implicit Method
Courant Number 0.75

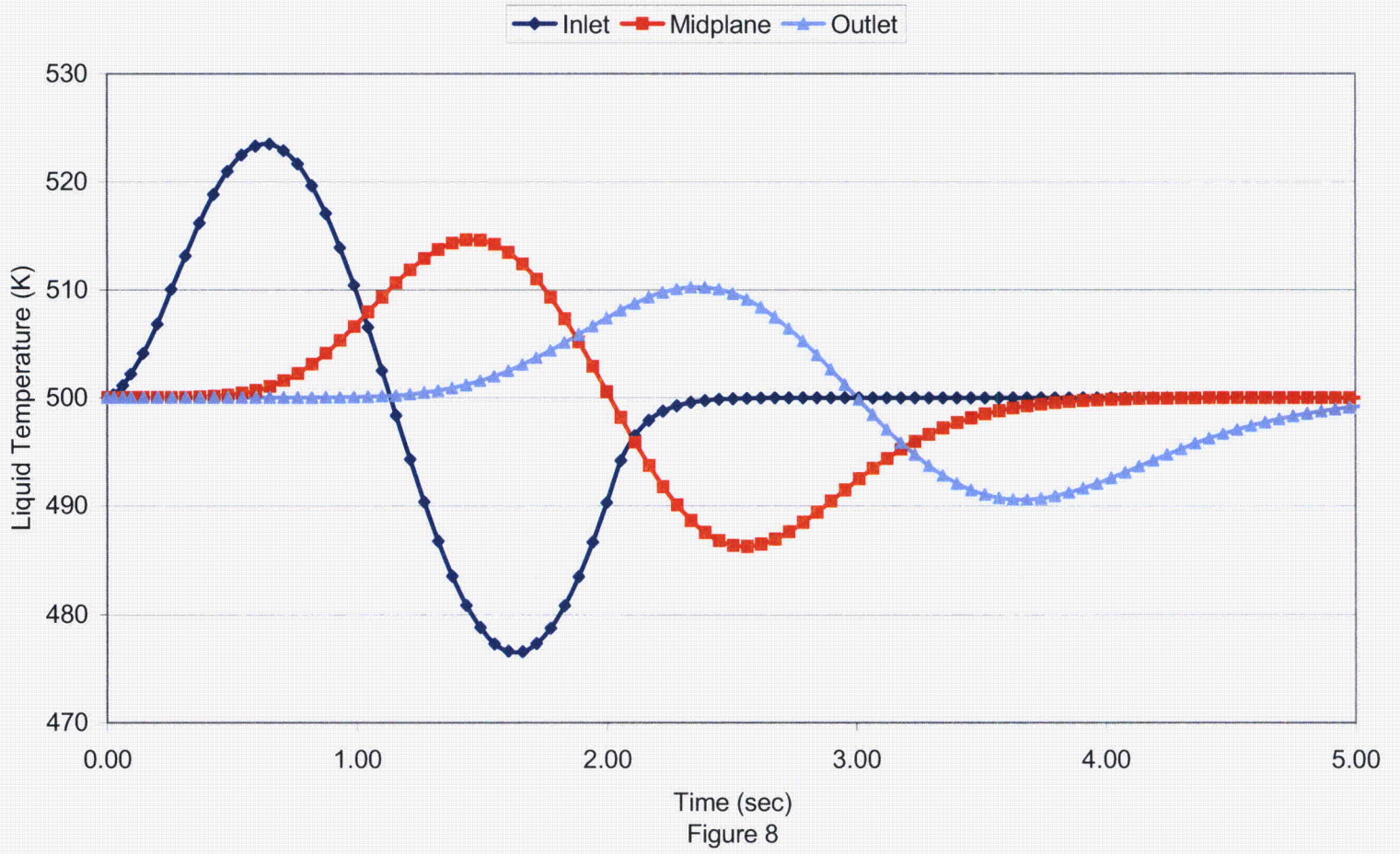


Figure 8

Review of NEDE-33083P, Supplement 1, December 2004

**TRACG APPLICATION FOR ESBWR STABILITY
ANALYSIS**

Jose March-Leuba

Oak Ridge National Laboratory

Jay W. Spore

Information Systems Laboratories

Table of Contents

Introduction.....	1
Summary and Major Conclusions.....	2
Detailed Review of LTR Sections	4
LTR Section 2 Licensing Requirements and Scope of Application	4
LTR Section 2.1 Licensing Compliance.....	4
LTR Section 2.2 Stability Design Criteria.....	4
LTR Section 2.5 Range of Application.....	5
LTR Section 3 Phenomena Identification and Ranking	6
LTR Section 4.0 Applicability of TRACG to ESBWR Stability Analysis.....	9
LTR Section 4.1 Model Applicability	9
LTR Section 4.2 Assessment Matrix	9
LTR Section 4.3 Other Topics Relevant To TRACG Modeling of Instability.....	13
LTR Section 4.4 TRACG Qualification against Peach Bottom Unit 2 Stability Data	14
LTR Section 5.0 Model Biases and Uncertainties.....	14
LTR Section 6.0 Application Uncertainties and Biases.....	15
LTR Section 8.0 Demonstration Analyses.....	15
LTR Section 8.1 Baseline Analysis	16
LTR Section 8.2 Sensitivities to High and Medium Ranked Parameters	17
LTR Section 8.4 Stability following AOOs.....	17
LTR Section 9.0 Plant Startup	17
LAPUR Confirmatory Calculations.....	20
LAPUR Results.....	20
Effect of Chimney Modeling	20
LAPUR Input Deck Description.....	21
References.....	22

Introduction

This Technical Evaluation Report (TER) documents our review of portions of NEDE-33083P, Supplement 1, "TRACG Application for ESBWR Stability Analysis" dated December 2004 (Reference 1), which documents General Electric's (GE) evaluation of the TRACG code for use on ESBWR stability calculations.

As stated in Reference 1, GE intends to use the TRACG code to calculate "stability margins during normal operation including anticipated transients." However, the procedure to estimate decay ratios using the TRACG code requires that the initial operating conditions are steady state, thus, it does not apply if the system is in a transient state. The TRACG code can be used to demonstrate that a particular transient is free from instability, but not to calculate its decay ratio during the transient. Stability margins for transients may be estimated with the TRACG code by re-running the code varying a parameter (e.g. core power) until an instability is observed.

In addition, Reference 1 states "TRACG is also used to analyze plant startup trajectories, to assure a smooth ascension in pressure and power with a minimum of flow oscillation" even though "stability during plant startup is not a licensing issue." While the conclusions of this review agree with the facts that (1) TRACG can be used to analyze the startup trajectory and (2) stability during startup is not likely to be a licensing issue, the scope of this review only covers the first statement (i.e., the technical capability of the TRACG code). The acceptability of the proposed startup procedures will be evaluated during design certification using the official ESBWR core design and parameters.

We must note that when we refer to TRACG in this report, we imply the TRACG code using the so-called "stability nodalization and methods." These methods are documented in Section 4.3 of Reference 1 "Other Topics Relevant to TRACG Modeling of Instability" and in Section 5.2 of reference 1 "Effects of Nodalization". They involve the use of explicit integration numerics in the channel component, as well as a fine nodalization scheme.

The scope of this review covers the evaluation of the capability of TRACG to calculate stability margins (i.e. calculating decay ratios), and demonstrating compliance with licensing limits for stability evaluation of the ESBWR during normal operations. Reference 1 and the scope of the review do not include instabilities that may result in dryout or post-CHF heat transfer (i.e. ATWS).

Summary and Major Conclusions

The primary goal of this review is to ascertain whether TRACG is capable of modeling ESBWR phenomena in order to calculate the ESBWR stability margins. Additional goals include a determination of the uncertainty of TRACG decay ratio calculations, and the development of acceptable stability criteria to be used for TRACG ESBWR calculations.

The conclusions from this review are:

1. The use of TRACG is acceptable to calculate the ESBWR stability margins during normal operation and at limiting steady state power and flow points during anticipated operational occurrences (AOO).
2. To ensure that TRACG ESBWR stability calculations are within the qualification basis, these calculations must follow the procedures outlined in Reference 1. These calculations must be reviewed to ensure that the following restrictions are satisfied
 - a. The number of TRACG thermal-hydraulic regions (i.e. channel groupings) in the core must be greater or equal than $[\]$. The channel groupings must capture the variations in inlet orificing, radial power and harmonics, hot channels, and geometry effects (i.e. super bundles of 16 bundles associated with a single chimney).
 - b. The axial nodalization in the core must follow the scheme described in Reference 1 Section 5.2 "Effects of Nodalization."
 - c. The calculation of the channel decay ratio must follow the procedure defined in Reference 1 Section 8.1.1 "Channel Stability Results."
 - d. The calculation of the core-wide decay ratio must follow the procedure defined in Reference 1 Section 8.1.2 "Core Wide Stability Results."
 - e. The calculation of the regional (out-of-phase) decay ratio must follow the procedure defined in Reference 1 Section 8.1.3 "Regional Stability Results."
3. The procedure documented in Reference 1 to calculate decay ratios using TRACG can only be applied to steady state operating conditions, not transients.
4. TRACG can be used to demonstrate that a particular transient (e.g. startup) is free from instability. TRACG can also be used to estimate the stability margin by repeating the transient calculation with different parameters until an instability is observed (e.g., different startup heat up rates)
5. Based on the uncertainty analysis provided in Reference 1, the uncertainty of TRACG ESBWR decay ratio calculations is less than or equal than 0.2. Therefore, the following safety criteria are adequate, and they guarantee compliance with GDC 12.
 - a. Core-wide decay ratio < 0.8

- b. Channel decay ratio < 0.8
 - c. Regional (out-of-phase) decay ratio < 0.8
6. The design acceptance criteria for ESBWR stability are design goals that ensure sufficient margin to unexpected occurrences and/or deviations from planned operation (e.g. fuel leaks that require repositioning of the control rods). The design acceptance criteria proposed in Reference 1, are adequate. The ESBWR design criteria are:
- a. Core-wide decay ratio < 0.4
 - b. Channel decay ratio < 0.4
 - c. Regional (out-of-phase) decay ratio < 0.4
7. The proposed TRACG procedures for calculation of ESBWR stability margins are best estimate for the expected conditions during the cycle. Deviations from these expected conditions will happen. In addition, the most likely mode of instability is expected to be regional (out-of-phase). Therefore, to ensure compliance with GDC 10, the ESBWR Reactor Protection System must incorporate an approved Detect and Suppress function. The review and approval of this function will be the subject of a separate submittal.
8. The use of TRACG is acceptable to demonstrate that the ESBWR response during startup procedures is adequate and free from instability.

Detailed Review of LTR Sections

LTR Section 2 Licensing Requirements and Scope of Application

LTR Section 2.1 Licensing Compliance

Two General Design Criteria (GDC) are typically associated with stability analysis. GDC 12 specifies that unstable oscillations must either be not possible or readily detected and suppressed. GDC 10 specifies that the reactor protection system must be capable of terminating any anticipated transients, including unstable power oscillations, without challenge to the fuel.

GE proposes to satisfy ESBWR Licensing Compliance with GDC 12 by demonstrating through TRACG analysis that instabilities are highly unlikely. Thus, compliance with GDC 10 must be demonstrated only for Anticipated Operational Occurrences (AOOs).

In addition to satisfying GDC 12 through analysis, GE proposes to include a detect and suppress (D&S) method to the reactor protection system as a backup. The details of this D&S method are not part of Reference 1, but should provide compliance with GDC 12 in the unlikely case that the analysis assumptions or methods are incorrect, and an instability develops.

The addition of the D&S protection backup allows the reduction of conservatism in the analysis. The proposed analysis methodology is essentially “best estimate”. The complete cycle is pre-calculated at the expected control rod patterns and the worst DR for the complete cycle is compared to the design criteria. In reality, unexpected occurrences happen. For example, a fuel leak would require a deviation from the predicted control rod pattern; thus, invalidating the best-estimate pre-calculation. GE proposes to deal with these unexpected occurrences not by adding conservatism to the calculation, but by adding the D&S protection backup and by using a very conservative design criterion. The proposed “ultimate” stability design criteria (See Section 2.2) are $DR < 0.8$ for all three modes (core-wide, out-of-phase, and channel); however, the design goals are to maintain all three $DR < 0.4$. By designing to a conservative DR, there would be sufficient margin to cover any unexpected operating condition.

The staff concurs with GE’s proposed Licensing Compliance approach. Designing to a conservative DR and adding a D&S protection backup satisfies the GDC 12 requirements.

LTR Section 2.2 Stability Design Criteria

TRACG calculations indicate that the Regional instability mode dominates the stability response of the reference ESBWR core. Staff confirmatory calculations with the LAPUR code exhibit a similar relation between the relative stability of the core-wide and regional modes in the reference ESBWR design. Thus, the margin to instability of the regional mode is a key design parameter for ESBWR. Stability margins for core-wide and channel instability, while relevant, are not as limiting for the reference ESBWR design, and they are not expected to be limiting for future design changes.

During the development of the Boiling Water Reactor Owners' Group (BWROG) Long Term Stability Solutions (LTS) in the early 1980's, a correlation was developed that attempted to bound all regional instability events observed to date within a region defined in the core-wide versus channel decay ratio. This correlation is sometimes called the "dog bite" correlation. With this methodology, the BWROG was able to circumvent a deficiency in their calculation methodology. At the time, no code was able to calculate the regional DR directly, so an approximate correlation was used.

Reference 1 recognizes that at least one ESBWR parameter is sufficiently different from operating reactors to require a modification of the dog-bite correlation. This parameter is the core diameter, which will result in a smaller eigenvalue separation for the first subcritical neutronic mode. Thus, the Reference 1 methodology proposes to modify in a conservative manner the dog-bite correlation to account for this difference. Other ESBWR design parameters may have similar effects, but we may not have sufficient operating/calculation experience to judge a priori what their effect on the ESBWR-specific dog-bite correlation may be.

Since TRACG is capable of directly calculating the limiting event (i.e., the regional DR), the staff believes that the TRACG ESBWR stability criteria should be based on calculated results, rather than an approximation that was developed based on operating-reactor experience.

In a letter to the NRC dated September 28, 2005 (Reference 2) GE has agreed with the staff position and modified the original stability design criteria, which was based exclusively on core-wide and channel decay ratio calculations ("dog-bite"). In Reference 2, GE proposes a stability criteria based on the following three criteria:

- Limiting channel decay ratio < 0.8
- Core decay ratio < 0.8 ;
- Regional decay ratio < 0.8

All these evaluations will be made at 95% content and 95% confidence, and the design goal will be to maintain the nominal values of the channel, core and regional decay ratios less than 0.4.

The staff concurs with these criteria.

LTR Section 2.5 Range of Application

Reference 1 states that, for this TRACG application, "the intended application is ESBWR stability analysis at normal operation including potentially more severe conditions resulting from AOOs".

To justify this application for ESBWR stability analysis at normal operation, GE has:

1. documented the methods and approximations used to model ESBWR with TRACG in normal operation,
2. performed a full CSAU analysis to determine the code applicability and expected uncertainties, and

3. performed demonstration stability analyses with a reference ESBWR design

Based on this analysis, the staff concurs that the range of TRACG applicability covers stability analysis at normal operation.

The applicability of TRACG to calculate safety parameters during Anticipated Operational Occurrences (AOO) is covered by a separate licensing topical report (LTR), "TRACG Application to ESBWR" NEDC-33083P" (Reference 3). The applicability of TRACG to ESBWR AOO's will be reviewed separately by the staff as part of ESBWR design certification. The application of Reference 1, as it pertains to AOOs is limited to predicting oscillations at more limiting power and flow conditions.

LTR Section 3 Phenomena Identification and Ranking

As part of the CSAU process, Reference 1 provides a phenomena identification and ranking table (PIRT) to delineate the important physical phenomena that impact the ESBWR decay ratio calculation by TRACG. The ESBWR stability PIRT is shown in Table 3.1-1 in Reference 1.

As stated in Reference 1, the PIRT serves a number of purposes. First, the phenomena are identified and compared to the modeling capability of the code to assess whether the code has the necessary models to simulate the phenomena. Second, the identified phenomena are cross-referenced to the qualification basis to determine what qualification data are available to assess and qualify the code models and to determine whether additional qualification is needed. Third, the High and Medium-ranked parameters are either varied over their uncertainty distributions or used at bounding values to obtain an overall uncertainty in the estimate of the safety parameters.

The following phenomena are identified as having high importance:

- [[

]]

- [[

-]]

The following phenomena are identified as having medium importance:

- [[

-]]

The following initial conditions or plant parameters were ranked as high or medium importance:

- [[
-
-
-
-
-
-

]]

- [[
-
-
-]]

In addition, the PIRT includes the following high importance derived parameters

- [[
-]]

[[

]]

TRACG simulations of ESBWR instabilities indicate a relatively large CPR margin. Therefore, phenomena associated with the prediction of dryout and film boiling, cladding deformation, etc. are considered to be of low importance. This implies that the application of TRACG to ESBWR instabilities is limited to normal operating conditions and certain steady state power and flow conditions resulting from an AOO and not to instabilities that may appear during an ATWS event or another transient that may result in dryout.

The core inlet subcooling that depends upon downcomer and feedwater flows and upon the mixing in the downcomer and lower plenum was not included in the PIRT for ESBWR instabilities. The implication is that the feedwater inflow is assumed to be well mixed in the downcomer and that the lower plenum is well mixed during instability transients. This assumption is valid at normal operating conditions and startup because core lower plenum stratification can be avoided during startup by operating the Reactor Water Cleanup/Shutdown Cooling System (RWCU/SDCS System) (References 4 and 5). Therefore this assumption may not be valid at low flow conditions in which there is lower plenum stratification or scenarios that involve cold water injection (such as injection of ECCS). Table 4.1-5a in Reference 6 lists the core inlet subcooling as a high importance parameter for ESBWR instabilities.

The PIRT is comprehensive, and it appears to give the appropriate rating to important stability phenomena.

LTR Section 4.0 Applicability of TRACG to ESBWR Stability Analysis

LTR Section 4.1 Model Applicability

TRACG is a two-fluid 1D and 3D thermal-hydraulic simulation tool that also includes the capability to do coupled thermal-hydraulic/3D transient neutronics analysis. The capabilities of TRACG in terms of the conservation equations solved, the correlations and models, the numerics, and the geometric modeling capability, are applicable to ESBWR instability analysis. The key phenomena identified in the ESBWR instability PIRT can be simulated with the TRACG computer code.

LTR Section 4.2 Assessment Matrix

The prediction of the important thermal-hydraulic phenomena for natural circulation and flow instabilities (i.e. void fraction, subcooled boiling, single phase and two-phase flow losses) has been assessed against separate effects tests, integral effects tests, and full plant data. The core void fraction assessments against FRIGG indicate that the fully developed nucleate boiling void fraction 1σ uncertainty is [[]] absolute voids, which is a very respectable level of uncertainty. For subcooled boiling, the uncertainty in void fraction increases to [[]] absolute voids. The increase in subcooled boiling uncertainty can be attributed to the [[]] uncertainty in the Saha-Zuber correlation for the prediction of the onset of subcooled boiling. The large diameter void data base (i.e. Ontario, Wilson, etc.) assessment indicates an uncertainty for the void fraction in the chimney of [[]] void. Pressure drop comparisons against full scale bundle data and separators indicate an overall uncertainty in the TRACG pressure drop models of [[]]. These two capabilities are the most important phenomena for the prediction of natural circulation flows. Specifically, the void fraction distribution and the pressure drop models are the dominant phenomena for determining natural circulation flows. Comparisons of TRACG with natural circulation flow rates in the SIRIUS test facility (Reference 7) indicate a bias of [[]] with a standard deviation of [[]]. Additional assessments for Dodewaard, CRIEPI, and PANDA are available in Reference 8 over a wide range of pressures, heat fluxes, and inlet subcoolings. The TRACG models and assessment indicate that TRACG can predict natural circulation flows and the uncertainty of these models can be propagated through a statistical model to determine the uncertainty in the final safety parameter (i.e. decay ratio). The dominant phenomena for natural circulation flow are modeled in TRACG and the accuracy is consistent with the available test data.

BWR power instability analysis involves density wave propagation, neutronics feedback via void coefficient, and fuel rod thermal response. Density waves propagate at the vapor velocity. Therefore, density wave propagation requires accurate void fraction profiles through the core and an accurate solution of the transient mass, energy, and momentum conservation equations and an accurate subcooled boiling model. The assessment of these models in Reference 7 indicates that TRACG accurately predicts density wave propagation and stability boundaries with a standard deviation of [[]] over a range of pressures, heat fluxes, and subcoolings. TRACG prediction of stability maps for CRIEPI at low pressure is also given in Reference 8.

The thermal-hydraulic modeling uncertainties given in Reference 1 were reviewed to determine consistency with available data and expectations. Reference 1 indicates the leakage path drill holes flow rate uncertainty is [[]], while the flow rate uncertainty for the side entry orifice and water rod orifice is [[]]. The leakage path drill holes represent 60% of the core bypass leakage flow and the flow through the finger spring leakage path represents 40% of the core bypass flow with an uncertainty of [[]]. The total estimated uncertainty for the core bypass flow is:

$$[[]] \quad (1)$$

If the leakage holes flow uncertainty was [[]] (i.e. similar to the side entry orifice (SEO) and water rod orifice), then the core bypass flow uncertainty would be:

$$[[]] \quad (2)$$

The [[]] uncertainty in the core bypass flow translates to a [[]] uncertainty in the core bypass flow loss. If the leakage path drill holes uncertainty was increased to [[]] giving the [[]] increase in core bypass flow, this would translate to a [[]] uncertainty in the core bypass flow loss. Therefore, it would not be a significant impact on the overall decay ratio uncertainty. GE also indicates in response to staff inquiries (Reference 9) there is prototypical data available that supports the [[]] uncertainty in leakage path drill holes flow rate and has been used in earlier submittals (Reference 10).

The important time scale for ESBWR power instabilities is the time required for a density wave to propagate through the ESBWR core. The time period for a BWR power instability has been found to be approximately twice the time required for a density wave to propagate through the ESBWR core. Calculated ESBWR frequency range is [[]] to [[]] depending upon the axial power profile (i.e. exposure) and whether the instability is core wide, hot channel, super bundle, or regional mode. Given a steady-state solution and the governing conservation equations, the density wave propagation time can be estimated by integrating the vapor velocity of a vapor particle transporting from the boiling boundary to the core exit:

$$L_b = \int_0^{t_p} V_g(z) dt \quad (3)$$

where,

L_b = Boiling length in the channel.

$V_g(z)$ = Vapor velocity, which is a function of the axial position and axial position is a function of time.

t_p = Transport time.

A standalone drift flux program for a single ESBWR channel was developed to estimate the steady-state void fraction and velocity profiles. The standalone drift flux program includes TRACG documented models (Reference 11) for the drift flux parameters and subcooled boiling. Based on this model the estimated density wave transport time for the ESBWR hot bundle is [[]] seconds, which implies an instability frequency of

[[]] Hz. This is slightly below the lower range of expected frequencies for the ESBWR. One explanation for the difference in transport times is the difference in void fraction profiles between TRACG and the standalone drift flux program. Comparison of the void fraction profile predicted by the drift flux standalone program to TRACG, TRACE (Reference 12), and RELAP5 (Reference 13) for the ESBWR hot channel is given in Figure 1.

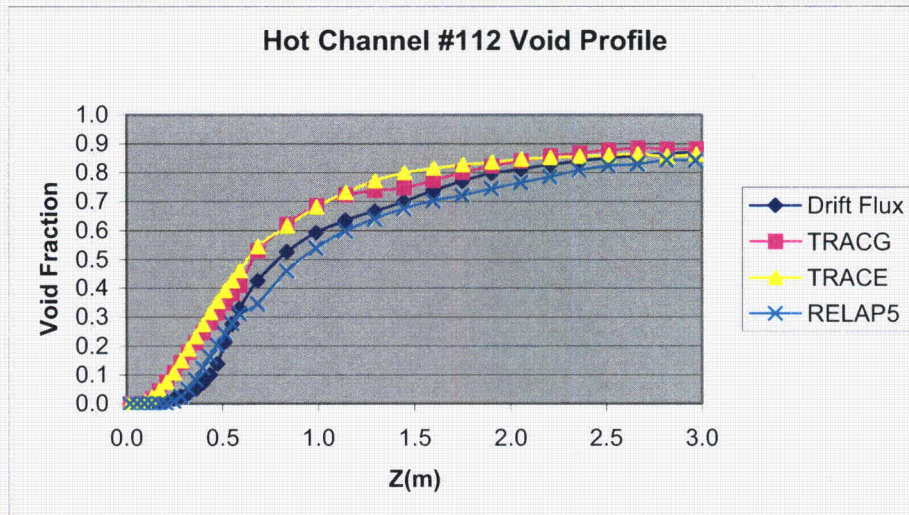


Figure 1. ESBWR Hot Channel Void Fraction Profile Predictions.

The TRACE models for subcooled boiling and bubbly flow and churn turbulent interfacial shear are similar to the TRACG models. Differences between the comparison of the drift flux model to TRACG and other codes are not significant given that the assessment of TRACG against bundle and large diameter void fraction data indicate that TRACG models are accurate.

Overall the comparison between TRACG, TRACE, and the standalone drift flux model supports the TRACG void fraction profiles. Differences between the drift flux model and TRACG can be attributed to the incompressible two-phase flow assumptions in the drift flux model and the lack of virtual mass terms in the drift flux model. RELAP5 is using a completely different interfacial shear package and is not expected to compare well with TRACE or TRACG.

The time period of oscillations for the SIRIUS test facility are greater than 10 seconds, while the time period of ESBWR power instabilities is [[]] seconds. There was a concern that the SIRIUS test facility was being used to support the TRACG power instability capability, when the time scales were significantly different.

The oscillations in the SIRIUS test facility are thermal-hydraulic and related to the transport time of density waves and enthalpy waves through the core and the chimney. For the ESBWR power instabilities in which power feedback is important, the time scale of importance is the density wave transport time through the heated core. The SIRIUS test facility data is used to assess the TRACG natural circulation and density wave propagation capabilities and is not intended to represent ESBWR power instabilities.

The important neutronics parameters for core wide and channel ESBWR power instabilities are void coefficient, delayed neutron fraction, direct moderator heating, exposure, and axial power profile. For regional ESBWR power instabilities the additional neutronics parameters are 3D neutron kinetics and the subcriticality of the first harmonic mode. For core wide and channel ESBWR power instabilities the void coefficient is the dominant parameter.

As a density wave with reduced void fraction propagates through a BWR channel, the void coefficient determines the increase in power associated with the increased neutron moderation. There is no operating data to compare for GE14 fuel design to assess the accuracy of the void coefficient models in TRACG. Reference 1 indicates that the estimation accuracy and uncertainty for the void coefficient is based on comparisons between the GE TGBLA04 code predictions and the Monte Carlo MCNP01 (Reference 14) predictions for 11 BWR bundle types, 9 different exposures and 3 different void fractions. This does provide a bias and uncertainty for the void coefficient that can be used in the TRACG statistical models to propagate the uncertainty to the final safety parameter calculation of the decay ratio. However, it assumes that MCNP01 results are an accurate representation of the BWR fuel assemblies. In addition, the 11 BWR bundle types do not include GE14 bundle design. Finally there is no uncertainty included in these analysis associated with actual nuclear isotope concentrations in the fuel rods at a given exposure. If we assume that:

1. the 11 BWR bundle types includes enough variability of the bundle designs, such that the GE14 bundle design is contained within that variability and
2. for a given set of nuclear isotope concentrations, MCNP01 accurately calculates the infinity multiplication factor,

then uncertainty in the actual nuclear isotope concentrations at a given exposure is still not included in this uncertainty analysis.

MCNP01 is an industry standard for the calculation of the k-infinity multiplication factor for nuclear fuel bundles and has a standard deviation of 0.00045 in the k-infinity values for the benchmark calculations that compare TGBLA to MCNP (Reference 9). The 11 BWR bundle types include a large variability of BWR bundle designs and the GE14 is expected to be contained within that variability. The uncertainty associated with exposure is addressed by performing stability calculations at BOC, MOC, and EOC.

The calculation of equilibrium cores at BOC, MOC, and EOC implies that a range of bundle exposures are analyzed. However, it is not obvious that the range of bundle exposures bounds the uncertainty associated with prediction of the nuclear isotopes associated with a given exposure.

Because of the radial pressure distribution across the top of the core and bottom of the chimneys, there is some sweep of the voids back into the top of the core bypass. There was a concern if the voiding of the bypass during instability resulted in additional uncertainty of the TRACG predicted 3D neutron kinetics.

The TRACG calculated sweep of voids back into the top of the core bypass does not propagate down to the heated region of the core. Therefore, there is no impact on the

neutronics associated with core bypass voiding during the ESBWR instability calculations.

The ESBWR baseline calculated channel decay ratio varies from $[\]$ to BOC to $[\]$ at EOC. There was a concern whether or not the channel decay ratio would be significantly different for a clean core before an equilibrium core has been established.

GE estimated that based on the reduced radial and axial peaking associated with an initial core, the ESBWR stability would be improved compared to an equilibrium core. An initial core design has not been finalized, but based on experience with other designs, there will be a reduction in the radial and axial peaking relative to an equilibrium core.

TRACG has been assessed for the dominant phenomena for ESBWR instabilities.

LTR Section 4.3 Other Topics Relevant To TRACG Modeling of Instability

In terms of numerics, the following four additional topics were identified:

1. Explicit integration scheme in the TRACG channel component.
2. Coupling of conduction solution with hydraulic solution.
3. Coupling of vessel component to channel components.
4. Coupling of 3D kinetics with thermal-hydraulic model.

The explicit integration scheme in the TRACG channel component was addressed in Reference 19 by comparing TRACG instability calculations with just the channel component using the explicit integration scheme with calculations where all fluid components in the model used the explicit integration scheme. The difference in calculated results were not significant. This implies use of the explicit integration scheme for the channel component for stability calculations is appropriate and acceptable. In addition, assessment of TRACG against FRIGG instability data also indicates that TRACG can accurately simulate BWR channel instability with the explicit integration scheme. In general, the fully implicit TRACG integration scheme results in additional damping in the numerical solution.

The coupling of the conduction solution with the hydraulic solution is acceptable for ESBWR instability calculations. Energy exchange between the heat structure conduction solution and the fluid component energy equation is consistent and energy is conserved consistent with the integration scheme.

The coupling of the vessel component to the channel components is acceptable for ESBWR instability calculations. Mass, energy, and momentum are conserved at the 3D mesh to 1D mesh cell faces consistent with the time level integration scheme (i.e. explicit or implicit).

Coupling of the 3D kinetics with thermal-hydraulic model involves an extrapolation of the 3D kinetics solution so that the new time fluid conditions can be calculated based on the estimated new time power levels. The 3D kinetics solution is then advanced based on feedback from the new time fluid conditions. There may be differences between the extrapolated 3D kinetics solution and the actual new time 3D kinetics solution. However,

TRACG uses changes in power, void fraction, etc. to control the time step size to ensure that these differences are not significant. Therefore, the coupling of the 3D kinetics with the thermal-hydraulic model is acceptable as demonstrated by the assessments against plant data.

LTR Section 4.4 TRACG Qualification against Peach Bottom Unit 2 Stability Data

TRACG decay ratio calculations have been qualified against results of the stability tests conducted at Peach Bottom 2 in April 1977. The reasons why GE chose the Peach Bottom tests are: (1) the availability of data, and (2) these tests were conducted at a low value of the decay ratio ($DR < 0.4$); the ESBWR is expected to operate under these low decay ratio conditions.

The results of the above benchmarks show that TRACG can calculate core-wide decay ratios for these types of very stable operating conditions. The standard deviation of the TRACG error in these benchmarks is smaller than the proposed 0.2 error to be used for the stability criteria (i.e., $DR < 0.8$ implies stability).

TRACG under-predicts the frequency of oscillation for the Peach Bottom tests, but this frequency under-prediction is common of most stability codes. GE states that the reason for the higher frequencies seen in the data has not been identified, but may be due to the method of extracting them from the transfer function.

The channel decay ratio was calculated by TRACG by introducing a [[]] inlet flow perturbation. The channel decay ratio is measured from the resulting core-inlet flow oscillation. Channel decay ratios were calculated for the Peach Bottom test conditions and results in very low values, as expected.

The regional stability mode is excited by perturbing [[

]]

The use of a pressure perturbation at the turbine inlet for the core-wide mode and flow perturbation for the channel and regional modes appear to yield good results to simulate instabilities. A sensitivity analysis was performed with different perturbation amplitudes and shapes. The results of this analysis indicate that the decay ratio results are not very sensitive to the amplitude or shape of the initial perturbation.

LTR Section 5.0 Model Biases and Uncertainties

GE has evaluated the model biases and uncertainties for all items from the PIRT table with a significant impact on the decay ratios. These items include all phenomena ranked High or Medium in the PIRT. Table 5.1-4 of Reference 1 documents the disposition of High and Medium ranked stability model parameters in the PIRT. This table shows the bias and standard deviation used for each of the PIRT phenomena to calculate the decay ratio uncertainty. The input uncertainties in Table 5.1-4 are reasonable; their numeric values are justified adequately in this section of Reference 1.

Section 5.2 of Reference 1 presents a study of the effects of nodalization on the calculated decay ratio. TRACG ESBWR stability analysis requires a specific nodalization scheme, which is described in Figure 5.2-1 of Reference 1. A fine axial nodalization is used in the core entrance to attempt to maintain a more constant Courant number (the core entrance velocity is slower than the core exit) and to provide more detailed modeling of the lower-void core regions, where void oscillations have the largest impact on stability. Radial nodalization involves collapsing the fuel bundles into approximately $[[\quad]]$ thermal-hydraulic channels. The proposed axial and radial nodalization has been used in the past for TRACG calculations of operating reactors' stability and has been found to be adequate for these calculations.

Section 5.3 of Reference 1 presents a study of the effects of scale. The key stability parameters and phenomena in ESBWR do not have significantly different scales than in operating reactors. In addition, full-scale tests have been performed on the channel components:

LTR Section 6.0 Application Uncertainties and Biases

Table 6.1-1 of Reference 1 documents the key plant initial conditions and their assumed error used for the uncertainty analysis. The magnitude of the errors used for the uncertainty analysis is well documented and the values are reasonable.

LTR Section 8.0 Demonstration Analyses

This section of Reference 1 describes the ESBWR TRACG modeling assumptions, and it documents the methodology used to calculate core-wide, channel, and regional (out-of-phase) decay ratios for ESBWR. In addition, this section of Reference 1 demonstrates:

1. TRACG is capable of modeling ESBWR stability phenomena
2. The reference ESBWR design satisfies the stability criteria proposed by GENE

The channel stability analysis is performed in TRACG by perturbing the flow to the high power channels while keeping the power constant. The calculation process is as follows:

1. $[[$
- 2.
- 3.
- 4.
- 5.
- 6.
- 7.

$]]$

The regional (out-of-phase) stability is evaluated in TRACG using a procedure very similar to the one used for the channel and core-wide stability above; however, it requires a “regional” channel grouping, [[

]] After establishing the channel groups, the decay ratio for regional oscillations is calculated using the following process:

1. [[
- 2.
- 3.
- 4.
- 5.
- 6.
- 7.

]]

To demonstrate the methodology, and to evaluate the stability of the ESBWR design, this methodology is applied in Reference 1 under baseline and steady state power and flow conditions associated with AOO conditions for Loss-of Feedwater Heater (LOFWH), which results in increased power; and Loss of Feedwater Flow (LOFW), which results in a lower flow. In addition, a sensitivity analysis to the High and Medium ranked phenomena identified in the PIRT was performed. The following sections document these results.

LTR Section 8.1 Baseline Analysis

This section of Reference 1 presents the stability results calculated by TRACG for the candidate ESBWR plant design, with 1132 bundles and a rated thermal power of 4500 MWt. This is intended as a demonstration of the applicability of TRACG to ESBWR stability analysis.

The TRACG ESBWR model includes [[]] thermal-hydraulic regions [[]]. An analysis was conducted at the various points in the cycle: Beginning of Cycle (BOC), Middle of Cycle (MOC) near the peak reactivity state, and End of Cycle (EOC). The core has a more pronounced bottom peak at BOC and is expected to be limiting for channel and regional stability. Decay ratios for core-wide stability are expected to be highest at MOC. Regional stability is strongly influenced by the sub-criticality of the higher order harmonics. The sub-criticality for the azimuthal mode ranges from [[]] at BOC to [[]] at EOC. The combination of the severe bottom peaking and lowest eigenvalue separation will result in the highest decay ratio for regional stability at BOC.

The above tendencies have been confirmed by both the TRACG and staff LAPUR calculations. Reference 1 shows the response of several channels to the perturbations (core-wide, channel, and out-of-phase), as well as the channel nodalization for core-wide and out-of-phase. The procedures defined in Reference 1 to generate the TRACG input cases model the relevant ESBWR physical phenomena with sufficient accuracy to yield good quality stability results.

LTR Section 8.2 Sensitivities to High and Medium Ranked Parameters

This section of Reference 1 presents the results of an analysis of the sensitivity of decay ratio results to the relevant input parameters identified in the PIRT. The maximum sensitivity is found to be related to the interfacial shear, as expected because it affects both void fraction and pressure drops. Figures 8.3-3 and 8.3-7 of Reference 1 show the results of the sensitivity analysis. They represent graphically the expected error in TRACG ESBWR calculations.

The results of these sensitivity analyses indicate that the TRACG ESBWR stability calculations are robust and, therefore, the TRACG results provide a reliable indication of the true ESBWR stability margin. The maximum decay ratio error for these sensitivity analyses was of the order of [[]], which is acceptable and justifies the use of the 0.2 calculation error criteria (i.e. $DR < 0.8$) proposed for use in ESBWR calculations

LTR Section 8.4 Stability following AOOs

Stability is a crucial design requirement for ESBWR because the rated power and flow conditions are the limiting conditions for stability during normal operation. However, following an AOO the power/flow conditions could be even more severe than at rated; therefore, AOO analyses must include an evaluation of stability. Two AOOs are identified in Reference 1 with potential to decrease the ESBWR stability margin: Loss-of-Feedwater Heater (LOFWH), which results in increased power; and Loss of Feedwater Flow (LOFW), which results in a lower flow.

The staff review concurs with GE's evaluation of the effects of AOOs on ESBWR stability margins. The two AOOs identified are the two likely scenarios that can reduce stability margins and, thus, must be analyzed during ESBWR licensing. Section 8.4 of Reference 1 documents the assumptions and procedures for these AOO analyses. TRACG is capable of modeling and predicting the resulting plant stability margins under these conditions.

LTR Section 9.0 Plant Startup

This review focuses on the capability of TRACG to model all the physical processes relevant to the stability of ESBWR. During normal operation, the stability mode of concern is the so-called density wave that produces flow and power oscillations with a frequency of 0.5 to 1 Hz. Because of its unique startup process, other instability modes are of concern during ESBWR startup. These instability modes include geysering instability and loop instabilities (also known as manometer or Type I instabilities). The TRACG capability of modeling both of these modes is described in Section 9 of Reference 1.

The startup process GE describes in Reference 1 for ESBWR involves the following steps

1. De-aerate coolant by pulling vacuum with mechanical pumps
2. Preheat coolant to 85C using either decay heat and/or auxiliary equipment (e.g. the reactor water cleanup system)
3. Isolate the primary at about 50 kPa by closing MSIV
4. Reach criticality by pulling control rods
5. The power is maintained constant at a low level (nominally 50 MW, but less than 85 MW) for a long period of time (3 to 7 hours)
6. When a pressure of 6.3 MPa is reached, the MSIVs are open, turbine is synchronized, and escalation to full power is achieved by pulling control rods.

The key in this startup procedure is maintaining a low-enough power during step 5 so that boiling occurs only in the top of the chimney and not inside the active core. Boiling occurs in the top of the chimney because of the difference of pressure due to elevation. As long as the power is low enough, subcooled boiling does not occur in the core while the pressure is low. By maintaining voids out of the core at low pressure, ESBWR prevents reactivity feedback issues, which could result in violent oscillations.

The above procedure was simulated with TRACG in Section 9 of Reference 1 and in the response to RAI 1 "Startup with Neutronic Feedback" (Reference 15). TRACG was capable of modeling this startup procedure.

The key difference as compared to normal operating conditions is the low pressure and low temperature. Thus, TRACG must be validated for these conditions, because thermal hydraulic instabilities tend to become more significant as the pressure is reduced, since the ratio of phase densities increases significantly as the pressure decreases. The assessment of TRACG models for void fraction is documented in Reference 8, and Reference 16. These qualifications cover a range of pressures down to 0.5 MPa and over a range of subcoolings as high as 38K. The TRACG models for void fraction have acceptable accuracy over a large range of conditions, however there is some indication that the uncertainty may increase as the pressure decreases. This is currently included in the overall uncertainty for TRACG void fraction predictions.

TRACG has been assessed in Reference 16 against ATLAS pressure drop data at 6.9 MPa, and FRIGG natural circulation data for a pressure range of 2 to 5 MPa. It has also been assessed in Reference 7 against SIRIUS natural circulation data down to a pressure of 2 MPa. Accurate comparison to natural circulation data requires both the capability to accurately simulate pressure losses as well as void fraction profiles. These comparisons indicate that the TRACG pressure drop models have acceptable accuracy over a range of pressures.

TRACG predicted the 1992 Dodewarrd startup within the accuracy of the available measurements. TRACG predicted relatively long time period manometer type oscillations associated with flashing in the chimney (i.e. not power oscillations associated with density wave transport times) that were not observed in the startup data, but would be difficult to detect with Dodewarrd instrumentation.

TRACG predicted thermal-hydraulic oscillations based on flashing in the CRIEPI chimney for pressures as low as 0.2 MPa and accurately predicts the stability map for this facility at low pressure. The long period oscillations were found to be related to manometer type oscillations associated with flashing in the chimney. CRIEPI has 1.8 m core and 5.5 m chimney. Similar oscillations were observed in PANDA, with 1.3 m core 9.5 m chimney at pressure 0.3 MPa. TRACG was also able to calculate these oscillations. As documented in Reference 7, TRACG accurately predicts stability map for SIRIUS test facility at 2 and 7.2 MPa.

Based on these assessments TRACG is capable of predicting instabilities during the proposed ESBWR startup. Therefore, we conclude that TRACG is an acceptable code to demonstrate during the design certification phase that the official ESBWR design and startup procedures are adequate and free from instability.

LAPUR Confirmatory Calculations

Confirmatory calculations were performed using the code LAPUR, V5.2 (Reference 17). Note that these calculations are not an exact replica of the TRACG analyses presented in Reference 1. These confirmatory calculations are intended to obtain an indication about the relative stability of the ESBWR design.

The major conclusion from these confirmatory calculations is that LAPUR confirms the stability results calculated by TRACG for ESBWR at nominal conditions. The LAPUR-calculated ESBWR decay ratios for all three density-wave instability modes (core-wide, out-of-phase, and channel) are very low (of the order of 0.1), indicating that the ESBWR has a high degree of stability.

LAPUR Results

LAPUR V5.2 was used to simulate the reference ESBWR nominal conditions at beginning and end of cycle. Typical LAPUR runs use quarter core symmetry and have four channels per thermal hydraulic region. The standard release of LAPUR V5.2 allows modeling up to 200 thermal hydraulic channels, which would cover all operating reactors. ESBWR is a special case, because 283 thermal-hydraulic regions are required to model a full quarter core. A simple modification to the LAPUR source code was implemented to allow for up to 512 thermal-hydraulic channels. This is a simple parameter change that was envisioned during the documentation and validation of Version 5.2. The new compiled code was benchmarked against the old code by using a 200-channel standard benchmark case used during the V5.2 validation.

Table 1 shows the results of LAPUR ESBWR modeling. As it can be observed, LAPUR predicts that the reference ESBWR nominal conditions are very stable.

Table 1. LAPUR Results for ESBWR at Nominal Conditions

	BOC		EOC	
	Decay Ratio	Frequency (Hz)	Decay Ratio	Frequency (Hz)
Core Wide	0.06	0.73	0.14	0.56
Out of Phase	0.11	1.00	0.08	0.66
Hot Channel	0		0	

Effect of Chimney Modeling

The LAPUR calculations indicate that the dynamic model used to simulate the chimney riser has little or no effect on the stability of the ESBWR.

The riser itself has a large effect on the core flow, but it has a very small friction pressure drop. However, once the core flow and power are fixed, the stability is not influenced by the presence of the chimney. So, the chimney plays a crucial role in setting up the steady state value of the core flow, but plays only a minor role during the unstable oscillations. This effect can be seen in

Table 2, where the results of a LAPUR calculation without chimney is reported. As seen in this table, the decay ratios calculated by LAPUR are not change by the presence of the chimney. Note: for this LAPUR calculation, the same core flow and core power was used as in the results in Table 1 - only the dynamic effect of the chimney is removed.

To ensure that LAPUR correctly models the chimney using the exit pipe component, we increased significantly the chimney friction and a change in the decay ratio was observed. The chimney friction had to be artificially increased by a factor of 100 before a noticeable change in calculated decay ratio was observed. We conclude that modeling of the chimney does not need to be very accurate to calculate the ESBWR stability performance. This conclusion is supported by the fact that the core exit void fraction is close to saturation (100%) and cannot change much when the flow oscillates. In addition, propagation time delay in the chimney allows for more than one void wave to be present, therefore the integrated buoyancy is small for oscillations at high frequency (~1 Hz).

Table 2. LAPUR Results for ESBWR without Chimney Model

	BOC		EOC	
	Decay Ratio	Frequency (Hz)	Decay Ratio	Frequency (Hz)
Core Wide	0.06	0.73	0.14	0.56
Out of Phase	0.11	1.00	0.08	0.66
Hot Channel	0		0	

LAPUR Input Deck Description

The complete LAPUR input decks (X & W) for the nominal ESBWR case are contained in a compact disk. Refer to Reference 17 for a description of the input deck cards. Here is a short description of the deck assumptions

1. This deck simulates the core with 283 thermal-hydraulic channels, which correspond to a one full quarter core. Each channel has its own axial power distribution as calculated with PANACEA (see Reference 18). The radial power distribution is modeled as full quarter core by specifying the channel powers calculated by PANACEA
2. LAPUR does not model partial-length fuel rods. The effect of the partial length rods is modeled by reducing the friction in the upper part of the core. The friction in the upper part of the core is ~73% lower than in the lower part (see card ID 36 and 37)
3. The chimney riser is modeled with LAPUR's exit pipe component (see card ID 46 to 52). With this approximation, each channel has its own riser, so there is no mixing at the core exit. This is a crude approximation, but justified by the fact that the chimney has very little effect on the density-wave instability.
4. The rest of the deck contains the standard core and fuel descriptions that would be used for any BWR in the fleet.

References

1. NEDE-33083P, Supplement 1, *TRACG Application for ESBWR Stability Analysis*, December 2004
2. Letter to the NRC from David Hinds (GENE) MFN 05-097, *Response to Action Items and RAIs Related to NEDE-33083P, TRACG Application for ESBWR Stability Analysis*, September 28, 2005
3. NEDE-33083P-A, *TRACG Application for ESBWR*, March 2005.
4. NEDC-33084P, *ESBWR Design Description*, August 2002, Page 2.4-24
5. *ESBWR Design Control Document, Tier 2, Chapter 4, Reactor* August 2005
6. NEDC-33079, Revision 1, *ESBWR Test and Analysis Description*, March, 2005
7. NEDC-33080P, *TRACG Qualification for ESBWR*, August 2002.
8. NEDC-32725P, Rev.1, Vol.1 and 2, *TRACG Qualification for SBWR*, August 2002
9. Letter to the NRC from David Hinds (GENE) MFN 05-146, *GE Response Request for Additional Information Letter No. 3 Related to NEDE-33083P, Supplement 1, "TRACG Application for ESBWR Stability Analysis,"* December 1, 2005
10. NEDE 23906P-A, Revision 1, *TRACG Application for Anticipated Operational Occurrences Transient Analysis*, April 2003
11. NEDE 32176P, Revision 2, *TRACG Model Description*, December 1999
12. J.W. Spore, et al, LANL document LA-UR-00-910, *TRAC-M/Fortran 90 (Version 3.0) Theory Manual*, March 2000
13. NUREG/CR-5535/Rev. 1, *RELAP5/MOD3.3 Code Manual Volume 1: Code Structure, System Models, and Solution Methods*, December 2001
14. J. F. Briesmeister, editor, *MCNP - A General Monte Carlo N-Particle Transport Code*, Version 4A, LA-12625, LANL, 1994
15. Letter to the NRC from George Stramback (GENE) MFN 05-052, *GE Response Request for Additional Information Related to NEDE-33083P, Supplement 1, "TRACG Application for ESBWR Stability Analysis,"* June 2, 2005
16. NEDE-32177P, Rev 2, *TRACG Qualification*, January 2000
17. NUREG/CR6696 *LAPUR5.2 Verification and Users Manual*, February 2001

18. Letter from Robert Gamble to NRC, MFN 04-077, *Additional Information on ESBWR Core Design – PANACEA Output Files*, August 9, 2004
19. Letter from George Stramback to NRC, MFN 05-133, *Responses to DSS-CD TRACG LTR RAls*, November 11, 2005

NRC Requests for Additional Information (RAIs) and GE Responses

RAI No.	NRC RAI Letter	GE Response Letter
1	MFN 05-008	MFN 05-052
2	MFN 05-008	MFN 05-052
3	MFN 05-008 MFN 05-085	MFN 05-052 MFN 05-097 [Revised Response to RAI 3 per MFN 05-085]
4	MFN 05-008	MFN 05-014
5	MFN 05-008	MFN 05-014
6	MFN 05-008	MFN 05-014
7	MFN 05-008	MFN 05-014
8	MFN 05-008	MFN 05-014
9	MFN 05-086	MFN 05-097 MFN 06-009 [Supplementary Information for RAI 9 per MFN 05-097]
10	MFN 05-136	MFN 05-146 MFN 05-146, Supplement 1 [Re-submittal with Correct Proprietary Designation]
11	MFN 05-136	MFN 05-146 MFN 05-146, Supplement 1 [Re-submittal with Correct Proprietary Designation]
12	MFN 05-136	MFN 05-146 MFN 05-146, Supplement 1 [Re-submittal with Correct Proprietary Designation]
13	MFN 05-136	MFN 05-146 MFN 05-146, Supplement 1 [Re-submittal with Correct Proprietary Designation]

NEDO-33083-A, Supplement 1, Revision 1

RAI No.	NRC RAI Letter	GE Response Letter
14	MFN 05-136	MFN 05-146 MFN 05-146, Supplement 1 [Re-submittal with Correct Proprietary Designation]
15	MFN 05-136	MFN 05-146 MFN 05-146, Supplement 1 [Re-submittal with Correct Proprietary Designation]
16	MFN 05-136	MFN 05-146 MFN 05-146, Supplement 1 [Re-submittal with Correct Proprietary Designation]
17	MFN 06-101	MFN 06-098

References:

1. MFN 05-008: NRC Letter from Amy E. Cubbage to Dr. Robert E. Gamble, GE, "Request for Additional Information Letter No. 1 Related to NEDE-33083P, Supplement 1, *TRACG Application for ESBWR Stability Analysis*," dated February 3, 2005.
2. MFN 05-014: GE Letter from Robert E. Gamble to NRC Document Control Desk, "GE Responses to NRC Request for Additional Information Related to NEDE-33083P, Supplement 1, *TRACG Application for ESBWR Stability Analysis*," dated February 22, 2005.
3. MFN 05-052: GE Letter from George Stramback to NRC Document Control Desk, "GE Responses to NRC Request for Additional Information Related to NEDE-33083P, Supplement 1, *TRACG Application for ESBWR Stability Analysis*," dated June 2, 2005.
4. MFN 05-085: NRC Letter from Amy E. Cubbage to Dr. Robert E. Gamble, GE, "Summary of Meeting Held on July 12, 2005, to Discuss Pre-Application Review Submittal Regarding the Application of the TRACG Code to ESBWR Stability (NEDC-33083P)," dated August 10, 2005.
5. MFN 05-086: NRC Letter from Amy E. Cubbage to Dr. Robert E. Gamble, GE, "Request for Additional Information Letter No. 2 Related to NEDE-33083P, Supplement 1, *TRACG Application for ESBWR Stability Analysis*," dated August 15, 2005.
6. MFN 05-097: GE Letter from David H. Hinds to NRC Document Control Desk, "Response to NRC Request for Additional Information Related to NEDE-33083P, *TRACG Application for ESBWR Stability Analysis*," dated September 28, 2005. [Revised Response to RAI 3 per MFN 05-085]

NEDO-33083-A, Supplement 1, Revision 1

7. MFN 05-136: NRC Letter from Amy E. Cabbage to Mr. David Hinds, GE, "Request for Additional Information Letter No. 3 Related to NEDE-33083P, Supplement 1, *TRACG Application for ESBWR Stability Analysis*," dated October 27, 2005.
8. MFN 05-146: GE Letter from David H. Hinds to NRC Document Control Desk, "GE Response to NRC Request for Additional Information Letter No. 3 Related to NEDE-33083P, Supplement 1, *TRACG Application for ESBWR Stability Analysis* (TAC #MC8168)," dated December 1, 2005.
9. MFN 05-146, Supplement 1: GE Letter from James C. Kinsey to NRC Document Control Desk, "GE Response to NRC Request for Additional Information Letter No. 3 Related to NEDE-33083P, Supplement 1, *TRACG Application for ESBWR Stability Analysis* (TAC #MC8168) Proprietary Designation," dated May 4, 2007. [Re-submittal with Correct Proprietary Designation for RAIs 10 through 16]
10. MFN 06-009: GE Letter from David H. Hinds to NRC Document Control Desk, "Supplementary Information for RAI No. 9 Related to NEDE-33083P, Supplement 1, *TRACG Application for ESBWR Stability Analysis*," dated January 10, 2006. [Supplementary Information for RAI 9 per MFN 05-097]
11. MFN 06-098: GE Letter from David H. Hinds to NRC Document Control Desk, "GE Response to Stability RAI Number 17 – ESBWR Chimney Nodalization," dated March 31, 2006.
12. MFN 06-101: NRC Letter from Amy Cabbage to Mr. David H. Hinds, GE, "Request for Additional Information Letter No. 4 Related to NEDE-33083P, Supplement 1, *TRACG Application for ESBWR Stability Analysis*," dated March 30, 2006.

RAI 1 [MFN 05-008]

Startup with Neutronic Feedback

The TRACG ESBWR startup simulations provided in NEDE-33083P, Supplement 1, do not include neutronic feedback. Even though core void generation occurs late in the transients analyzed (when the pressure is significant), the calculations shown are not conclusive because the void feedback could conceivably result in large power oscillations when coupled to operator actions to maintain the reactor at power.

Please provide a TRACG simulation of ESBWR startup that includes the neutronic feedback. Use the limiting heat up rate. Describe in detail the control model used to simulate operator actions to maintain the reactor at power during the startup transient.

RAI 1 Response [MFN 05-052]

A TRACG simulation of ESBWR startup with the neutronic feedback was performed using the limiting heat up rate. In this analysis, the 269 control rods are divided into 10 groups. The grouping of these control rods and the withdrawal sequence during the startup are similar to those used for operating plants. Results of this simulation have demonstrated that at the limiting heat up rate, no difficulties and no large power oscillations were encountered during the start up transient.

This TRACG calculation was performed with the activation of the 3D kinetics model. The calculation was initiated at the end of the de-aeration period with the steam dome pressure at 0.52 bar and RPV water at 82 C, similar to those calculations documented in NEDE-33083P, Supplement 1. The water level was maintained near the top of the separators. The MSIVs were closed to isolate the RPV. Initially, all control rods are in fully inserted position.

The 269 control rods in ESBWR are divided into 10 groups and the rod group positions are shown in Figure RAI 1-1. Rod Group # 10 represents the control rods for the 25 control cells. The grouping of control rods and the withdrawal sequence during the startup are similar to those used for operating plants. The withdrawal speeds for each of these groups during the transient are specified as TRACG input to simulate the operator actions to maintain the reactor at power during the startup transient. These rod groups are slowly withdrawn to maintain the total reactivity close to 0.0 and the total power level is maintained at around []MW until the RPV pressure reaches [] Subsequently, the MSIVs are opened and the power level is increased in steps (by means of additional rod withdrawals) to achieve rated pressure at []

Figure RAI 1-2 shows the withdrawal fraction for all control rods. Groups 1, 2 and 3 are fully withdrawn in 720 seconds. With these 3 groups at fully withdrawn position, the control rod withdrawal fraction is 0.37, i.e., 67% of all rods are in fully inserted position. At this time, the total reactor reactivity (Figure RAI 1-3) becomes greater than 0.0 (critical). Groups 4 and the next several groups are withdrawn with slower speed to avoid rapid change in total reactivity and reactor power.

Figure RAI 1-4 shows the total reactor power. For the first 1500 seconds, the total reactor power consists mainly of decay heat (~ 20 MW). []

]] The total reactivity varies around 0.0 and the total power variation around 85 MW is the result of the continuous withdrawal of the control rods. The power is controlled below 150 MW, until the MSIVs are opened. No significant core void is calculated until the MSIVs are opened at 12900 seconds, when the temperature and pressure are near the operating conditions. The heatup rate for this case is 53 C/hour, which is slightly below the maximum allowed rate considering thermal stress of 55 C/hour.

Figure RAI 1-5 shows the steam dome pressure response for this case. The RPV pressurizes to 6.3 MPa in 3.6 hours (12900 seconds) and the MSIVs are opened. With the MSIV open the power is limited by BOP systems not by heatup rate. The control rods are withdrawn further to step up the power and to reach the rated pressure at 4.4 hours. At this time, Rod Groups 1 to 7 are fully withdrawn and Group 8 is 50% withdrawn. Groups 9 and 10 (25 control cell rods) are in fully inserted position. The control rod withdrawal fraction is 0.73.

Figure RAI 1-6 shows the core inlet subcooling as a function of time. The local inlet subcooling drops from an initial value around [[]] as the system pressurizes to 6.3 MPa. The core flow transient response is shown in Figure RAI 1-7. There are two periods with small flow noise: around 2000 s corresponding to the step increase in power (Figure RAI 1-4) and around 4500 seconds corresponding to some void initiation at the top of separators (Figure RAI 1-8). Steady void fraction is established at the top of the separators after 9000 s. There are no fluctuations in the neutron flux during these periods. The flow result is similar to the case with no reactor kinetics modeled.

Figure RAI 1-9 shows core void in the highest power bundles. Vapor generation begins at the top of the high power bundles at 4500 s. At this time the pressure is about 5 bar. Voids propagate to cell 30 at about 11000 s, by which time the system pressure is above 30 bar. Figure RAI 1-10 depicts the exit flows in the high power bundle. This trace follows the core average flow response shown in Figure RAI 1-7. Figure RAI 1-11 shows the exit flows in the peripheral bundles. The peripheral bundles are in upflow throughout the transient.

Margins to thermal limits (CPR) were calculated for this startup case. The thermal margin for the high power bundles is shown in Figure RAI 1-12. Large margins are maintained throughout. Figure RAI 1-13 is the corresponding plot for the peripheral bundles. Again, large margins are maintained throughout the transient.

[[

]]

Figure RAI 1-1 ESBWR Control Rod Groups for Startup Simulation

[[

Figure RAI 1-2 Withdrawal Fraction for all Control Rods

]]

[[

Figure RAI 1-3 Total Reactivity

]]

[[

Figure RAI 1-4 Reactor Power

]]

[[

Figure RAI 1-5 Steam Dome Pressure

]]

[[

Figure RAI 1-6 Core Inlet Subcooling

]]

[[

Figure RAI 1-7 Core Inlet flow

]]

[[

]]

Figure RAI 1-8 Separator Void Fraction

[[

]]

Figure RAI 1-9 Hot Bundle void Fraction

[[

Figure RAI 1-10 Hot Bundle Exit Flow

]]

[[

Figure RAI 1-11 Peripheral Bundle Exit Flow

]]

[[

Figure RAI 1-12 Hot Bundle CPR

]]

[[

Figure RAI 1-13 Peripheral Bundle CPR

]]

RAI 2 [MFN 05-008]

ODYSY Calculation

Provide a frequency domain ODYSY calculation for ESBWR beginning of cycle (BOC) conditions. Provide a comparison between the channel, core-wide, and out-of-phase decay ratios calculated by ODYSY and TRACG.

RAI 2 Response [MFN 05-052]

ODYSY is a GE frequency domain code that has been approved by the NRC for channel and core wide stability evaluations [1]. The NRC has not reviewed the application of ODYSY for out-of-phase stability calculations. Background on this application is provided below.

GE is not seeking approval for the ODYSY code for ESBWR stability analysis. Calculations were performed with ODYSY specifically to respond to the RAI for channel, core wide and out-of-phase regional decay ratios.

ODYSY Model Outline:

ODYSY defines an open loop transfer function of the reactor, which can be used to evaluate stability characteristics. The major components are defined using first-principles governing equations. A small perturbation from steady-state is assumed and the effect on each component model is evaluated by linearizing the governing equations. A Laplace Transform of each perturbation response is performed and transfer functions are constructed to relate model output to perturbations in the input variables. Once the open loop transfer function is assembled, its frequency response is calculated. The frequency response is used to determine the decay ratio of the system at those conditions.

The major components of the reactor core model are the neutronics model, fuel heat transfer model, and thermal-hydraulic model. Multiple parallel channels are allowed by the model. A one-dimensional axial neutronics model is employed. The recirculation loop external to the core models the thermal-hydraulics in the upper plenum, separators, downcomer and lower plenum. The steam lines and control systems are not modeled as part of the stability evaluation but are accounted for in the system initial conditions.

For the out-of-phase mode decay ratios, a point kinetics solution is employed and the open loop transfer function and decay ratio is calculated for each harmonic mode with its associated subcriticality. The decay ratio calculated for the fundamental mode with zero subcriticality corresponds to the core-wide mode. This method follows the approach first proposed by March-Leuba [2]. The core-wide decay ratios obtained with the 1-D and point kinetics models are compared and serve to support the weighting of the neutronic parameters in the point kinetics model.

Neutron Kinetics for Regional Oscillations - Higher Harmonic Modes

The regional mode of instability excites a higher order mode of the neutronics equations. The higher harmonic modes are subcritical at steady-state operating conditions. However, under certain conditions, these modes can be excited because of the transient core thermal hydraulics. To evaluate regional stability, the reactor transfer functions are calculated for the harmonic modes as well as for the fundamental mode. This section discusses the form of the neutronic equation to be solved for the harmonic modes of the neutronics.

The one-group space-time dependent neutron kinetics equation can be written as:

$$\frac{1}{v^*} \frac{\partial \phi(r,t)}{\partial t} = (F(r,t) - L(r,t))\phi(r,t) - \sum_{n=1}^N \frac{\partial C_n(r,t)}{\partial t} \quad (2-1)$$

$$\frac{\partial C_n(r,t)}{\partial t} = \beta_n F(r,t)\phi(r,t) - \lambda_n C_n(r,t)$$

where $L(r,t)$ is the destruction operator and $F(r,t)$ is the production operator.

$$F = \frac{\Sigma_1}{\Sigma} \cdot \frac{K\Sigma}{\mu_0} \quad (2-2)$$

$$F - L = \frac{\Sigma_1}{\Sigma} \left(\frac{K_\infty \Sigma}{\mu_0} - DB^2 - \Sigma \right)$$

The destruction and production operators are time dependent because of void and Doppler feedback effects. These operators are denoted as a sum of a time-independent steady-state part and a time-varying transient part as follows:

$$L(r,t) = L_0(r) + \delta L(r,t) \quad (2-3)$$

$$F(r,t) = F_0(r) + \delta F(r,t)$$

The neutron flux $\phi(r,t)$ and delayed neutron precursor density $C_n(r,t)$ can be expanded into infinite series of harmonic modal components:

$$\phi(r,t) = n_0 \phi_0(r) + \sum_{m=1}^{\infty} n_m(t) \phi_m(r) \quad (2-4)$$

$$C_n(r,t) = \frac{c_{n,0} \phi_0(r)}{v^*} + \sum_{m=1}^{\infty} \frac{c_{n,m}(t) \phi_m(r)}{v^*}$$

where $n_m(t)$ and $c_{n,m}(t)$ are time-dependent expansion coefficients of the different flux density modes ϕ_m . n_0 and $c_{n,0}$ are the amplitudes of the steady-state neutron flux and neutron precursor concentration, respectively.

The lower order spatial harmonics can be approximated by the static λ -modes [3].

$$L_0(r)\phi_m(r) = \frac{1}{\lambda_m} F_0(r)\phi_0(r) \quad (2-5)$$

where λ_m is the m^{th} lambda mode eigenvalue. The subcritical reactivity associated with the m^{th} harmonic mode is defined as:

$$\Delta\rho_m = \text{eigenvalue separation} = \frac{1}{\lambda_m} - \frac{1}{\lambda_0}$$

where λ_0 is the largest (fundamental) eigenvalue.

The eigen functions are orthogonal, such that:

$$\langle \phi_m^+, F_0 \phi_j \rangle = \int_{\text{Core}} \phi_m^+(r) F_0(r) \phi_j(r) dr = V_1 \delta_{mj} \quad (2-6)$$

$$\langle \phi_m^+, \frac{\phi_j}{v^*} \rangle = \int_{\text{Core}} \phi_m^+(r) \frac{\phi_j(r)}{v^*} dr = V_2 \delta_{mj} \quad (2-7)$$

where ϕ^+ is the adjoint neutron flux, V_1 and V_2 are normalizing factors and δ_{mj} is the Kronecker delta.

Substituting Equations (2-3) and (2-4) into Equations (2-1), multiplying by the adjoint flux and integrating over the reactor core yields the modal point kinetics equations. The orthogonality relationships Equations (2-6) and (2-7) have been used in this process.

$$\frac{dn_m(t)}{dt} = -\frac{\Delta\rho_m + \beta}{\Lambda_m} n_m(t) + \sum_{n=1}^N \lambda_n c_{n,m}(t) + \frac{\rho_{m0}(t)}{\Lambda_m} n_0 + \sum_{j=1}^{\infty} \frac{\rho_{mj}(t)}{\Lambda_m} n_j(t) \quad (2-8)$$

$$\frac{dc_{n,m}(t)}{dt} = \frac{\beta_{ni}}{\Lambda_m} n_m(t) - \lambda_n c_{n,m}(t)$$

where the intermodal reactivity, $\rho_{mj}(t)$, and Λ_m are defined as:

$$\rho_{mj}(t) = \frac{\langle \phi_m^+, (\delta F - \delta L)(r, t) \phi_j \rangle}{\langle \phi_m^+, F_0 \phi_m \rangle} \quad (2-9)$$

$$\Lambda_m = \frac{\langle \phi_m^+, \frac{\phi_m}{V^*} \rangle}{\langle \phi_m^+, F_0 \phi_m \rangle} \quad (2-10)$$

The last term in Equation (2-8) for the neutron density contains a summation of an infinite number of nonlinear terms coupling the mth order harmonic with all other harmonics. In the linear approximation, this cross product is neglected.

For regional oscillations, we are concerned with the first azimuthal harmonic mode; if we set m=1, the inter-modal reactivity and subcritical reactivity become:

$$\rho_{10}(t) = \frac{\langle \phi_1^+, (\delta F - \delta L)(r, t) \phi_0 \rangle}{\langle \phi_1^+, F_0 \phi_1 \rangle} \quad (2-11)$$

$$\Delta\rho_1 = \text{eigenvalue separation} = \frac{1}{\lambda_1} - \frac{1}{\lambda_0} \quad (2-12)$$

For one-group diffusion theory, the neutron flux is self-adjoint. Thus, $\phi_1^+(r) = \phi_1(r)$, and the reactivity is weighted by the product of the fundamental mode flux and the first harmonic mode flux normalized by the square of the first harmonic mode flux.

Application to ODYSY

By linearizing, Laplace transforming and combining Equations (2-8), we get the neutronics transfer function as:

[[

]]

Here ρ_{10} represents the weighted inter-modal reactivity for the first azimuthal mode given by Equation 2-11, and $\Delta\rho_1$ is the eigenvalue separation between the fundamental and first harmonic modes, given by Equation 2-12.

Channel Grouping and Data Averaging

Stability analysis with ODYSY is performed by dividing the core into a number of thermal-hydraulic channel 'groups'. This grouping of fuel channels is based on similarities in thermal-hydraulic characteristics, as well as their location in the core and the relative power level. (ESBWR has only GE14 fuel). In particular, for the analysis of harmonic modes, the product of

the fundamental mode neutron flux and the harmonic mode neutron flux is used to differentiate channel groups. A typical regional stability analysis may employ up to 19 channel groups. Sensitivity studies on channel grouping have been performed, which show that 19 groups are sufficient to characterize BWR cores. A special option in PANACEA calculates the higher mode flux solutions and provides the harmonic flux distribution and eigenvalue separation.

In order to use Equation (2-13) for the neutronics transfer function, it is necessary to compute the core integrated values ρ_0 and λ_1 from Equations (2-11) and (2-10).

[[

]]

ODYSY Results

As requested, ODYSY analysis was performed at BOC for a core power of 4500 MWt. The same PANACEA wrapup file as used for the TRACG analysis was used as the basis for the nuclear parameters for the core wide stability analysis. The initial conditions used for the analysis are shown in Table 2-1. The grouping of the channels by power level is shown in Figure 2-1 for core wide analysis and in Figure 2-2 for regional mode analysis.

The open loop transfer function between channel flow and pressure drop for channel stability is shown in Figure 2-3. The margin to stability is evaluated from the shortest distance from $(-1, 0j)$ to the OLTF locus. The channel decay ratio was calculated to be

[[
]] Because the channel ratio is very low, the precision in its determination is low and the agreement is acceptable.

The open loop transfer function for core-wide stability is shown in Figure 2-4. This model uses the standard 1-D neutronics model in ODYSY based on radial weighting of

nuclear data from PANACEA. The transfer function represents the response in feedback power to a perturbation in core power. The core decay ratio obtained from this transfer function is [[

]] The agreement is good.

The regional stability analysis employs a point kinetics model. The capability to perform rigorous weighting of the PANACEA neutronic parameters through a data processing code is not available, so an approximate approach has been used as discussed in the previous section. [[

]]

Results for the OLTF for the first harmonic are shown in Figure 2-7. [[

]]

The values calculated by TRACG for the regional mode are a decay ratio of [[

]]

The TRACG and ODYSY results for channel, core and regional stability are compared in Table 2-2.

Sensitivity Studies

There is a substantial difference between the corrected and uncorrected void coefficient for the point kinetics application. As a sensitivity study, the regional stability calculation was repeated with the uncorrected fit. The results are shown in Figure 2-8. The decay ratio increased to [[

]]. These results are closer to the TRACG results. In any case, the TRACG results bound the uncertainty in the ODYSY void coefficient.

Sensitivity studies were also made to explore the reason for the low channel decay ratios. The channel grouping corresponding to the regional mode analysis was used for the study. The key parameter here is the ratio of single-phase to two-phase pressure drop. The ESBWR channel has a higher ratio (0.50) relative to standard BWR fuel because of the shorter overall length and a proportionately longer region above the part length rods. This ratio was progressively decreased by increasing the spacer and upper tieplate losses. Figure 2-9 shows the results for the channel decay ratio. The single-phase to two-phase

pressure drop ratio was decreased all the way to 0.23, which produced a channel decay ratio of [[]]. The regional decay ratio was also evaluated as the pressure distribution was changed. There was a corresponding increase in the regional decay ratio, driven by the dominant channels. As the single-phase to two-phase pressure drop ratio was decreased all the way to 0.23, the regional decay ratio increased to [[]] (Figure 2-10). These trends indicate that the low channel decay ratio is tied to the high single-phase to two-phase pressure drop ratio for the ESBWR bundles, which in turn leads to a low regional decay ratio.

Table 2-1 : Initial Conditions for ODYSY Analysis

[[

]]

Table 2-2 : Comparison of ODYSY and TRACG Results
 Core Power = 4500 MWt; Peak Channel Power = 5.10 to 5.13 MW; BOC

[[

						TRACG

]]

[[

]]

Figure 2-1: ODYSY Channel grouping for Core Wide Analysis

[[

]]

Figure 2-2: ODYSY Channel Grouping for Regional Stability Analysis

[[

Figure 2-3 Channel Transfer Function

]]

[[

Figure 2-4 Core Transfer Function

]]

[[

Figure 2-5 Comparison of 1D and Point Kinetics Results

]]

[[

Figure 2-6 Original and Corrected Fits for Void Reactivity

]]

[[

Figure 2-7 Transfer Function for First Harmonic Mode

[[

]]

Figure 2-8 Harmonic Mode Sensitivity to Void Coefficient

]]

[[

Figure 2-9 Sensitivity of Channel Decay Ratio to Pressure Distribution

[[

Figure 2-10: Sensitivity of Regional Decay Ratio to Pressure Distribution

References:

1. J. S. Post and A. K. Chung, "ODYSY Application for Stability Licensing Calculations", NEDC-32992P-A, July 2001.
2. J. March-Leuba and E.D. Blakeman, "A Mechanism for Out-of-Phase Power Instabilities in Boiling Water Reactors", Nucl. Sci. Eng., 107, p. 173 , 1991.
3. K. Hashimoto, "Linear Modal Analysis of Out-of-Phase Instability in Boiling Water Reactor Cores", Ann. Nucl. Energy, 30, No.12, pp.789-797, 1993.

RAI 3 [MFN 05-008] [MFN 05-085]

TRACG Calculation of Instability Threshold

Perform a series of TRACG steady-state calculations at BOC conditions with increasing powers until unstable power oscillations develop to demonstrate the power-margin to instability.

RAI 3 Response [MFN 05-052] [MFN 05-097 (Revised Response per MFN 05-085)]

Starting with the rated core design at 4500 MWt at BOC conditions, control rods were withdrawn to increase the core power level. The inserted rods were pulled out uniformly in steps to increase the core power to 5000, 5200 and 5400 MWt. The last power level is higher than the thermal scram point. At each power level, a steady state was established. Channel and core wide stability was evaluated at each state by observing the response to a perturbation from the steady state. These calculations were made using the same process followed for the calculations shown in the Licensing Topical Report. Even at 5400 MWt, TRACG calculated a substantial margin to instability. Regional stability evaluations were also made at an elevated power of 5200 MWt, slightly below the scram power level. The regional decay ratio was found to be well below 1.0 at this power level.

The details of the calculations are provided below. The results of the calculations are summarized in Table RAI 3-2.

The initial conditions for the three elevated power levels are shown in Table RAI 3-1. The corresponding axial power shapes for the average and peak power bundle are shown in Figures RAI 3-1 to RAI 3-3. Stability analysis was performed at the higher power levels using the same techniques employed in the report NEDE-33083 Supplement 1. Channel decay ratios were evaluated by perturbing instantaneously the velocities in the inlet single-phase region of the bundle. Core decay ratios were evaluated by perturbing the steamline pressure and observing the core power response. For regional stability, channels on either side of the axis of symmetry of the harmonic flux shape were perturbed in opposite directions and the channel power responses were evaluated.

The channel stability results are shown in Figures RAI 3-4 through RAI 3-6. The decay ratio increased from [[

]]

The core wide power responses to pressure perturbations are shown in Figure RAI 3-7 through RAI 3-9. The core decay ratio was of the order of [[

]]

For the regional analysis, calculations were made at 5200 MW to see if instability in the regional mode would occur at a lower power than the scram power level. The harmonic flux shape for the core at 5200 MW is shown in Figure RAI 3-10. The products of the fundamental and harmonic flux shapes are shown in Figure RAI 3-11. Based on these, the channel grouping shown in Figure RAI 3-12 was developed. This is slightly different from the one used at 4500 MW in the report because of differences in the rod pattern harmonic flux shape. Regional stability was then evaluated by perturbing the inlet velocities to the channel groups in opposite directions on the two sides of the line of harmonic symmetry. Figure RAI 3-13 shows the power response for two channel groups on opposite sides of the line of symmetry, confirming the

NEDO-33083-A, Supplement 1, Revision 1

regional mode of the perturbation. Figure RAI 3-14 shows the response of several channel groups on the same side of the line of symmetry. The maximum decay ratio is [[]].

Table RAI 3-1: Initial Conditions at Higher Power Levels

[[

]]

Table RAI 3-2: Stability Results at Higher Powers

[[

]]

[[

Figure RAI 3-1 Axial Power Profiles for Average and Peak Bundles at 5000 MW

[[

]]

Figure RAI 3-2 Axial Power Profiles for Average and Peak Bundles at 5200 MW

]]

[[

Figure RAI 3-3 Axial Power Profiles for Average and Peak Bundles at 5400 MW

[[

]]

Figure RAI 3-4 Channel Flow Response to Inlet Velocity Perturbation (5000 MW)

]]

[[

Figure RAI 3-5 Channel Flow Response to Inlet Velocity Perturbation (5200 MW)

[[

]]

Figure RAI 3-6 Channel Flow Response to Inlet Velocity Perturbation (5400 MW)

]]

[[

Figure RAI 3-7 Core Power Response to Pressure Perturbation (5000 MW)

[[

]]

Figure RAI 3-8 Core Power Response to Pressure Perturbation (5200 MW)

]]

[[

Figure RAI 3-9 Core Power Response to Pressure Perturbation (5400 MW)

[[

]]

Figure RAI 3-10 First Harmonic Flux Shape at 5200 MW

]]

[[

]]

Figure RAI 3-11 Product of the Fundamental and First Harmonics (5200MW)

[[

]]

Figure RAI 3-12 Channel Grouping for Regional Analysis at 5200 MW

[[

Figure RAI 3-13 Channel Power Response – Channels on Opposite Sides of Line of Symmetry]]

[[

Figure RAI 3-14 Channel Power Response – Channels on Same Side of Line of Symmetry]]

RAI 4 [MFN 05-008]

3D Power Distribution

Please provide the 2D (channel powers) and 3D power distributions for BOC, middle of cycle (MOC), and end of cycle (EOC) in electronic format.

RAI 4 Response [MFN 05-014]

The 2D and 3D power distributions for BOC, MOC and EOC are contained in file MFN 05-014 2D&3D Power Dist. Xls on the enclosed CD.

RAI 5 [MFN 05-008]

Subcritical Mode Power Distribution

Please provide the 2D and 3D power distributions for the calculation shown in Figure 8.1-5 of the first subcritical mode at BOC conditions in electronic format. Also, please provide a short description of the calculation tools used for this calculation.

RAI 5 Response [MFN 05-014]

The 2D and 3D power distributions for the first harmonic mode (Figure 8.1-5) are contained in the file: MFN 05-014 RAI Harmonic Shape.xls on the enclosed CD.

A description of calculational tool for the calculation of the harmonic flux shapes is provided below:

Calculation of Harmonic Modes of the Neutron Flux Distribution

The HARMONICS module in PANAC11 has been developed to support the analysis of BWR stability. The module has the ability to generate harmonic modes of the neutron flux distribution.

The method used is based on the well-known Gram-Schmidt orthogonalization process. Let A represent the diffusion operator and let ϕ_i be the i -th eigenfunction of the diffusion operator corresponding to the eigenvalue λ_i . Then,

$$A\phi_i = \lambda_i\phi_i \quad \text{Eq. (1)}$$

The eigenfunctions of this operator form a complete orthonormal set. Therefore,

$$\langle \phi_i, \phi_j \rangle = \delta_{ij} \quad \text{Eq. (2)}$$

For this solution, the inner product is defined as the summation over all nodes in the core. This is not strictly correct, since it does not account for the spatial variation of the flux within each node, but it does a very good approximation. Any function, ψ , may be expanded in terms of ϕ_i as

$$\psi = \sum_{i=0}^N a_i \phi_i, \quad \text{Eq. (3)}$$

$$= \sum_{i=0}^N \langle \phi_i, \psi \rangle \phi_i \quad \text{Eq. (4)}$$

Suppose that the eigenfunctions are ordered such that:

$$\lambda_0 > \lambda_1 \geq \lambda_2 \geq \dots \geq \lambda_i \geq \dots \quad \text{Eq. (5)}$$

ϕ_0 then represents the fundamental mode, which may be determined by the “power” iteration method. The power iteration method may also be used to find the first harmonic, provided that the initial iterate contains a component of the first harmonic and provided that at the end of each iteration, all traces of the fundamental mode are removed. The first requirement is met by choosing a random distribution as the initial guess:

$$\psi^0 = \bar{\phi}_0 (R - 1/2) \quad \text{Eq. (6)}$$

where $\bar{\phi}_0$ is the average of the fundamental mode over the entire core and R is a random distribution of numbers between zero and one. The second requirement is met by subtracting the fundamental mode flux from the n -th iteration as follows:

$$\tilde{\psi}^n = \psi^n - \frac{\langle \phi_0, \psi^n \rangle}{\langle \phi_0, \phi_0 \rangle} \phi_0 \quad \text{Eq. (7)}$$

The division by $\langle \phi_0, \phi_0 \rangle$ assures proper normalization during the process. This iterative procedure converges albeit slowly. Studies have shown that the L_2 norm of the residuals given by

$$\left[\frac{1}{N} \langle \phi_i^n - \phi_i^{n-1}, \phi_i^n - \phi_i^{n-1} \rangle \right]^{1/2} \quad \text{Eq. (8)}$$

is more effective as the convergence criterion than the usual convergence parameter:

$$\text{Max}_i(\phi_i^n / \phi_i^{n-1}) - \text{Min}_i(\phi_i^n / \phi_i^{n-1}) \quad \text{Eq. (9)}$$

Calculation of the higher harmonics proceeds in a similar way, except that all previous harmonics must be subtracted after each iteration. For the m-th harmonic:

$$\tilde{\psi}^n = \psi^n - \sum_{i=0}^{m-1} \frac{\langle \phi_i, \psi^n \rangle}{\langle \phi_i, \phi_i \rangle} \phi_i \quad \text{Eq. (10)}$$

RAI 6 [MFN 05-008]

Pressure Drops

Please provide the pressure drop and void fraction as function of elevation for BOC conditions. Provide it at least for a hot channel and an average channel along with their power and flow conditions.

RAI 6 Response [MFN 05-014]

The pressure drop and void fraction profiles for hot and average power channels are contained in the file: MFN 05-014 Channel Data.xls on the enclosed CD.

RAI 7 [MFN 05-008]

TRACG Time Traces

Please provide the time trace data for Figures 8.1-8 through 11, and 8.1-19 through 20 in electronic format.

RAI 7 Response [MFN 05-014]

The time trace data for the requested figures are contained in the file: MFN 05-014 Data for DR figures.xls on the enclosed CD.

RAI 8 [MFN 05-008]

ESBWR Design Parameters

Please provide the following ESBWR design parameters:

(Table is not repeated here)

RAI 8 Response [MFN 05-014]

The requested information is provided in the table below.

Parameter	Units	Value
Number of fuel rods per bundle		92
Channel height (in heated length)	cm	304.8
Heat transfer area per unit axial length	cm	296.59 (lower part), 251.46 (above PLR)
Channel flow area	cm ²	91.59 (lower part); 103.34 (above PLR)
Hydraulic diameter	cm	1.00 (lower part), 1.29 (above PLR)
Density of the fuel	g/cm ³	10.40
Fuel pellet diameter	cm	0.8763
Cladding heat capacity	cal/cm ³ . °C	0.502 @ 277 °C
Cladding thermal conductivity	cal/cm. s. °C	0.0379 @ 277 °C
Cladding thickness	cm	0.066
Gap heat transfer coefficient	cal/cm ² .s. °C	0.10 to 0.24
Gap width	cm	0.00889

RAI 9 [MFN 05-086]

TRACG calculations indicate that the Regional instability mode dominates the stability response of the reference ESBWR core. Staff confirmatory calculations with the LAPUR code exhibit a similar relation between the relative stability of the core-wide and regional modes in the reference ESBWR design. Thus, the margin to instability of the regional mode is a key design parameter for ESBWR. Stability margins for core-wide and channel instability, while relevant, are not as limiting for the reference ESBWR design, and they are not expected to be limiting for future design changes.

During the development of the Boiling Water Reactor Owners' Group (BWROG) Long Term Stability Solutions (LTS) in the early 1980's, a correlation was developed that attempted to bound all regional instability events observed to date within a region defined in the core-wide vs channel decay ratio. This correlation is sometimes called the "dog bite" correlation. With this methodology, the BWROG was able to circumvent a deficiency in their calculation methodology. At the time, no code was able to calculate the regional DR directly, so an approximate correlation was used.

The TRACG LTR submittal recognizes that at least one ESBWR parameter is sufficiently different from operating reactors to require a modification of the dog-bite correlation. This parameter is the core diameter, which will result in a smaller eigenvalue separation for the first subcritical neutronic mode. Thus, the LTR methodology proposes to modify in a conservative manner the dog-bite correlation to account for this difference. Other ESBWR design parameters may have similar effects, but we may not have sufficient operating/calculations experience to judge a priori what their effect on the ESBWR-specific dog-bite correlation may be.

Since TRACG is capable of directly calculating the limiting event (i.e., the regional DR), the staff believes that the TRACG ESBWR stability criteria should be based on calculated results, rather than an approximation that was developed based on operating-reactor experience. Please provide the rationale for GE's proposed approach regarding regional instability.

RAI 9 Response [MFN 05-097]

GE has adopted the core decay ratio vs. channel decay ratio stability map for the ESBWR to maintain consistency with the accepted practice for operating BWRs. GE recognizes that the regional boundary ("dog-bite correlation") could be different for the ESBWR and has accounted for the differences, primarily core size, through differences in the magnitude of the core subcriticality. Taken together with the large margins to the dog-bite correlation, GE believes adequate margins to regional stability can be maintained.

However, GE agrees that the capability in TRACG to directly calculate the regional decay ratio provides a technically superior basis for evaluating margins for regional stability. GE agrees to modify the approach used for analysis as follows:

The stability design criteria will be modified to be:

Limiting channel decay ratio < 0.8

Core decay ratio < 0.8;

Regional decay ratio < 0.8 .

All these evaluations will be made at 95% content and 95% confidence.

The design goal will be to maintain the nominal values of the channel, core and regional decay ratios less than 0.4.

The Licensing Topical Report NEDE-33083P, Supplement 1, "TRACG Application for ESBWR Stability Analysis" will be revised to reflect these changes. A Monte Carlo analysis for regional stability will be added to Section 8 of the report. It is not possible to vary the harmonic shape and subcriticality during Monte Carlo trials. The Monte Carlo analysis will be performed at the limiting point in the cycle (BOC, MOC or EOC). This will cover the range of harmonic subcriticalities and neutronic parameters over the cycle.

GE Supplementary Information for RAI No. 9 [MFN 06-009 (Supplementary Information per MFN 05-097)]

The modified approach used for ESBWR stability analysis as follows:

- The stability design criteria will be modified to be:
 - Limiting channel decay ratio < 0.8
 - Core decay ratio < 0.8 ;
 - Regional decay ratio < 0.8 .
- All these evaluations will be made at 95% content and 95% confidence.
- The design goal will be to maintain the nominal values of the channel, core and regional decay ratios less than 0.4.

The results for the regional stability Monte Carlo analysis are provided below:

[[

]]

RAI 10 [MFN 05-136]

MCNP is used to determine biases and uncertainty in void coefficient. What is the accuracy of the MCNP calculations? Monte Carlo calculations involve some finite number of histories, which implies some uncertainty for the results. The microscopic cross-sections data base used by the Monte Carlo calculation also has some uncertainty associated with it. The burnup calculation that identifies the concentrations for the isotopes at a given burnup has uncertainty. The uncertainty in the burnup calculation translates to an uncertainty in the Monte Carlo calculation. There is an uncertainty associated with the manufacturing tolerances for the fuel rods in terms of enrichment fraction, etc. How are these uncertainties included into the ESBWR instability calculations? TRACG includes internal biases and uncertainty for the k-infinite void coefficient based on the differences between MCNP and GE lattice code simulations. This implies that the MCNP calculations are exact. Has the uncertainty in the MCNP calculations been included in these TRACG internal biases and uncertainty functions?

RAI 10 Response [MFN 05-146] [MFN 05-146, Supplement 1 (Re-submittal with Correct Proprietary Designation)]

The MCNP uncertainty in the calculated k-infinity values has a standard deviation of [[]] based on the stochastic variability of the calculations at the number of histories that were specified [[]]. The MCNP k-infinity uncertainty translated into approximately [[]] uncertainty in the void coefficient at 40% instantaneous void that increases gradually to around [[]] instantaneous void. The uncertainty due to MCNP goes up for higher voids because k-infinity goes down whereas the MCNP standard deviation in k-infinity is approximately constant. The burnup calculation is performed in TGBLA and the isotopes are specified to MCNP for different exposures. [[]]

]]

All these uncertainties are elements in the overall uncertainty in the void coefficient since uncharacterized uncertainties in MCNP relative to TGBLA cause the variation in the pair-by-pair comparisons to increase. [[

]] The void history impact results in a bias in much the same way as having the incorrect exposure. Both are accommodated in the process by determining the cycle exposure where the calculated stability response is most severe.

RAI 11 [MFN 05-136]

The biases and uncertainty in void coefficient is based on comparing the results for the TGBLA06 and MCNP01 calculations for 11 different lattices at different void fractions and exposures. Is the GE14 design one of the 11 different lattices? Are the biases and uncertainties associated with the GE14 design bounded by the response surface developed for the 11 different lattices?

RAI 11 Response [MFN 05-146] [MFN 05-146, Supplement 1 (Re-submittal with Correct Proprietary Designation)]

The lattices are characterized according to the fuel rod array and whether or not they are fully or partially rodged. At the lattice level there is no geometric difference in the 10x10 GE12 design and the 10x10 GE14 design. [[

]] Thus, this set provides good coverage for the GE14 bundles. The void coefficient bias and uncertainty is well characterized for the entire range of instantaneous void fractions and exposures as was indicated in NEDE-32906P-A, Revision 1.

RAI 12 [MFN 05-136]

Is there any voiding calculated in the water rods during a typical ESBWR instability calculation with TRACG? There is some core bypass voiding calculated in the periphery of the core due to the down flow at the top of the core bypass. The biases and uncertainty in void coefficient is based on assuming the water rods and core bypass are at zero void fraction. Is the additional uncertainty in reactor kinetics associated with water rods voids and/or core bypass bounded by the response surface used by TRACG?

RAI 12 Response [MFN 05-146] [MFN 05-146, Supplement 1 (Re-submittal with Correct Proprietary Designation)]

There is no voiding in the water rods. The liquid temperature at the top of the water rod at the steady-state conditions is about 4K below saturation temperature, which is illustrated in the Figure below..

[[

]]

RAI 13 [MFN 05-136]

NEDE-33083P, Supplement 1 page 5-11 lower tie-plate leakage (drilled holes) has an uncertainty of 5%, while on the same page the sharp-edge orifice for water rod has uncertainty of 10%. Why is the uncertainty of the flow through drilled holes less than the uncertainty for a calibrated sharp-edge orifice?

RAI 13 Response [MFN 05-146] [MFN 05-146, Supplement 1 (Re-submittal with Correct Proprietary Designation)]

The uncertainty for the flow through the drilled holes in the lower tieplate is based on measurements in prototypical hardware and has been used before in earlier submittals (NEDE-32906 P-A). The uncertainty in the water rod flow is conservatively estimated. The calibrated orifice in the water rod will have a smaller uncertainty than the drilled holes. However, the water rod has (smaller) flow losses in the inlet and exit holes and the wall friction. Rather than accounting for these separately, a bounding estimate of 10% was used. Tables 8.2-1 and 8.2-2 in NEDE-33083P, Supplement 1 show that the sensitivity of the channel and core decay ratios to these parameters is very small.

RAI 14 [MFN 05-136]

BOC is bounding exposure for channel decay ratio. MOC is bounding exposure for core decay ratio. What about a clean core (i.e. zero exposure) rather than an equilibrium cycle? Have any calculations been completed for completely fresh core (i.e. zero exposure)?

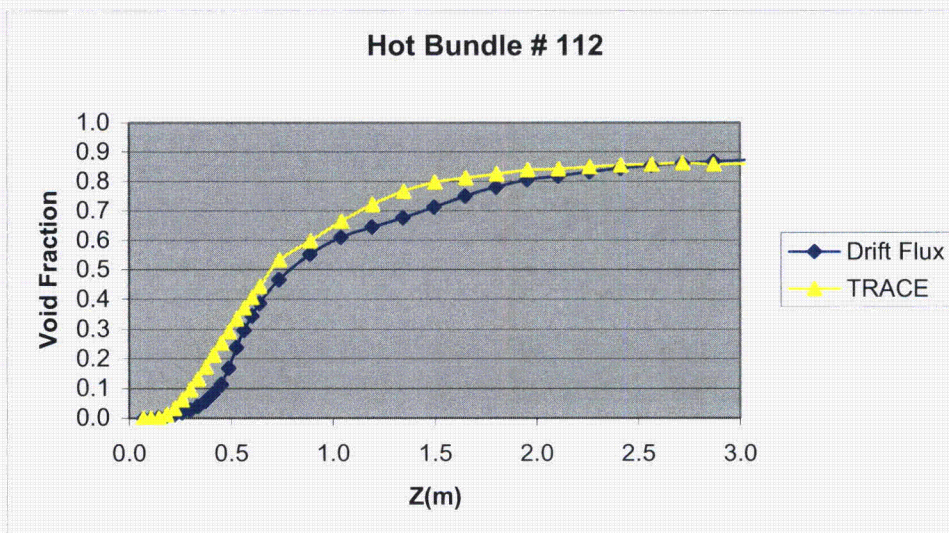
RAI 14 Response [MFN 05-146] [MFN 05-146, Supplement 1 (Re-submittal with Correct Proprietary Designation)]

An initial core design has not been developed for the ESBWR. For purposes of demonstrating the application methodology, an equilibrium core was judged to be sufficient. The actual initial core will be analyzed using the approved methodology at COL.

The process of developing an initial core design begins with the equilibrium core. The characteristics of the equilibrium core are replicated by replacing the burned fuel with fuel that is lower in enrichment and gadolima. The final design following iteration usually results in a somewhat flatter radial and axial peaking to compensate for higher local peakings in the higher enrichment bundles. The flatter axial peaking is favorable for channel and regional stability. The flatter radial peaking will typically lead to a higher subcriticality for the first harmonic mode relative to the common "ring of fire" radial peaking pattern. The void coefficient is less negative at BOC than later in the cycle, and should be slightly less negative for the initial core because of the absence of plutonium in the fuel. Overall, the stability performance of the initial core at BOC is expected to be similar or slightly better than for BOC for the equilibrium core. Given the margins to the stability design criteria demonstrated in Section 8.3 of NEDE-33083P, Supplement 1, use of an initial core should not be a major perturbation to the analysis results.

RAI 15 [MFN 05-136]

As part of the staff's review your interfacial drag models in TRACG, a calculation was performed that predicts void fraction as a function of elevation in the hot bundle. This was performed using TRACE and a standalone drift flux calculation that uses the models in Ref. 1. The staff found that the results were slightly different. This was expected since there are modeling differences between TRACE and the TRACG models in Ref. 1.



TRACG uses the Rouhani-Bowring model² for the energy distribution in subcooled boiling while TRACE uses the Lahey's mechanistic model³. The models are essentially the same, except the TRACE model does not include the pumping factor.

TRACG Model:

$$q_l = q_w \text{ if } h_l < h_{ld}$$

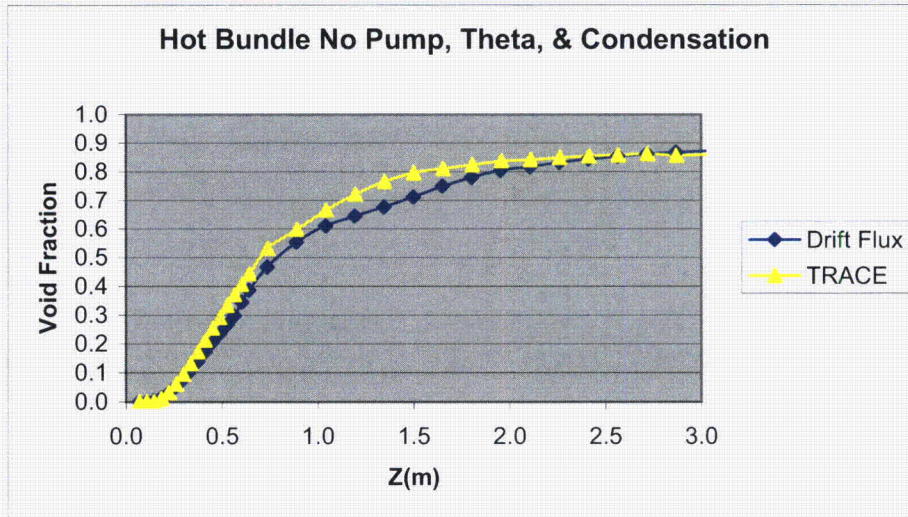
$$q_l = q_w \left[\left(\frac{h_f - h_l}{h_f - h_{ld}} \right) \left(1 + \left(\frac{h_l - h_{ld}}{h_f - h_l} \right) \left(\frac{\varepsilon}{1 + \varepsilon} \right) \right) \right] \text{ if } h_l > h_{ld}$$

The TRACE model has ε set to zero (i.e. the pumping factor).

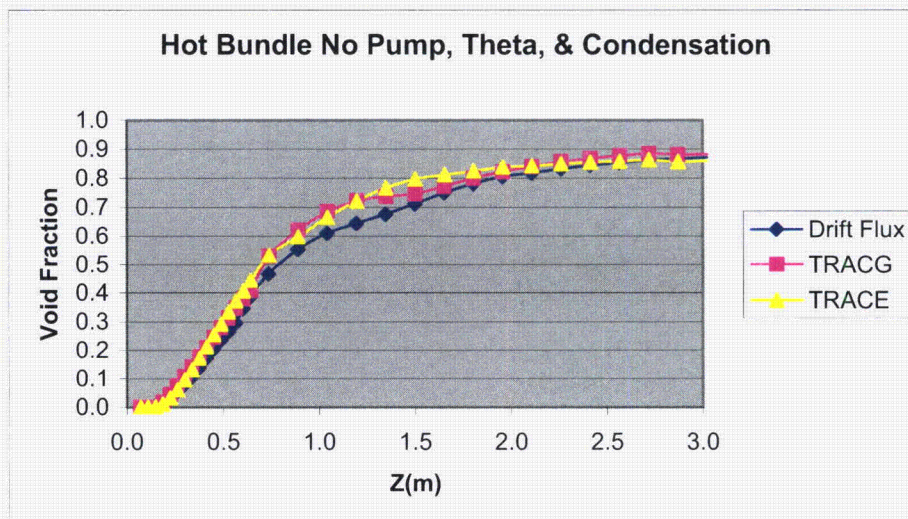
Another difference is that TRACE does not include the theta factor for modification⁴ of Co in the subcooled boiling regime, while the TRACG model description indicates that this factor is included.

$$C_{o, sb} = C_o \left(\frac{h_l - h_{ld}}{h_f - h_{ld}} \right)$$

The standalone drift flux model was modified to set the pumping factor to zero, remove the theta factor for modification⁴ of Co in the subcooled boiling regime, and ignore condensation in the subcooled boiling regime. The cases were re-run and the two results agree quite well.



These void fraction profiles were then compared to the TRACG data in the MS Excel file MFN 05-014 Channel Data.



NEDO-33083-A, Supplement 1, Revision 1

This also agreed quite well, which was not expected. The staff expected that in the subcooled region the TRACG data would agree with the drift flux model in the prior to the modifications since that model is using the same models in Ref. 1.

Please provide the following so that the staff may understand or resolve the differences:

- a) Confirmation that the pumping factor and theta factor are used in TRACG.
- b) Axial power profile for the ESBWR hot bundle at steady-state.
- c) Location of the grid spacers and the form loss used for the grid spacers and the flow area for the grid spacers.
- d) Provide a density wave propagation time based on the TRACG results.

RAI 15 Response [MFN 05-146] [MFN 05-146, Supplement 1 (Re-submittal with Correct Proprietary Designation)]

- a) The code listing for TRACG04 was checked and it was confirmed that both the pumping factor theta factor are coded as described in the TRACG Model Description (Reference 1).
- b) Axial power profiles for the ESBWR hot bundle (channel #112) are illustrated in the Figure below

[[

]]

c) The pressure drop due to singular losses ΔP_s is calculated in TRACG according to following equation (Ref 1.)

$$\Delta P_s = C \frac{G^2}{2\rho_l} \Phi_{10\text{hom}}^2$$

where

C – loss coefficient

G – mass flux (kg/(s*m²))

ρ_l – liquid density (kg/m³)

$\Phi_{10\text{hom}}^2$ – homogeneous two-phase multiplier

$$\Phi_{10\text{hom}}^2 = 1 + x \left(\frac{\rho_l}{\rho_v} - 1 \right)$$

ρ_v – vapor density (kg/m³)

x – flow quality

The local losses for the central channel are shown in the Table below

[[

]]

d) The density wave propagation time can be evaluated based on the phase shift between inlet and outlet flows. The inlet and outlet flows for the hot channel #112 (BOC, Channel stability analysis, inlet flow perturbation 20%) are illustrated in the Figure below. The density wave propagation time is [[]]

[[

]]

RAI 16 [MFN 05-136]

Fig. 3-11 in Ref. 5 indicates that for the Sirius test at 72 bars pressure the density-wave oscillations have a period > 10 seconds. The height of the core for the Sirius test is ~ 1.7 m compared to 3.0 m for the ESBWR. The ESBWR calculated power oscillations have a period ~ 1.3 seconds. The time period of the power oscillations in the ESBWR are related to the time required for a density wave to transport through the core. However, the density wave oscillations for the Sirius test with a shorter core have a period that is approximately an order of magnitude larger than the time period for the ESBWR power oscillations. It is assumed that the longer time period for the Sirius test is because the Sirius test is at constant power and therefore the density wave oscillation includes the time associated with a density wave propagating through the chimney. Please provide an explanation for the time period associated with the density wave oscillations in the Sirius test.

RAI 16 Response [MFN 05-146] [MFN 05-146, Supplement 1 (Re-submittal with Correct Proprietary Designation)]

The SIRIUS tests do not demonstrate classic density wave oscillations. Rather, these tests display a Type 1 Instability (see Figure 9.1-1 of NEDE-33083P, Supplement 1). These oscillations are initiated when voiding starts in the chimney region. An increase in the void fraction in the chimney leads to an increase in the natural circulation flow, which in turn tends to quench the voids (e.g. Figure 3-9 in Reference 5 shows the void fraction in the chimney dropping to zero during each oscillation). This type of periodic behavior is more significant at low pressures due to the larger density difference between the phases. The oscillations are terminated when the heat flux is increased further and a steady void fraction is established in the core and chimney. The time period of these oscillations is related to the transport time for enthalpy changes through the core and chimney as a result of changes in flow. Hence the time

periods are of the order of 10 to 15 seconds rather than the much shorter time periods for density wave oscillations, which are driven by void propagation through the core.

References for RAI 15 and RAI 16:

- 1) J.G.M. Andersen, et al, "TRACG Model Description," NEDE-32176P, Revision 2, Class 3, December, 1999.
- 2) R.T. Lahey, *Two-Phase Flow in Boiling Water Reactors*, NEDO-13888, July 1974.
- 3) R. T. Lahey, "A Mechanistic Subcooled Boiling Model," Proc. of the Sixth International Heat Transfer Conference, 1, Toronto, Canada, 1978, pp 293-295.
- 4) J.A. Findlay and G.E. Dix, "BWR Void Fraction Correlation and Data," NEDE-21565, January 1977.
- 5) J.R. Fitch, et al, "TRACG Qualification for ESBWR," NEDC-33080P, August, 2002.
- 6) ESBWR Design Description, NEDC-33084p, Class III, DRF 0000-0007-3896, August, 2002.

RAI 17 [MFN 06-101]

Submit calculations demonstrating that the chimney does not affect the density wave stability of ESBWR. As discussed at the ACRS thermal-hydraulic subcommittee meeting on March 14, 2006, the calculations are performed with finer nodalization of the chimney region and the explicit integration scheme. ["This RAI was sent to you via electronic mail on March 15, 2006."]

RAI 17 [MFN 06-098]

Provide calculations demonstrating that the chimney does not affect the density wave stability of ESBWR. To perform these calculations, re-nodalize the chimney with a finer nodalization and use the explicit integration scheme.

RAI 17 Response [MFN 06-098]

The reference nodalization of the ESBWR for stability analysis is shown in Figure 5.2-1 of NEDE-33083P, Supplement 1. The chimney region is represented by Levels 10 through 16. The height of Level 10 is [[]], and the height of Levels 11 through 16 is [[]]. For the nodalization study, Level 10 was subdivided into [[]] levels and Levels 11 through 16 were subdivided into [[]] levels each, resulting in [[]] levels in the chimney region of approximately [[]] each. The chimney node height then becomes similar to the channel node size of [[]]. The total number of levels in the vessel increased from [[]].

A steady state calculation was performed with the new nodalization. Stability analysis for the MOC conditions was then performed with the new nodalization. [[

]].

Figure RAI 17-1 shows the propagation of voids from the boiling boundary up the channel. The exit void fraction perturbation is out of phase with the void fraction perturbation in the boiling boundary node. The magnitude of the void perturbation is largest in the lower part of the bundle and decreases at the channel exit. Figure RAI 17-2 shows the propagation of the void fraction through the chimney. The magnitude of the perturbation is reduced relative to that in the core, and it propagates through the chimney with minimal damping. Figure RAI 17-3 shows the magnitude of the pressure drop perturbations in the core and chimney. The pressure drop perturbations are dominated by the core. The core power response to the perturbation is shown in Figure RAI 17-4. Also shown is the core power response for the original nodalization of the chimney. There is virtually no difference in the power response traces, and consequently in the decay ratio. This confirms that the original nodalization of the chimney was adequate and there is no effect of the finer nodalization. This can be attributed to the fact that the perturbations in the chimney pressure drop are much smaller than those in the core. Hence, the propagation of voids through the chimney plays only a minor role in determining the decay ratio and resonant frequency.

[[

Figure RAI 17-1: Void propagation through Core (Detailed Chimney Nodalization)

]]

[[

Figure RAI 17-2: Void propagation through Chimney (Detailed Chimney Nodalization)

]]

[[

Figure RAI 17-3: Core and Chimney Pressure Drop Perturbations (Detailed Chimney Nodalization)

[[

Figure RAI 17-4: Core Power Response (Standard and Detailed Chimney Nodalizations)

TABLE OF CONTENTS

Acronyms and Abbreviations	ix
1.0 Introduction	1-1
1.1 Background	1-1
1.2 Purpose and Scope	1-1
1.3 Scope of Review	1-3
2.0 Licensing Requirements and Scope of Application	2-1
2.1 Licensing Compliance	2-1
2.2 Stability Design Criteria	2-1
2.3 TRACG Analysis Approach For Licensing Compliance	2-5
2.3.1 Conformance with CSAU Methodology	2-5
2.4 Implementation Requirements	2-9
2.4.1 Review Requirements For Updates	2-9
2.5 Range of Application	2-9
3.0 Phenomena Identification And Ranking	3-1
3.1 ESBWR Stability PIRT	3-1
4.0 Applicability Of TRACG To ESBWR STABILITY ANALYSIS	4-1
4.1 Model Applicability	4-1
4.2 Assessment Matrix	4-1
4.3 Other Topics Relevant To TRACG Modeling of Instability	4-12
4.3.1 Explicit Integration Scheme for the Channel Component	4-12
4.3.2 Coupling of Conduction and Hydraulic Equations	4-12
4.3.3 Coupling of the Vessel and Channel Components	4-13
4.3.4 Coupled 3-D Kinetics and Thermal-Hydraulics Model	4-13
4.4 TRACG Qualification against Peach Bottom Unit 2 Stability Data	4-15
4.4.1 Test Conditions and Test Results	4-15
4.4.2 TRACG Analysis	4-15
4.4.3 Sensitivity Studies	4-16
4.4.4 Channel Decay Ratio	4-16
5.0 Model Biases and Uncertainties	5-1
5.1 Model Parameters and Uncertainties	5-1
5.2 Effects of Nodalization	5-20
5.2.1 Vessel Nodalization for ESBWR Stability Analysis	5-20
5.2.2 Detailed Nodalization Scheme for the Channel Component	5-20
5.2.3 Channel Grouping for Stability Applications	5-21
5.3 Effects of Scale	5-27
5.3.1 Full Scale Test Coverage	5-27
5.3.2 Operating Plant Data	5-27
5.4 Sensitivity Analysis	5-31
6.0 Application Uncertainties and Biases	6-1
6.1 Key Initial Conditions and Plant Parameters	6-1
7.0 Combination of Uncertainties	7-1
7.1 Traditional Bounding Analysis	7-1

7.2	Statistical Treatment of Overall Computational Uncertainty	7-1
7.3	Comparison of Approaches for Combining Uncertainties	7-2
7.3.1	Propagation of Errors	7-3
7.3.2	Response Surface Technique	7-3
7.3.3	Order Statistics (OS) Method – Single Bounding Value	7-4
7.3.4	Normal Distribution One-Sided Upper Tolerance Limit	7-6
7.4	Recommended Approach for Combining Uncertainties	7-6
7.5	Implementation of Statistical Methodology	7-9
7.5.1	Conformance with Design Limits	7-9
8.0	Demonstration Analyses	8-1
8.1	Baseline Analysis	8-1
8.1.1	Channel Stability Results	8-2
8.1.2	Core wide Stability Results	8-3
8.1.3	Regional Stability Results	8-4
8.2	Sensitivities to High and Medium Ranked Parameters	8-25
8.2.1	Channel Decay Ratio	8-25
8.2.2	Core Decay Ratio	8-25
8.3	Statistical Analysis of ESBWR Stability	8-29
8.3.1	Channel Decay Ratio Statistical Analysis	8-29
8.3.2	Core Wide Decay Ratio Statistical Analysis	8-30
8.3.3	REGIONAL Decay Ratio Statistical Analysis	8-30
8.3.4	Comparison with Design Limits	8-31
8.4	Stability following Anticipated Operational Occurrences (AOOs)	8-40
9.0	Plant Startup	9-1
9.1	Phenomena Governing Oscillations during Startup	9-1
9.2	Applicability of TRACG for Startup Calculations	9-6
9.3	TRACG Analysis of Typical Startup Trajectories	9-9
9.3.1	ESBWR Plant Startup	9-9
9.3.2	TRACG calculations for Simulated Startup Scenarios	9-9
9.4	Summary of ESBWR Startup Performance	9-19
10.0	References	10-1

LIST OF TABLES

Table 2.3-1: 2-8
Code Scaling, Applicability and Uncertainty Evaluation Methodology 2-8
Table 3.1-1: 3-4
Phenomena Governing ESBWR Stability Transients..... 3-4
Table 3.1-1: 3-8
Initial Conditions and Plant Parameters..... 3-8
Table 4.2-1 4-3
Stability Phenomena and TRACG Model Capability Matrix 4-3
Table 4.2-2: 4-8
Qualification Assessment Matrix for High and Medium Ranked ESBWR Stability Phenomena 4-8
8
Table 4.4-1: 4-17
PB2 Operating Conditions for Stability Tests 4-17
Table 4.4-2: 4-17
PB2 Stability Test Results 4-17
Table 4.4-3: 4-17
TRACG Channel Grouping for PB2 Core..... 4-17
Table 4.4-4: 4-18
Comparison of TRACG Predictions with Test Data..... 4-18
Table 4.4-5: 4-18
Sensitivity to Applied Perturbations 4-18
Table 5.1-1: 5-12
Bias and Uncertainty in Pressure Drop for 9x9 and 10x10 SEO and Lower Tie Plates..... 5-12
Table 5.1-2: 5-12
Bias and Uncertainty in Pressure Drop for 9x9 and 10x10 Spacers..... 5-12
Table 5.1-3: 5-13
Bias and Uncertainty in Pressure Drop for 9x9 and 10x10 Upper Tie Plates..... 5-13
Table 5.1-4: 5-18
Disposition of High and Medium Ranked Stability Model Parameters 5-18
Table 5.2-1: 5-23
Void Distribution at the Top of the Bypass Region..... 5-23

Table 5.3-1:	5-29
Range of Key Stability Parameters - ESBWR vs. Operating Plant Data.....	5-29
Table 6.1-1:	6-2
Key Plant Initial Conditions.....	6-2
Table 7.3-1:	7-2
Methods for Combining Uncertainty	7-2
Table 7.4-1	7-8
Comparisons of Methods for Combining Uncertainties	7-8
Table 8.1-1: TRACG Channel Grouping (MOC).....	8-6
Table 8.1-2:	8-7
Higher Harmonic Mode Sub-criticality at Different Exposures	8-7
Table 8.1-3:	8-7
Initial Conditions for Channel and Core Stability Analysis	8-7
Table 8.1-4:	8-8
Initial Conditions for Super Bundle Stability Analysis	8-8
Table 8.1-5:	8-8
Regional Stability: Decay Ratio by Subgroup	8-8
Table 8.2-1:	8-27
Sensitivity of Channel Decay Ratio to High and Medium-Ranked PIRT Parameters	8-27
Table 8.2-2:	8-28
Sensitivity of Core Decay Ratio to High and Medium-Ranked PIRT Parameters	8-28
Table 8.3-1:	8-32
Parameters and Distributions for Monte Carlo Trials.....	8-32
Table 9.2-1:	9-8
Comparison of Non-dimensional Parameters: CRIEPI vs. ESBWR.....	9-8
Table 9.2-2:	9-8
Comparison of Non-dimensional Parameters: Dodewaard vs. ESBWR	9-8

LIST OF ILLUSTRATIONS

Figure 2.2-1: Stability Acceptance Criteria for BWRs..... 2-3

Figure 2.2-2: Proposed Stability Map for ESBWR 2-4

Figure 3.1-1: Schematic of ESBWR Vessel and Internals 3-9

Figure 3.1-2: Top View of ESBWR Chimney and Core Region..... 3-10

Figure 4.3-1: Data Transfer Between TRACG Models 4-14

Figure 4.4-1: Test Conditions on PB2 Power/Flow Map 4-19

Figure 4.4-2: Average Axial Power Shapes for Stability Tests 4-19

Figure 4.4-3: Power Response to Pressure Perturbation for Test PT1 4-20

Figure 4.4-4: Power Response to Pressure Perturbation for Test PT2 4-20

Figure 4.4-5: Power Response to Pressure Perturbation for Test PT3 4-21

Figure 4.4-6: Power Response to Pressure Perturbation for Test PT4 4-21

Figure 4.4-7: TRACG Predictions of Decay Ratio versus Data 4-22

Figure 4.4-8: Sensitivity to Core Flow Perturbation Amplitude..... 4-22

Figure 4.4-9: Sensitivity to Number of Channel Groups (Test PT2)..... 4-23

Figure 4.4-10: Channel Decay Ratio for Test PT3 4-23

Figure 5.1-1: TGBLA06 Void Coefficient Relative Bias and Relative Standard Deviation for
Various Exposures (GWd/MT)..... 5-4

Figure 5.1-2. FRIGG OF64 Void Fraction Data – Subcooled Boiling..... 5-7

Figure 5.1-3. Void Fraction Sensitivity to PIRT23..... 5-7

Figure 5.1-4. Sensitivity of Fuel Center to Fluid Temperature Difference for 8x8 Fuel..... 5-9

Figure 5.1-5. Sensitivity of Fuel Center to Fluid Temperature Difference for 9x9 Fuel..... 5-9

Figure 5.1-6. Void Fraction Deviations for Tests Applicable to Regions with Large Hydraulic
Diameter 5-15

Figure 5.1-7 Sensitivity of TRACG Prediction of Average Void Fraction in EBWR Test Facility
to PIRT Multiplier on Interfacial Drag Coefficient..... 5-16

Figure 5.1-8 Probability Distribution for Multiplier on Interfacial Drag Coefficient 5-16

Figure 5.2-1: Axial and radial nodalization for ESBWR Stability Analysis 5-24

Figure 5.2-2: Channel Nodalization Studies from Reference 2 5-25

Figure 5.2-3: R- θ Nodalization for ESBWR Stability Analysis 5-25

Figure 5.2-4: Channel Grouping for ESBWR Stability Analysis 5-26

Figure 5.3-1: Comparison of Power and Flow per Bundle for ESBWR vs. Operating BWRs	5-30
Figure 5.3-2: Variation in Harmonic Sub-criticality vs. Core Size	5-30
Figure 7.3-1. Schematic Process for Combining Uncertainties	7-5
Figure 8.1-1. TRACG ESBWR Vessel R-Z Modeling	8-9
Figure 8.1-2: R- θ Nodalization of ESBWR Core Region showing Average Power (MW) in Each Region	8-10
Figure 8.1-3: TRACG Channel Grouping for ESBWR Core	8-11
Figure 8.1-4: Core Average Axial Power Shape at Different Exposures	8-12
Figure 8.1-5: Flux Distribution for First Azimuthal Harmonic with Axis of Symmetry	8-13
Figure 8.1-6: Flux Distribution for Second Azimuthal Harmonic with Axis of Symmetry	8-14
Figure 8.1-7: ESBWR Natural Circulation Operation with Limiting Conditions for Stability Analysis	8-15
Figure 8.1-8: Hot Bundle Flow Response to Transient Inlet Flow Perturbation	8-16
Figure 8.1-9: Hot Super Bundle Flow Response to Transient Inlet Flow Perturbation	8-16
Figure 8.1-10: Core Power Response to Transient Turbine Inlet Pressure Perturbation	8-17
Figure 8.1-11: Sensitivity to Perturbation Size	8-17
Figure 8.1-12: Power Distribution by Channel in Large Sectors in Ring 1	8-18
Figure 8.1-13: Power Distribution by Channel in Large Sectors in Ring 2	8-18
Figure 8.1-14: Finer Channel Grouping by Power Level	8-19
Figure 8.1-15: Sensitivity to Detailed Channel Grouping	8-20
Figure 8.1-16: Power Distribution for First Harmonic	8-21
Figure 8.1-17: Core Map showing Products of Fundamental and First Harmonic Powers (Regions with highest absolute values are shown in dark brown)	8-22
Figure 8.1-18: Channel Grouping for Regional Stability Calculation (darker colored regions have higher absolute peaking)	8-23
Figure 8.1-19: Channel Power Responses to Out-of-Phase Flow Perturbation	8-24
Figure 8.1-20: Symmetrically Located Channel Power Responses to Out-of-Phase Flow Perturbation	8-24
Figure 8.3-1: Monte Carlo Trials for Channel Decay Ratio	8-33
Figure 8.3-2: Monte Carlo Results for Channel Flow	8-33
Figure 8.3-3: Monte Carlo Results for Channel Decay Ratio	8-34
Figure 8.3-4: Monte Carlo Trials for Core Decay Ratio	8-34
Figure 8.3-5: Correlation between Core Decay Ratio and Power/Flow Ratio	8-35

Figure 8.3-6: Monte Carlo Results for Core Flow.....	8-35
Figure 8.3-7: Monte Carlo Results for Core Decay Ratio	8-36
Figure 8.4-1: Stability in Expanded Operating Map.....	8-42
Figure 8.4-2: Loss of Feedwater Heater Transient	8-42
Figure 8.4-3: Core Power Response to Pressure Perturbation (Scram Power Level).....	8-43
Figure 8.4-4: Hot Channel Flow Response to Inlet Flow Perturbation (Scram Power Level). ..	8-43
Figure 8.4-5: Core Power Response to Pressure Perturbation at Reduced Level.....	8-44
Figure 8.4-6: Hot Channel Response to Inlet Flow Perturbation at Reduced Level.....	8-44
Figure 9.1-1: Generalized Stability Map showing Type 1 and Type 2 Instability [28].....	9-4
Figure 9.1-2: Indications of Periodic Behavior during Dodewaard Startup [29]	9-4
Figure 9.1-3: Thermal – Hydraulic Conditions during Startup [28].....	9-5
Figure 9.1-4: Enthalpy Profiles for Different Heatup Rates	9-5
Figure 9.3-1: ESBWR Startup Trajectory.....	9-11
Figure 9.3-2: ESBWR Reactor Water Cleanup/Shutdown Cooling System – Schematic Diagram	9-11
Figure 9.3-3: TRACG Startup Simulation: Reactor Power Trajectories	9-12
Figure 9.3-4: TRACG Startup Simulation: Pressure Response	9-12
Figure 9.3-5: TRACG Startup Simulation – Core Inlet Subcooling.....	9-13
Figure 9.3-6: TRACG Startup Simulation – Core Inlet Flow.....	9-13
Figure 9.3-7: Separator Void Fraction (50 MW heatup)	9-14
Figure 9.3-8: Separator Void Fraction (85MW heatup)	9-14
Figure 9.3-9: Separator Void Fraction (125 MW heatup)	9-15
Figure 9.3-10: Hot Bundle Void Fraction (50 MW heatup).....	9-15
Figure 9.3-11: Hot Bundle Void Fraction (85 MW heatup).....	9-16
Figure 9.3-12: Hot Bundle Void Fraction (125 MW heatup).....	9-16
Figure 9.3-13: Hot Bundle Exit Flow	9-17
Figure 9.3-14: Peripheral Bundle Exit Flow.....	9-17
Figure 9.3-15: Hot Bundle CPR.....	9-18
Figure 9.3-16: Peripheral Bundle CPR.....	9-18

ACRONYMS AND ABBREVIATIONS

Term	Definition
AOO	Anticipated Operational Occurrence
BOC	Beginning of cycle
BT	Boiling Transition
BWR	Boiling Water Reactor
CCFL	Counter Current Flow Limitation
CHAN	Fuel Channel component in TRACG
CPR	Critical Power Ratio
CSAU	Code Scaling, Applicability and Uncertainty
DSS-CD	Detect and Suppress Solution – Confirmation Density
DVC	Dynamic Void Coefficient
ECCS	Emergency Core Coolant System
EOC	End Of Cycle
ESBWR	Economic Simplified Boiling Water Reactor
FTTC	Fuel Thermal Time Constant
FW	Feedwater
FWTR	Feedwater temperature reduction
GDC	General Design Criteria
GESTAR	General Electric Standard Application for Reload Fuel
GEXL	GE Boiling Transition Correlation
GT	Guide Tube
H	High Importance
HT	Heat Transfer
ICPR	Initial Critical Power Ratio
L	Low Importance
LOCA	Loss Of Coolant Accident
LTP	Lower Tieplate
LTR	Licensing Topical Report
M	Medium Importance
MCPR	Minimum Critical Power Ratio
MOC	Middle Of Cycle
NA	Not Applicable
NRC	Nuclear Regulatory Commission

Term	Definition
OLMCPR	Operating Limit MCPR
PANAC11	PANACEA, GE BWR Core Simulator
PIRT	Phenomena Identification and Ranking Table
PHE	Peak Hot Excess
RFACT	R Factor
SAFDL	Specified Acceptable Fuel Design Limit
SEO	Side entry orifice
TRACG	Transient Reactor Analysis Code (GE proprietary version)
UTP	Upper Tieplate
1-D	One Dimensional
1P	Single Phase Pressure Drop
2P	Two Phase Pressure Drop
3-D	Three Dimensional

1.0 INTRODUCTION

1.1 BACKGROUND

Under certain conditions, Boiling Water Reactors (BWRs) may be susceptible to coupled neutronic/thermal-hydraulic instabilities. These instabilities are characterized by periodic power and flow oscillations and are the result of density waves (i.e., regions of highly voided coolant periodically sweeping through the core). If the flow and power oscillations become large enough, and the density waves contain a sufficiently high void fraction, the fuel cladding integrity safety limit could be challenged.

Operating BWRs are implementing detection and mitigation solutions such as Detect and Suppress Solution – Confirmation Density (DSS-CD) [4]. These solutions consist of hardware and software that provide for reliable, automatic detection and suppression of stability related power oscillations, in the event that these plants enter the low flow region of the operating map. In the Economic Simplified Boiling Water Reactor (ESBWR), the highest power to flow ratio (and hence the smallest stability margin) is encountered at rated operation. Thus, it is essential that the ESBWR operate with substantial margin to instability at rated power. This requirement is met by imposing very conservative design criteria on the decay ratio. Detect and Suppress solutions will also be implemented, but only to serve as a backup in the very unlikely event that oscillations are encountered.

The TRACG computer code is used for the analysis of ESBWR stability margins. TRACG is a General Electric (GE) proprietary version of the Transient Reactor Analysis Code (TRAC). TRACG uses advanced one-dimensional and three-dimensional methods to model the phenomena that are important in evaluating the operation of BWRs. TRACG has been approved by the NRC for ESBWR LOCA (ECCS and containment) analysis. [24]. The application of TRACG for Anticipated Operational Occurrences (AOOs) and for ATWS overpressure calculations for operating BWRs has also been approved by the NRC [3], [31]. Currently, the NRC is reviewing the use of TRACG for BWR stability analysis in connection with the DSS-CD application [5].

TRACG has a multi-dimensional, two-fluid model for the reactor thermal hydraulics and a three-dimensional reactor kinetics model. The models can be used to accurately simulate a large variety of test and reactor configurations. These features allow for realistic simulation of a wide range of BWR phenomena, and are described in detail in the TRACG Model Description Licensing Topical Report [1].

TRACG has been extensively qualified against separate effects tests, component performance data, integral system effects tests and operating BWR plant data. The details are presented in the TRACG Qualification Licensing Topical Report [2]. Specific qualification studies for tests simulating passive BWR design features are reported in References 6 and 7.

1.2 PURPOSE AND SCOPE

The TRACG computer code is used to perform licensing analysis of the ESBWR. This report presents the methodology for application of TRACG to the ESBWR for stability analysis.

TRACG is specifically used for the following categories of analyses:

- Stability margins during normal operation including anticipated transients.

TRACG is also used to analyze plant startup trajectories, to assure a smooth ascension in pressure and power with a minimum of flow oscillation. Stability during plant startup is not a licensing issue; however, large MCPR margins are demonstrated for the startup scenario in this report.

This report describes the methodology to calculate key safety parameters and to quantify the uncertainties when applying the TRACG code to the ESBWR for the evaluation of stability margins. Thus, this report presents TRACG application methodology for ESBWR stability analysis. This document demonstrates the acceptable use of TRACG analysis results for licensing the ESBWR power plant within the applicable licensing bases.

The stability analysis will statistically account for the uncertainties and biases in the models and plant parameters using a Monte Carlo method for the Normal Distribution One-Sided Upper Tolerance Limit (ND-OSUTL) if the output distribution is normal, or the Order Statistics method if it is not (Section 7). Conservative values may be used in place of probability distributions for some plant parameters for convenience. The uncertainties and biases considered include the following:

- Model uncertainties
- Experimental uncertainties and any uncertainties related to test scale-up
- Plant uncertainties
- Process measurement errors
- Manufacturing tolerances

Some of these uncertainties are fuel type dependent. Therefore, periodic changes in the statistical analysis may be required as the core design changes. The statistical analysis process is defined in this report and criteria to be used to change this analysis are provided.

Representative results are shown that illustrate the application methodology and demonstrate the margins to the design limits. The overall analysis approach followed is consistent with the Code Scaling Applicability and Uncertainty (CSAU) analysis methodology [8]. Conformance with the CSAU methodology is demonstrated in Section 2. The sensitivity of the figure of merit (decay ratio) to the initial conditions is established in this report.

Section 2.0 describes the licensing requirements and the scope of the TRACG application to ESBWR stability. Section 3.0 describes the identification and ranking of phenomena relevant to stability. Section 4.0 describes and justifies the applicability of TRACG models for stability analysis. Section 5.0 describes the model uncertainties. Section 6.0 describes the application uncertainties and biases. Section 7.0 describes the method used for the combination of uncertainties. Section 8.0 provides a demonstration analysis and typical results. A discussion of plant startup in natural circulation is provided in Section 9.0.

1.3 SCOPE OF REVIEW

GE requests that the NRC approve TRACG for analyzing and demonstrating compliance with licensing limits for stability evaluation of the ESBWR.

The Licensing Topical Reports: TRACG Model Description [1]; TRACG Qualification; [2], TRACG Qualification for SBWR Volumes 1 and 2 [6], and TRACG Qualification for ESBWR [7] are incorporated by reference as part of the review scope.

2.0 LICENSING REQUIREMENTS AND SCOPE OF APPLICATION

2.1 LICENSING COMPLIANCE

The licensing basis for stability must comply with the requirements of 10 CFR 50, Appendix A, "General Design Criteria for Nuclear Power Plants". The Appendix A criteria related to stability are Criteria 10 and 12.

Criterion 10 (Reactor Design) requires that:

"The reactor core and associated coolant, control, and protection systems shall be designed with appropriate margin to assure that specified acceptable fuel design limits are not exceeded during any condition of normal operation, including the effects of anticipated operational occurrences."

Criterion 12 (Suppression of Reactor Power Oscillations) requires that:

"The reactor core and associated coolant, control, and protection systems shall be designed to assure that power oscillations which can result in conditions exceeding specified acceptable fuel design limits are not possible or can be reliably and readily detected and suppressed."

The ESBWR licensing basis for stability satisfies GDC 12 by designing the reactor system such that significant power oscillations are not possible. A high degree of confidence is established that oscillations will not occur by imposing conservative design criteria on the channel¹, core wide and regional decay ratios under all conditions of normal operation and anticipated transients.

Because oscillations in power and flow are precluded by design, the requirements of GDC 10 are met through the analysis for AOOs, and are automatically satisfied with respect to stability.

As a backup, the ESBWR will implement a Detect and Suppress solution as a defense-in-depth system. The details of the solution will be developed during the ESBWR Construction and Operating License (COL) phase.

2.2 STABILITY DESIGN CRITERIA

Compliance with General Design Criterion 12 is assured by implementing design criteria for the decay ratio. GE uses a stability criteria map of core decay ratio vs. channel decay ratio to establish margins to stability (Figure 2.2-1). Stability acceptance criteria for BWRs are established on this map at core decay ratio = 0.8 and limiting channel decay ratio = 0.8, with an allowance for regional mode oscillations in the top right corner of the defined rectangle. These boundaries were established considering model uncertainties of the order of 0.2 in the core and channel decay ratio in the GE analysis methods (FABLE and ODYSY). There is also margin in the regional boundary, which is drawn below available plant regional oscillation data, though the

¹ "Channel" is used interchangeably with "Bundle" in this report and denotes a fuel bundle and its channel box.

amount of conservatism has not been quantified. These criteria have been approved by the NRC for application of ODYSY to the E1A Long Term Stability Solution [12], [13].

The ESBWR core size of 1132 bundles is significantly larger than the largest operating BWR (ABWR with 872 bundles). The sub-criticality of the azimuthal harmonic, which is relevant for regional oscillations, decreases with core size. The regional stability boundary is expected to move inwards in the Core Decay ratio vs. Channel Decay Ratio plane as the sub-criticality decreases. Rather than modifying the operating plant stability map, the regional decay ratio will be calculated directly and compared with an acceptance criterion of 0.8. The margin of 0.2 in the calculation of the regional decay ratio is reasonable and consistent with the values for the channel and core decay ratios. Figure 2.2-2 shows the three-dimensional stability map and the design criteria for channel, core and regional stability.

The design goal is for the nominal values of the core, channel and regional decay ratios at rated power and flow to be less than 0.4, or about half the design criteria. This is consistent with the BWR design philosophy of maintaining the decay ratios in the flow control range approximately half of the limiting values.

The design requirement is for the core, channel and regional decay ratios to be less than the acceptance criteria of 0.8 at the 2σ level of uncertainty. Because the ESBWR is a new plant and there are no plant data, the uncertainties will include operating state and model uncertainties, even though there is already an explicit allowance for model uncertainty in the acceptance criteria.

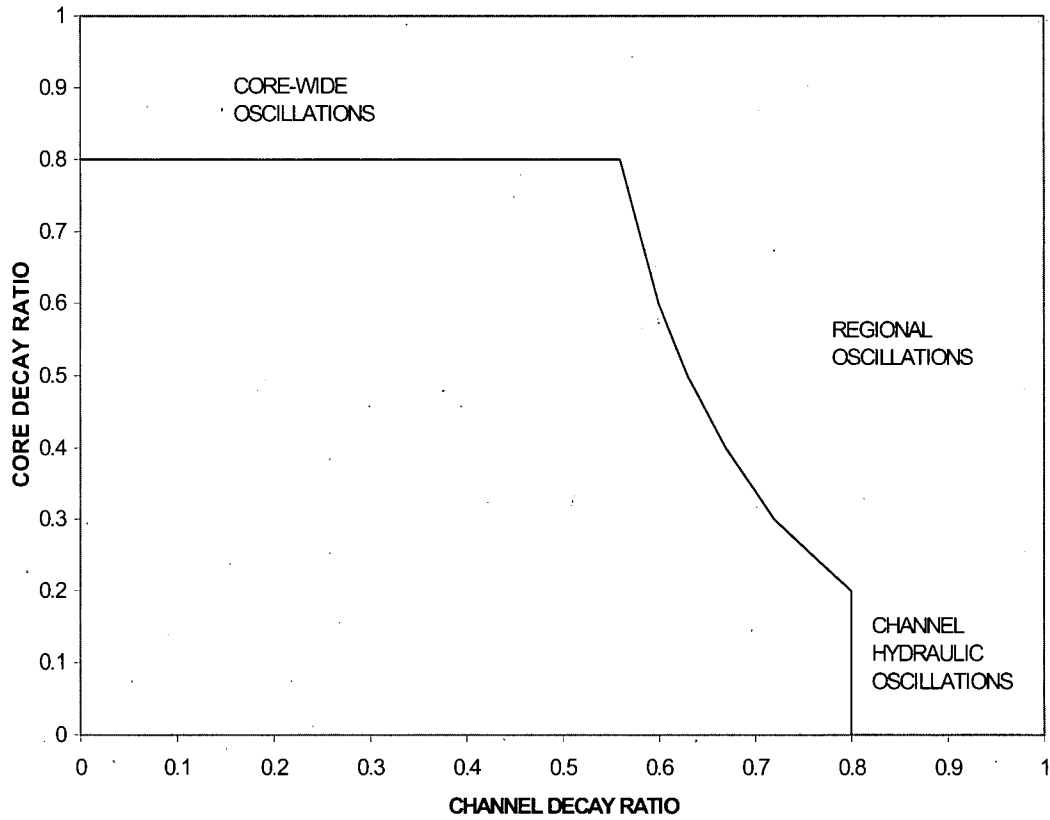


Figure 2.2-1: Stability Acceptance Criteria for BWRs

[[

a

]]

Figure 2.2-2: Proposed Stability Map for ESBWR

2.3 TRACG ANALYSIS APPROACH FOR LICENSING COMPLIANCE

The overall TRACG demonstration analysis approach for ESBWR stability analysis is consistent with the Code Scaling, Applicability and Uncertainty (CSAU) analysis methodology [8], and addresses the applicable elements of the NRC-developed CSAU evaluation methodology as described in the next section.

2.3.1 CONFORMANCE WITH CSAU METHODOLOGY

The CSAU report describes a rigorous process for evaluating the total model and plant parameter uncertainty for a nuclear power plant calculation. Further details on the CSAU methodology are contained in the NRC-issued Regulatory Guide 1.157 [9]. The CSAU methodology incorporates the elements of phenomena identification and ranking, documentation of models, assessment against Separate Effects Tests (SETs) and Integral System Tests (ISTs) for the key phenomena, and quantification of uncertainties due to the models, scaling and plant parameters. In the CSAU process, the overall model uncertainty is derived from the propagation of individual model uncertainties through code calculations; experimental comparisons are used as a check on the derived uncertainty.

The CSAU methodology consists of 14 steps, as outlined in Table 2.3-1.

The 14 CSAU steps are summarized in the following paragraphs. The objectives for each step are evaluated by indicating how they will be addressed in this report.

[1]. Specify scenario.

Stability analysis is performed at the limiting operating conditions including power, flow and exposure. Anticipated Operational Occurrences (AOOs) that might lead to more severe initial conditions for stability are also considered.

[2]. Select nuclear plant.

The Nuclear Power Plant (NPP) which is the basis for this application report is the 4500 MWt ESBWR, an optimized version of the plant described in the ESBWR Design Description [10].

[3]. Identify and rank phenomena.

All processes and phenomena that occur during an event do not equally influence plant behavior. The most cost efficient, yet sufficient, analysis reduces all candidate phenomena to a manageable set by identifying and ranking the phenomena with respect to their influence on the primary safety criteria. The processes and phenomena associated with each component are examined. After the processes and phenomena have been identified, they are ranked with respect to their effect on the primary safety criteria for the event. A phenomena identification and ranking table (PIRT) is established to guide the subsequent uncertainty quantification. The PIRTs for stability are reported in Section 3.

[4]. Select frozen code.

TRACG04 is the frozen code selected for the analysis.

[5]. Document code.

The details of the models are contained in the TRACG Model Description LTR [1]. A summary description of the TRACG assessment is provided in Section 2.3.2. Details are contained in the TRACG Qualification LTRs [2], [6], [7]. This report describes the application process. The User' Manual [11] provides guidance on the use of the code.

[6]. Determine code applicability.

To demonstrate applicability, one must begin with capability. Capability to calculate an event for a nuclear power plant rests on four elements: (1) conservation equations, which provide the code capability to address global processes; (2) constitutive correlations and models, which provide code capability to model and scale particular processes; (3) numerics, which provide code capability to perform efficient and reliable calculations; and (4) structure and nodalization, which address code capability to model plant geometry and perform efficient and accurate plant calculations. All four elements must be considered when evaluating the code capability for a specific application. Code capability is only one aspect needed to demonstrate that the code is applicable. Applicability also implies that the capability of the code has been demonstrated by actually applying the code in the intended manner with acceptable results. The capability of TRACG to model phenomena that are important to ESBWR simulations has been addressed in Section 4.1. Qualification aspects are addressed in Section 4.2.

[7]. Establish assessment matrix.

The determination of uncertainty for a computer code must be based on a sufficient data set, which necessarily will include both separate and integral effects tests and available plant data. The assessment matrix must cover all phenomena and components that were identified and ranked 'High' in the PIRT for the selected events for the nuclear power plant. The stability PIRTs are documented in Section 3.0. The assessment coverage of the PIRTs is summarized in Table 4.2-2.

[8]. Define nodalization for plant calculations.

The plant model must be nodalized finely enough to represent both the important phenomena and design characteristics of the nuclear power plant but coarsely enough to remain economical. In principle, nodalization can be treated as an individual contributor to code uncertainty; however, quantification of nodalization uncertainty can be very costly. Thus, the preferred path is to establish a standard nodalization based on the assessment against separate and integral effects tests. Nodalization studies have been performed in assessing this test data in order to determine the level of detail necessary to represent the important phenomena and then consistent levels of detail have been applied to establish standard noding schemes for the ESBWR. The standard ESBWR

nodalization for TRACG for stability applications is defined based on the qualification studies and is described in Section 5.

[9]. Determine code and experiment uncertainty.

Comparisons with separate effects tests are used to quantify the uncertainty in the individual models and correlations. Typically, experimental uncertainty is inherent in these comparisons and is not separated out. Quantification of the uncertainties in the model parameters is discussed in Section 5. The impact on the primary safety parameters for the nuclear power plant can be determined by varying the inputs to the individual models by a specified amount (e.g. $\pm 1\sigma$). The overall uncertainty of the code in simulating the important phenomena for ESBWR stability is addressed fully in Section 8.

[10]. Determine effects of scale.

The differences for similar physical processes, at scales up to and including full scale, should be evaluated to establish a statement of potential scaling effects. For TRACG, this has been done by evaluating the experimental basis for the individual models and correlations against full-scale plant conditions, by performing qualification against separate-effects tests, integral effects tests at different scales and full-scale plant data, and by using a plant nodalization based on the qualification studies. Specific evaluations for stability are addressed in Section 5.

[11]. Determine effects of plant operating conditions.

Uncertainties in the nuclear power plant simulations may result from uncertainties in plant operating state or in plant process parameters. For example, the plant power distribution is a function of burnup history and control rod pattern prior to the transient. For the ESBWR, these uncertainties are accounted for by using the cycle exposure that leads to the highest decay ratios (Section 6). Uncertainties in setpoints will be treated by using analytical limits for these parameters.

[12]. Perform plant sensitivity calculations.

Nuclear power plant calculations for a given event are used to determine the code's output sensitivity (in the primary safety criteria parameters) to various plant operating conditions that arise from uncertainties in the reactor state at the initiation of the transient event or in plant process parameters. Similarly, nuclear power plant calculations are used to address the uncertainties introduced by the code models and correlations. In this manner, the sensitivities of the safety-related quantities to these parameters are evaluated individually or collectively. The sensitivity studies for stability are documented in Section 8.

[13]. Combine biases and uncertainties.

In this step, all the biases and uncertainties are combined into an overall bias and uncertainty. There are different techniques that can be used, as discussed in Section 7. The results of the stability analysis are shown in Section 8.

[14]. Determine total uncertainty.

The statement of total uncertainty for the code for ESBWR stability analysis is given in terms of the difference between the bounding and nominal results.

**Table 2.3-1:
Code Scaling, Applicability and Uncertainty Evaluation Methodology**

CSAU Step	Description	Addressed In
1	Scenario Specification	Normal operation, AOOs, plant startup
2	Nuclear Power Plant Selection	ESBWR 4500 MWt
3	Phenomena Identification and Ranking	Table 3.1-1
4	Frozen Code Version Selection	TRACG04
5	Code Documentation	References [1,2,6,7,11]
6	Determination of Code Applicability	Table 4.2-1
7	Establishment of Assessment Matrix	Table 4.2-2
8	Nuclear Power Plant Nodalization Definition	Section 5
9	Definition of Code and Experimental Accuracy	Section 5
10	Determination of Effect of Scale	Section 5
11	Determination of the Effect of Reactor Input Parameters and State	Section 6
12	Performance of Nuclear Power Plant Sensitivity Calculations	Section 8
13	Determination of Combined Bias and Uncertainty	Section 8
14	Determination of Total Uncertainty	Section 8

2.4 IMPLEMENTATION REQUIREMENTS

The implementation of TRACG into actual licensing analysis of ESBWR stability is contingent upon completion of the following implementation requirements:

- Review and approval by the NRC of:
 1. The uncertainties documented in Section 5.
 2. The statistical process for analyzing stability margins described in Section 7.
- Calculation of overall biases and uncertainties to be applied to best-estimate calculations of decay ratios as shown in Section 8.

2.4.1 REVIEW REQUIREMENTS FOR UPDATES

In order to effectively manage the future viability of TRACG for ESBWR stability licensing calculations, GE proposes the following requirements for upgrades to the code to define changes that (1) require NRC review and approval and (2) that will be on a notification basis only.

2.4.1.1 UPDATES TO TRACG CODE

Modifications to the basic models described in Reference 1 may not be made for ESBWR stability licensing calculations without NRC review and approval.

Features that support effective code input/output may be added without NRC review and approval.

2.4.1.2 UPDATES TO TRACG MODEL UNCERTAINTIES

New data may become available with which the specific model uncertainties described in Section 5 may be reassessed. If the reassessment results in a need to change specific model uncertainty, the specific model uncertainty may be revised for ESBWR stability licensing calculations without NRC review and approval as long as the process for determining the uncertainty is unchanged.

2.4.1.3 UPDATES TO TRACG APPLICATION METHOD

Revisions to the TRACG application method described in Section 7 may not be made for ESBWR stability licensing calculations without NRC review and approval.

2.4.1.4 CYCLE SPECIFIC UNCERTAINTIES IN SAFETY PARAMETERS

Biases and uncertainties in the decay ratios are developed for the ESBWR plant using the process described in this report. This process will be implemented for the first operating cycle for the ESBWR. The magnitudes of these biases and uncertainties may change for future core designs and do not require NRC review and approval. The values of the uncertainties will be transmitted to the NRC for information if the stability margin is significantly impacted.

2.5 RANGE OF APPLICATION

The intended application is ESBWR stability analysis at normal operation including potentially more severe conditions resulting from AOOs.

3.0 PHENOMENA IDENTIFICATION AND RANKING

The critical safety parameter for evaluating stability margin is the decay ratio. The phenomena identification and ranking table (PIRT) is used to delineate the important physical phenomena that impact the decay ratio. PIRTs are ranked with respect to their impact on the critical safety parameters. For example, the decay ratio is determined by the reactor response to perturbations in core flow or system pressure. The coupled core neutronic and thermal-hydraulic response to void propagation through the core is determined by the void reactivity, fuel rod thermal inertia and core pressure distribution.

3.1 ESBWR STABILITY PIRT

All processes and phenomena that occur during a transient do not equally influence plant behavior. Disposition analysis is used to reduce all candidate phenomena to a manageable set by identifying and ranking the phenomena with respect to their influence on the critical safety parameters. The processes and phenomena associated with each component are examined, and then ranked with respect to their effect on the critical safety parameters for the event.

PIRTs are developed with only the importance of the phenomena in mind and are independent of whether or not the model is capable of handling the phenomena and whether or not the model shows a strong sensitivity to the phenomena. For example, two phenomena may be of high importance yet may tend to balance each other so that there is little sensitivity to either phenomenon. Both phenomena are of high importance because the overall balance between these competing phenomena is important.

Table 3.1-1 was originally developed to identify the phenomena that govern BWR/3-6 stability responses, and represents a consensus of GE expert opinions. The phenomena were then reviewed for the ESBWR and some changes were incorporated. The differences between the operating plants and the ESBWR have been identified in the table. The stability transient events have been categorized into three distinct groups:

- Channel thermal-hydraulic instability,
- Core-wide instability, and
- Regional instability.

For each event type, the phenomena are listed and ranked for each major component in the reactor system. The ranking of the phenomena is done on a scale of high importance to low importance or not applicable, as defined by the following categories:

- **High importance (H):** These phenomena have a significant impact on the decay ratio and should be included in the overall uncertainty evaluation.
- **Medium importance (M):** These phenomena have minor impact on the decay ratio and may be excluded in the overall uncertainty evaluation.
- **Low importance (L) or not applicable (NA):** These phenomena have no impact on the decay ratio and need not be considered in the overall uncertainty evaluation.

In the PIRT (Table 3.1-1), the High and Medium ranked phenomena are highlighted in red. Differences between the ESBWR PIRT and that for the operating BWRs (regardless of ranking) are marked in green.

The parameters that are important for stability are those that determine the natural circulation flow, density wave propagation in the core and the feedbacks to the density wave propagation. The natural circulation flow is governed by the resistance and density distribution in the flow loop. The important resistances in the flow loop are in the core, separators and to a smaller extent, the lower plenum. The density distribution depends on the void fractions in the chimney, core, and separators. Density wave propagation and phase lags are dependent on the core velocities and void distribution as well as the core pressure drop distribution. Feedbacks include those between the core density and neutron flux, and between the neutron flux and fuel rod heat flux. For the regional mode of oscillation, the sub-criticality of the higher order harmonics of the neutron flux distribution is an important parameter.

Differences between the ESBWR PIRT and the corresponding table for operating plants result from two sources:

1. Differences in geometrical configuration

The ESBWR incorporates a tall chimney region to enhance natural circulation (Figure 3.1-1). The partitioned chimney introduces a number of new phenomena to be considered. Each chimney cell receives the flow from a group of 16 bundles together with the core bypass region between these 16 bundles (Figure 3.1-2). The chimney cells communicate with each other at the top of the chimney (6 m above the top of the core) and also through the top guide at the top of the bypass region. Because the 16 bundles feeding a chimney are coupled to a common chimney cell, the stability of this group of bundles (dubbed a "super bundle") is also evaluated. Chimney cells in the peripheral region of the core have a lower void fraction and higher density than those in the central region. Thus, the pressure at the bottom of a peripheral chimney cell is higher than for a central chimney cell. The pressure difference can result in a small flow down from a peripheral cell through the top guide and into the central chimney cells. The axial resistance of the top guide and the radial resistance across the bypass region play a role in determining the magnitude of this recirculation flow and possible ingestion of steam into the top of the bypass region.

2. Different figure of merit

Because sustained oscillations are precluded in the ESBWR, the figure of merit is the decay ratio. Phenomena related to CPR or core heatup are not important for the ESBWR and have been relegated to the "Low" importance category.

For the core region, Table 3.1-1 also tabulates a number of derived parameters (e.g. ratio of core power to core flow) important to reactor stability. While these can be obtained as ratios of parameters defined earlier in the table, in many cases the ratios are better indicators of stability margins than the individual parameters.

Table 3.1-1 evaluates initial conditions and plant parameters for their importance to stability. These are not physical phenomena but determine the plant state, and have been kept separate from the phenomena in Table 3.1-1.

The PIRT serves a number of purposes. First, the phenomena are identified and compared to the modeling capability of the code to assess whether the code has the necessary models to simulate the

phenomena. Second, the identified phenomena are cross-referenced to the qualification basis to determine what qualification data are available to assess and qualify the code models and to determine whether additional qualification is needed. Third, the High-ranked parameters are varied over their uncertainty distributions to obtain an overall uncertainty in the estimate of the safety parameters.

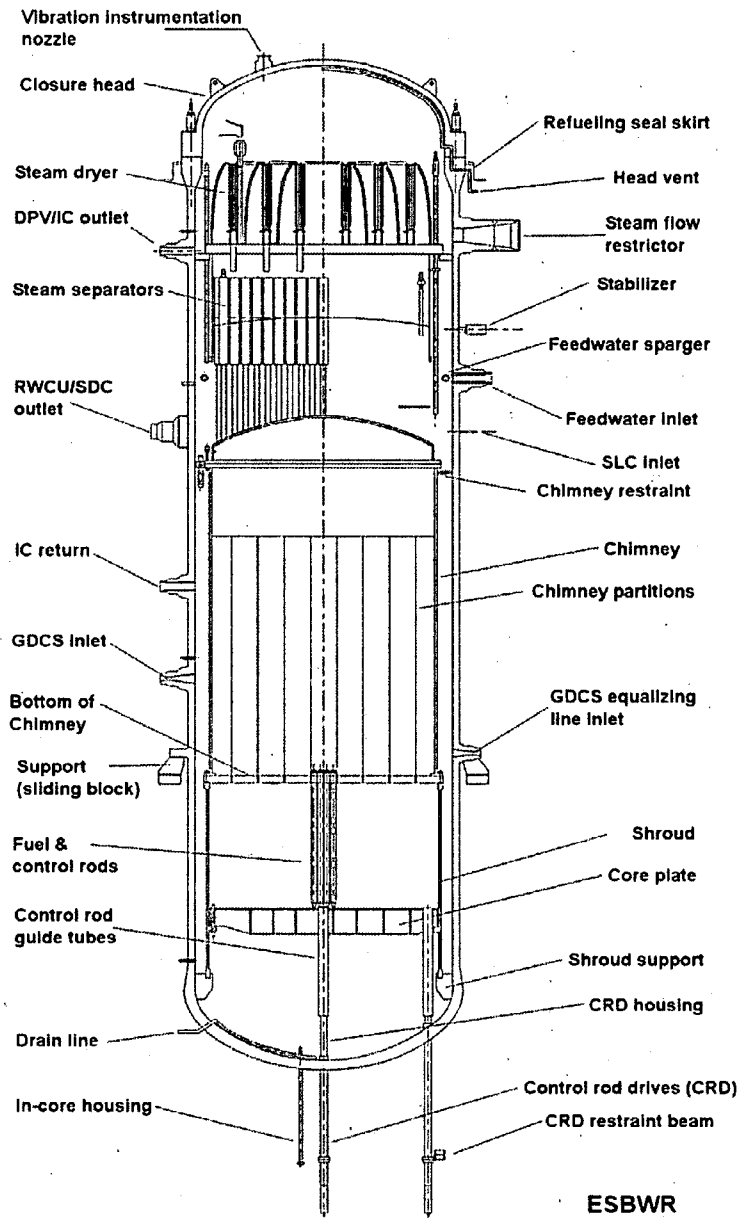


Figure 3.1-1: Schematic of ESBWR Vessel and Internals

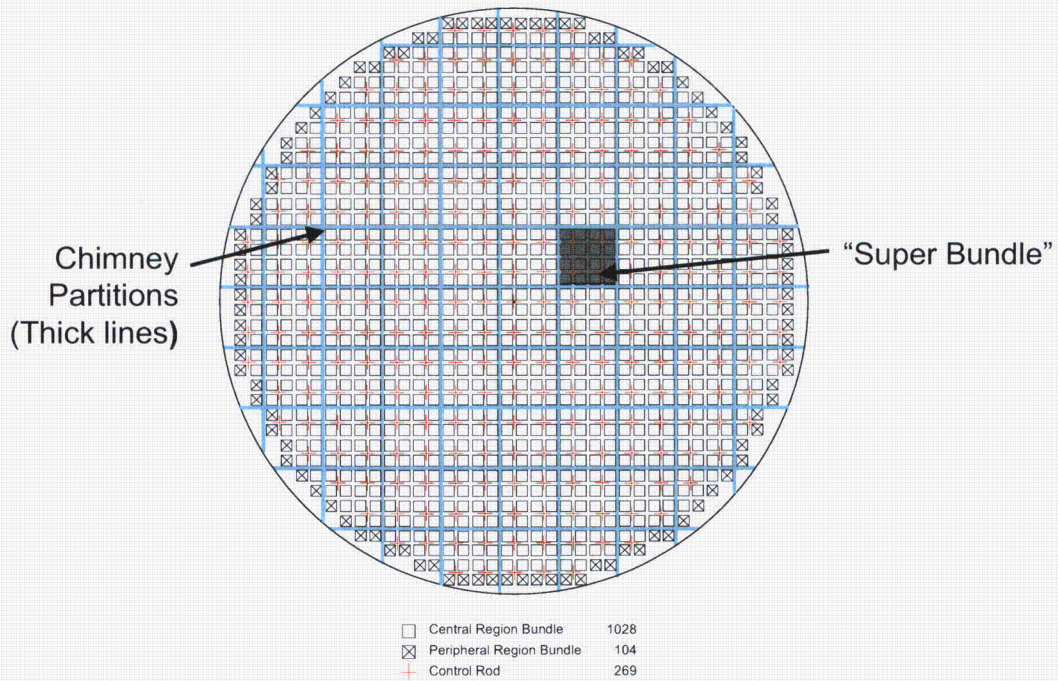


Figure 3.1-2: Top View of ESBWR Chimney and Core Region

4.0 APPLICABILITY OF TRACG TO ESBWR STABILITY ANALYSIS

This section demonstrates the applicability of TRACG for the analysis of stability for ESBWR through a two-step process. First, the phenomena identified in Section 3 are compared to the modeling capability of the code to determine that the code has the necessary models to simulate the phenomena. Second, the assessment basis of the TRACG code for stability applications is examined.

4.1 MODEL APPLICABILITY

The capability of the code to simulate an event for a nuclear power plant depends on four elements:

- Conservation equations, which provide the code capability to address global processes,
- Correlations and models, which provide the code capability to model and scale particular processes,
- Numerics, which provide the code capability to perform efficient and accurate calculations, and
- Structure and nodalization, which address the code capability to model plant geometry and perform efficient and accurate calculations.

Consequently, these four elements must be considered when evaluating the applicability of the code to the event of interest for the nuclear power plant calculation. The key phenomena for stability analysis were identified in the PIRTs in the previous section. The capability of the code to simulate the key phenomena is addressed, documented and supported by code qualification in References 1,2,5,6 and 7. The results are summarized in this section.

The complete list of phenomena is cross-referenced to the model capabilities in Table 4.2-1. The table shows that TRACG has models to treat the relevant phenomena for stability analysis.

4.2 ASSESSMENT MATRIX

The identified phenomena are cross-referenced to the qualification basis to determine what qualification data are available to assess and qualify the code models, and to determine whether additional qualification is needed for some phenomena.

The qualification assessment of TRACG models is summarized in Table 4.2-2. For each PIRT phenomenon that is ranked High or Medium, the relevant elements from the Qualification LTR [2] are identified. The table shows that for almost all the governing stability-related phenomena, TRACG qualification has been performed against a wide range of data. Data from separate-effects tests, component tests, integral system tests and plant tests as well as operating plant data have been used to qualify the capability of TRACG to model the phenomena.

The exceptions where there is no data coverage are: lower plenum radial flow resistance; core bypass region axial and radial flow resistance; and chimney cell interactions. The flow resistances are based on handbook correlations. Large uncertainties will be applied to these parameters in the statistical process of calculating upper bounds for the decay ratio. There is no direct data for chimney cell interactions, but there are no new phenomena to be considered. The response of

individual channels, which are part of a 16-bundle cluster under a chimney cell, is analyzed in detail as part of channel stability evaluations.

A large part of the assessment basis (particularly for neutronics related phenomena) consists of plant stability data. These data are primarily for onset of oscillations; i.e., at decay ratios close to 1. It was judged necessary to expand this data base to include plant data at low decay ratios, typical of ESBWR operation. For this purpose, additional TRACG assessment results versus Peach Bottom stability data with low decay ratio are included later in this section.

NEDO-33083-A, Supplement 1, Revision 1

4.3 OTHER TOPICS RELEVANT TO TRACG MODELING OF INSTABILITY

This section addresses other topics relevant to TRACG modeling of instability, including the selection of numerical integration scheme and numerical formulations used for stability analysis.

4.3.1 EXPLICIT INTEGRATION SCHEME FOR THE CHANNEL COMPONENT

TRACG uses a fully implicit integration technique for the heat conduction and hydraulic equations when integrating from time step n to time step $n+1$. In the implicit formulation, the convective terms are calculated based on the new properties at time step $n+1$. The fully implicit technique is the default option. The governing hydraulic equations in the implicit form are provided in Section 8.2 of Reference 1. For time domain stability calculations, an optional explicit integration technique is employed for the channel component. To minimize numerical damping, the use of the explicit scheme changes the convective terms to use the current properties at time step n in place of the new properties at time step $n+1$.

The TRACG thermal-hydraulic instability modeling using the explicit integration scheme has been evaluated for adequacy by comparison to experimental data from the FRIGG facility, as discussed in Section 3.7 of Reference 2. Two types of tests were run in the FRIGG facility. One test series used a pseudo random signal imposed on the system to determine the system response as a function of frequency. A second test series provided a more deterministic measurement of the onset of unstable behavior. In these tests, which started from steady-state natural circulation operation, the system power was slowly increased until the onset of unsteady behavior was observed. This second series of tests have been simulated by TRACG. Comparisons of TRACG predictions of the channel power for the onset of limit cycle oscillations to the power measured in the tests is considered the best assessment of the code's ability to predict the onset of unstable operation.

4.3.2 COUPLING OF CONDUCTION AND HYDRAULIC EQUATIONS

The coupling scheme used for the conduction and hydraulic equations does not change for stability applications, relative to AOOs.

The heat transfer coupling between the structures and the hydraulics is treated implicitly, when the implicit integration technique is used. For this purpose, the heat conduction equation is solved in two steps, and thus integration of the combined equations involves the following steps:

- (1) The heat conduction equation for structures is linearized with respect to fluid temperatures. The result of this step is a system of linear equations for structure temperatures and surface heat flow as functions of the fluid temperatures.
- (2) The hydraulic equations are solved using an iterative technique. This step results in new values for the fluid pressures, void fraction, temperatures and velocities.
- (3) A corrector step is utilized for the hydraulic solution. Due to the use of an iterative solution technique, the conservation of the properties is affected by the convergence. The corrector step is employed to correct any lack of conservation due to imperfect convergence.

- (4) Back-substitution into the heat conduction equation is performed to obtain new temperatures for structures.

The linearization of the heat conduction equation and subsequent back-substitution (Steps 1 and 4) are described in Section 8.1 of Reference 1. The hydraulic solution (Steps 2 and 3) is described in Section 8.2 of Reference 1.

4.3.3 COUPLING OF THE VESSEL AND CHANNEL COMPONENTS

The coupling scheme used between the vessel component and the channel components does not change for stability applications, relative to AOOs. A network solution scheme is applied, as described in Section 8.2.2 of Reference 1. For stability calculations, the numerical method is selected on a component-by-component basis. Explicit integration is used for the channel component and the other components use the implicit numerical method. When a component using an implicit numerical method is connected to a component using the explicit numerical method, the new time step fluid properties are convected between the two components. Thus the component using the implicit numerical method is fully implicit for all nodes. The explicit component is fully explicit for all nodes except for a node connecting to an implicit component, which will use a mixture of old time step and new time step properties in the convective terms. Old time step properties are used in the convection to other cells in the explicit component and new time step properties are used in the convection at a face connecting to an implicit component. With this approach conservation of mass and energy balances is assured.

4.3.4 COUPLED 3-D KINETICS AND THERMAL-HYDRAULICS MODEL

The coupled 3-D kinetics and thermal-hydraulics model used does not change for stability applications, relative to AOOs. The 3-D kinetics model is described in Section 9 of Reference 1.

TRACG solves the three-dimensional (3-D) transient neutron diffusion equations using one neutron energy group and up to six delayed neutron precursor groups. The basic formulation and assumptions are consistent with the GE 3-D BWR Core Simulator [14]. The neutron flux and delayed neutron precursor concentrations at every (i,j,k) node are integrated in time in response to moderator density, fuel temperature, boron concentration or control rod changes. [[

]]

[[

]]

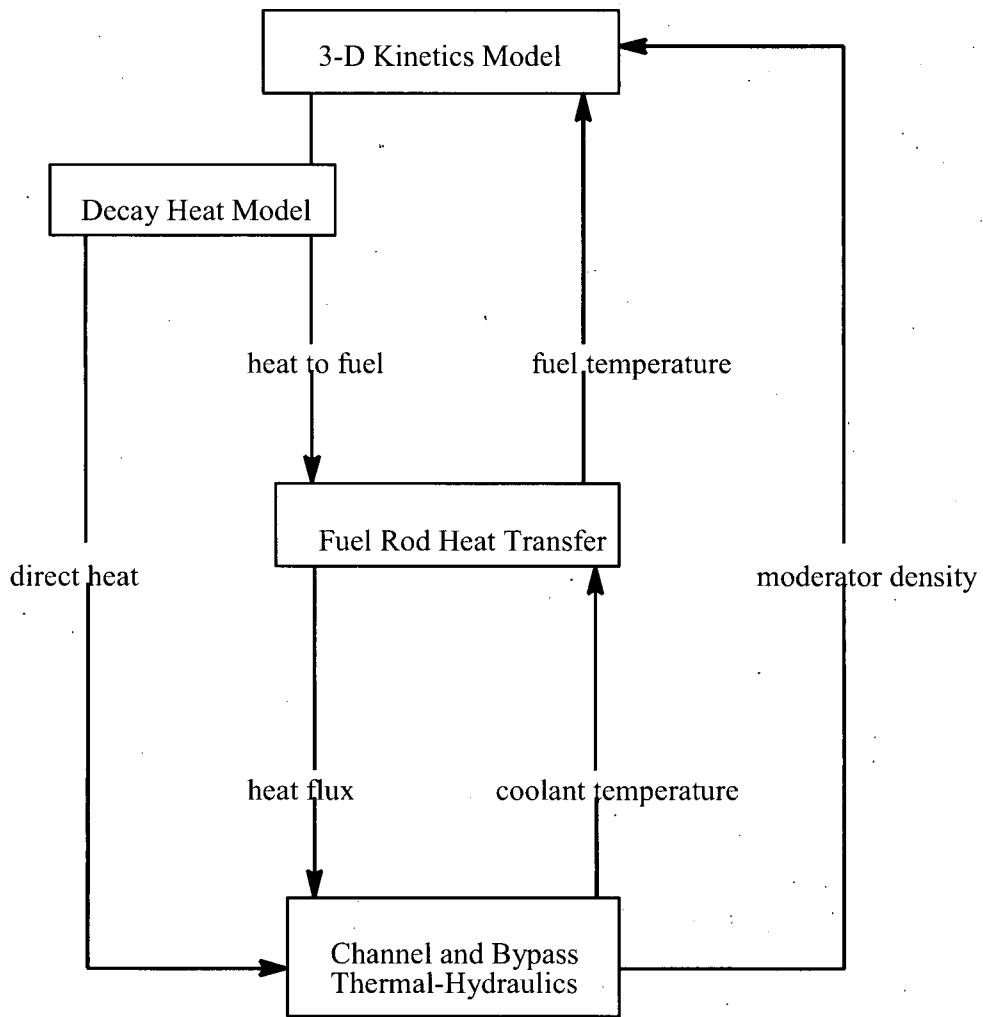


Figure 4.3-1: Data Transfer Between TRACG Models

4.4 TRACG QUALIFICATION AGAINST PEACH BOTTOM UNIT 2 STABILITY DATA

Low flow stability tests were conducted at Peach Bottom 2 at the end of Cycle 2 on April 14, 15 and 16, 1977 [23]. Chronologically, these tests were performed during the same period as the well-known turbine trip tests, in between Turbine Trip 1 (April 9) and Turbine Trip 2 (April 23). The stability tests (PT1 through PT4) were conducted along the low-flow end of the rated power-flow line, and along the power-flow line corresponding to minimum pump speed. The reactor core stability margin was determined from an empirical model fitted to the experimentally derived transfer function measurement between core pressure and the APRM (Average Power Range Monitor) neutron flux signal. Both periodic and pseudo-random binary signals were applied to the pressure regulator set point as the input signal.

The pseudo-random binary perturbation technique was found to be an operationally simple and precise technique for measuring BWR core stability margins. The tests demonstrated large stability margins (low decay ratios) for the Peach Bottom 2 Cycle 2 core design.

4.4.1 TEST CONDITIONS AND TEST RESULTS

The operating conditions at which the low flow stability tests were conducted are listed in Table 4.4-1. The minimum core flow that could be achieved at test conditions PT2, PT3 and PT4 was limited to about 20% of rated recirculation pump speed rather than natural circulation core flow, as originally planned. The test points are shown on the power-flow map in Figure 4.4-1. The process computer average axial power distributions for the four tests are shown in Figure 4.4-2. The experimentally obtained transfer function between APRM A and core pressure was fit to a second order function with one real zero and two complex poles. In the Laplace domain the transfer function is of the form:

$$G(s) = \frac{K_p(\tau_1 s + 1)}{s^2 / \omega_1^2 + 2\delta_1 s / \omega_1 + 1}$$

where δ_1 is the damping ratio, ω_1 the natural frequency and K_p is the gain. The decay ratio is then calculated as:

$$\ln DR = \frac{-2\pi\delta_1}{\sqrt{1-\delta_1^2}}$$

Data for resonant frequency, damping ratio and decay ratio are presented in

Table 4.4-2 for the four tests.

4.4.2 TRACG ANALYSIS

The TRACG input decks used for PB2 Turbine Trip Test 1 (TT1) were the starting point for the TRACG analysis. As the stability tests were conducted just a week following TT1, the exposure accounting data generated for TT1 were applicable for the stability tests. PANAC wrapups were created for the specific test by modifying the initial conditions (flow, power, pressure, core inlet enthalpy and control rod pattern). Figure 4.4-2 shows the average axial power shapes from the process computer for the four tests. The TRACG input deck used for TT1 was modified to nodalize the fuel channels more finely near the boiling boundary, as discussed in Section 5.2. The PB2 core, consisting of 7x7 and 8x8 fuel, was modeled with eight channel groups, as shown in Table 4.4-3.

Stability analysis was performed by perturbing the turbine inlet pressure. Various types of perturbations were tried. Results were insensitive to the method of perturbation (as shown later in this section). A pressure pulse of 0.06 MPa (10 psi) for 1 second has been used in the cases for which results are reported below.

Figure 4.4-3 shows the power response to a pressure pulse applied at the turbine inlet for Test PT1. A decay ratio and frequency of oscillation can be extracted from this trace. The decay ratio is not exactly constant for the non-linear system. In order to have a common basis for comparison, the decay ratio has been defined as the ratio of the amplitudes of the second negative peak to the first negative peak. The power responses to pressure perturbations for the test conditions PT2, PT3 and PT4 are shown in Figure 4.4-4 to Figure 4.4-6. Measured and calculated decay ratios and frequencies are compared in Table 4.4-4. Calculated decay ratios are also compared with data in Figure 4.4-1. Generally, TRACG is a little conservative in its predictions. For these four data points, the TRACG calculations have a mean error of [[]] and a standard deviation of [[]]. TRACG calculates a damped natural frequency of about [[]] Hz, considerably lower than the [[]] Hz measured in the tests. The frequencies calculated by TRACG correlate well with the transit time for the vapor through the high power channels. The reason for the higher frequencies seen in the data has not been identified, but may be due to the method of extracting them from the transfer function.

4.4.3 SENSITIVITY STUDIES

TRACG sensitivity studies were performed for Test PT1 to evaluate the effect of the nature of the perturbation applied to initiate the power response. The sensitivity studies and results are reported in Table 4.4-5. Rectangular pressure pulses of different amplitude were applied for different durations. A triangular pressure pulse was also applied in one case. Finally, two perturbations in core flow of different amplitude were tried. The results are insensitive to the magnitude, shape and duration of the pressure pulses. Only the smaller core flow perturbation led to a slightly larger decay ratio – largely due to a small amplitude power response (Figure 4.4-8). These results provide confidence in this technique of estimating decay ratios. Subsequently, the rectangular pressure pulse of 0.06 MPa for 1 s has been used for the other calculations.

The sensitivity to core nodalization, specifically channel grouping, was also evaluated for all four tests. The core was modeled with 19 channel groups, conventionally used for regional stability calculations with TRACG. The results (shown in Figure 4.4-9 for Test PT2) were virtually identical for the two cases. Thus, the 8-group nodalization is judged to be adequate for these calculations.

4.4.4 CHANNEL DECAY RATIO

There are no measurements of the channel decay ratio. TRACG calculations of channel decay ratio were made by perturbing the inlet flow to an individual channel, with the power kept constant. The resulting channel flow response for conditions corresponding to PT3 is shown in Figure 4.4-10. The channels are very stable, with decay ratios close to zero.

**Table 4.4-1:
PB2 Operating Conditions for Stability Tests**

Test Number	Reactor Power		Core Flow Rate		Core Pressure	Core Inlet Enthalpy
	MWt	% Rated	kg/s	% Rated	MPa	kJ/kg
PT1	1995	60.6	6629	51.3	6.895	1183
PT2	1702	51.7	5419	42.0	6.839	1174
PT3	1948	59.2	4903	38.0	6.929	1182
PT4	1434	43.5	4903	38.0	6.888	1179

**Table 4.4-2:
PB2 Stability Test Results**

Test Number	Closed Loop Resonant Frequency (Hz)	Damping Coefficient	Decay Ratio
PT1	0.44	0.318	0.12
PT2	0.47	0.319	0.12
PT3	0.44	0.168	0.34
PT4	0.40	0.190	0.30

**Table 4.4-3:
TRACG Channel Grouping for PB2 Core**

Channel Component #	Bundle Type	Channel Location	Number of Physical Channels	Channel Average Power (MW)
11	7X7	CENTRAL	68	2.77
14	8X8	CENTRAL	20	3.13
12	7X7	CENTRAL	240	2.64
15	7X7	CENTRAL	176	2.61
16	8X8	CENTRAL	60	2.96
17	8X8	CENTRAL	104	2.94
18	7X7	CENTRAL	4	3.11
13	7X7	PERIPHERAL	92	1.69

**Table 4.4-4:
Comparison of TRACG Predictions with Test Data**

]]

**Table 4.4-5:
Sensitivity to Applied Perturbations**

]]

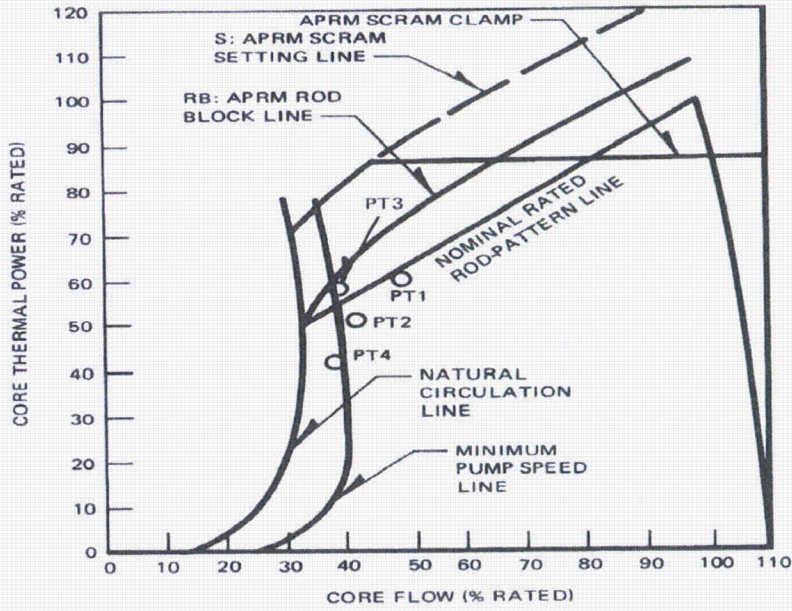


Figure 4.4-1: Test Conditions on PB2 Power/Flow Map

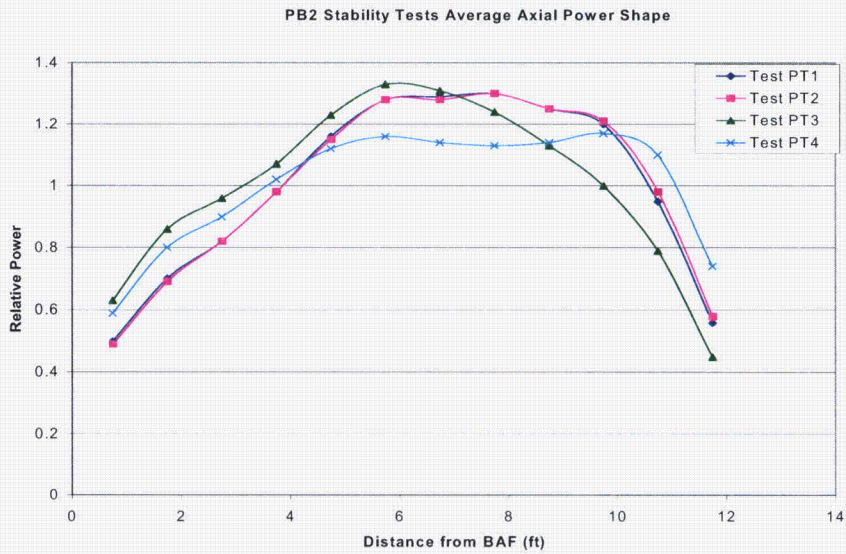


Figure 4.4-2: Average Axial Power Shapes for Stability Tests

[[

]]

Figure 4.4-3: Power Response to Pressure Perturbation for Test PT1

[[

]]

Figure 4.4-4: Power Response to Pressure Perturbation for Test PT2

[[

]]

Figure 4.4-5: Power Response to Pressure Perturbation for Test PT3

[[

]]

Figure 4.4-6: Power Response to Pressure Perturbation for Test PT4

[[

]]

Figure 4.4-7: TRACG Predictions of Decay Ratio versus Data

[[

]]

Figure 4.4-8: Sensitivity to Core Flow Perturbation Amplitude

[[

]]

Figure 4.4-9: Sensitivity to Number of Channel Groups (Test PT2)

[[

]]

Figure 4.4-10: Channel Decay Ratio for Test PT3

5.0 MODEL BIASES AND UNCERTAINTIES

The model biases and uncertainties for all items from the PIRT table (Table 3.1-1), which have been identified as having a significant impact on the decay ratios, have been evaluated. The subset of phenomena ranked High or Medium is included in the Qualification Assessment Matrix (Table 4.2-2). Overall model biases and uncertainties for the stability application are assessed for each high and medium ranked phenomenon by using a combination of comparisons of calculated results to: (1) separate-effects test facility data, (2) integral test facility test data, (3) component qualification test data and (4) BWR plant data. Where data are not available, cross-code comparisons or engineering judgment are used to obtain approximations for the biases and uncertainties. For some phenomena that have little impact on the calculated results, it is appropriate to simply use a nominal value or to conservatively estimate the bias and uncertainty. Table 5.1-4 provides the dispositions of the high and medium ranked stability model parameters from Table 4.2-2.

5.1 MODEL PARAMETERS AND UNCERTAINTIES

This section discusses the uncertainties associated with each item that has been identified as having an impact on the decay ratio for either channel, core wide or regional stability. The ID, description, and highest ranking (M for Medium and H for High) are listed for each item. The results are summarized in Table 5.1-4.

A11 Lower Plenum Radial Resistance, M

The lower plenum radial resistance is a contributor to the overall loop resistance that determines the natural circulation flow through the core. While this is a minor resistance compared to the core and separators, the uncertainty is fairly large because of the complex path through the guide tubes. [[

]]

B2 Bypass Void Distribution, M

The bypass void fraction is controlled by the vapor generation in the bypass and the relative velocity between the phases. Heat generation in the bypass region and wall heat transfer from the fuel bundles determine the vapor generation in the bypass region. Heat generation is due to direct moderator heating (B13). The uncertainty in the wall heat transfer is due to nucleate boiling heat transfer and is not a major contributor. The void fraction is determined by the relative velocity between the phases, which depends on the interfacial shear. The uncertainty in the interfacial shear is defined in Item C2AX. It is possible for voids to be drawn into the top of the bypass region from the chimney in the peripheral region. The magnitude of the void fraction due to this effect is governed by the axial and radial resistance at the top of the bypass (B14).

B13 Bypass Direct Moderator Heating, M

The direct moderator heating is the result of energy released into the moderator as the fast neutrons are slowed down and due to gamma absorption. The uncertainty is defined in Item C3DX.

B14 Bypass Axial and Radial Resistance, M

The chimney cells formed by the partitions in the chimney communicate at the bottom via the top of the core bypass region. The peripheral chimney cells are at a higher pressure at the bottom level with respect to the central chimney cells because of the higher static head in these cells. The pressure differential results in a small downflow at the top of the bypass in the peripheral cells and a crossflow to the central region of the bypass where the flow turns upwards and returns to the chimney. This circulation pattern can draw steam into the bypass from the chimney region. The extent to which voids exist at the top of the bypass depends on the relative magnitude of the bypass resistance to the flow resistance of the flow openings at the bottom of the chimney. [[

]].

C1AX Void Coefficient, H

TRACG04 uses a 3-D neutron kinetics model based on the PANACEA [14] neutronics parameters as they are implemented in PANAC11. The nodal reactivity is calculated in terms of the infinite multiplication factor, migration area, fast group removal cross-section and fast group diffusion coefficient. All of these parameters are calculated in terms of the moderator density. The infinite multiplication factor is also dependent on a history-weighted moderator density and nodal exposure.

[[

]]

[[

]]

Figure 5.1-1: TGBLA06 Void Coefficient Relative Bias and Relative Standard Deviation for Various Exposures (GWd/MT)

C1DX 3-D Kinetics and Power Shape, H

TRACG has a 3-D neutron kinetics model, based on the PANACEA formulation [14]. The TRACG kinetics model has been qualified against stability data for various BWRs, viz. LaSalle 2, Leibstadt. Steady-state power distribution comparisons have been made with data from several plants [2] and PANACEA predictions. The uncertainty of the kinetics model is determined by the uncertainty in scram reactivity, void and Doppler coefficient. For stability evaluations which involve the response to small perturbations, only the void reactivity is relevant.

C1EX Delayed Neutron Fraction, H

The delayed neutron fraction is important in determining the neutronic response speed. This parameter is a function of the fuel type and exposure. The variability in delayed neutron fraction is covered by considering the full range of fuel types and core exposures. Note that the dynamic void coefficient (obtained by dividing the void coefficient by the delayed neutron fraction) is a better parameter for stability evaluations than the void coefficient. Thus, observations related to the dynamic void coefficient in subsequent sections refer to both C1AX and C1EX. Similarly, the parameter CS4 (sub-criticality of the 1st harmonic) is conventionally represented in dollars by dividing the difference in eigenvalues for the fundamental and first harmonic modes by the delayed neutron fraction.

C1FX Sub-criticality of First Harmonic Mode, H

The sub-criticality of the first harmonic mode governs the likelihood of regional oscillations. The sub-criticality must be overcome by the gain of the hydraulic transfer function. Hence, the smaller the sub-criticality, the easier it is to excite the harmonic mode oscillations. This parameter is covered by considering the cycle exposure that produces the lowest sub-criticality.

C2AX Interfacial Shear, H

Although this PIRT phenomenon is entitled "Interfacial Shear", it more generally concerns representation of the uncertainties of TRACG model parameters that affect the prediction of void fraction in the core and bypass. The core and bypass are distinguished from the regions of the vessel discussed under E2 and F1 by their comparatively small hydraulic diameters. As described in the AOO application report [3], data from the FRIGG test facility [19], which form the basis for the GE design void correlation, are the most relevant data for pressures near the normal operating range. TRACG02 predictions of the FRIGG void fraction data for fully developed nucleate boiling showed a small positive bias in absolute void fraction of [[]] and a standard deviation of [[]] [3]. The uncertainty observed in these data comparisons was reflected in the TRACG02 model through a PIRT multiplier (PIRT22) on the interfacial shear parameter (C_o-1). The relatively small bias in the predictions, especially in comparison with the experimental uncertainty of [[]] in the void fraction measurement, was used to justify the choice of an unbiased mean of [[]] for PIRT22. From an examination of the dependence of void fraction predictions on PIRT22, it was concluded that a PIRT22 standard deviation of [[]] would appropriately represent the prediction standard deviation of [[]]. (As described in the AOO application report [3], the error in the TRACG

predictions is somewhat larger for subcooled boiling. This is attributed to uncertainty in the onset of net vapor generation, which is covered under C2BX.)

The predictions of the FRIGG data were repeated with TRACG04. The results gave a bias of [[]] and a standard deviation of [[]], differing only slightly from the results obtained using TRACG02. Thus, the uncertainty (standard deviation [[]]) in PIRT22 has been retained.

C2BX Subcooled Boiling, H

For stability evaluations, interfacial heat transfer is a factor only in the subcooled boiling region. The void fraction in the subcooled flow regime is quite insensitive to the magnitude of the heat transfer coefficients at the interface between the bubbles and the subcooled liquid, as long as a reasonable value is used. The void fraction is more sensitive to the liquid enthalpy at which net vapor generation occurs (h_{ld}), and to the distribution of the surface heat flux going into vapor generation versus liquid superheat at the wall (q''_1). The Saha-Zuber criterion is used for h_{ld} and the Rouhani-Bowring model is used to calculate the fraction of the wall heat flux to the liquid, q''_1 [1]. Of these, the void fraction is most affected by h_{ld} . Reference 20 shows that the scatter in the prediction of the subcooling at the net vapor generation point, $h_f - h_{ld}$, can be bounded by \pm [[]]. Comparisons to 8x8 bundle void fraction data show that the larger scatter in the void fraction for low qualities in the subcooled boiling region ([[]]) for the fully developed nucleate boiling region) is covered when a [[]] perturbation is applied to the subcooling for the onset of net vapor generation. The mean error is also slightly larger for subcooled boiling ([]). The statistical analysis of the comparison to the subcooled void fraction data is shown in Figure 5.1-2.

A [[]] variation in the subcooling for onset of net vapor generation corresponds to an average of [[]] and a maximum of [[]] variation in the void fraction for the subcooled boiling region. Therefore a 1σ uncertainty of [[]] is assigned for this model. The impact on the calculated void fraction at the FRIGG test conditions of a PIRT multiplier (PIRT23) value of [[]] is seen in Figure 5.1-3.

[[

]]

Figure 5.1-2. FRIGG OF64 Void Fraction Data – Subcooled Boiling

[[

]]

Figure 5.1-3. Void Fraction Sensitivity to PIRT23

C3AX Pellet Heat Distribution, H

The pellet power distribution is calculated by lattice physics codes and provided as an input to TRACG. Uncertainties in this parameter are reflected in the pellet temperature distribution, which is the parameter for which data are available. [[

]] Sensitivity studies show that the distribution calculated by lattice physics codes provides conservative results compared to a flat power distribution.

C3BX Pellet Heat Transfer Parameters, H

The TRACG fuel rod model is based on the GESTR model [21]. The uncertainty in measured fuel centerline to coolant temperature differences is [[]] and includes uncertainty in gap size and conductance, pellet conductivity and power distribution. The uncertainties in pellet power distribution, pellet conductivity and gap conductance are lumped into a single uncertainty in the fuel conductivity, in qualifying the overall model against fuel temperature data. The dominant resistance is the pellet conductivity; an [[]] variation in the pellet conductivity corresponds to the [[]] observed uncertainty in the centerline to coolant difference, while the gap conductance needs to be varied by a factor of [[]] to produce the same variation in the temperature difference as shown in Figure 5.1-4 and Figure 5.1-5. In these figures, PIRT27 is a multiplier on the fuel thermal conductivity and PIRT28 is the multiplier on the gap conductance. When the gap conductance is increased, the resistance over the gap becomes insignificant compared to the thermal resistance of the pellet, and it is not possible to vary the temperature difference to the 2σ level needed to produce a 95% probability estimate. Furthermore, normal distribution in the gap conductance would not produce a normal distribution in the center to fluid temperature difference due to the highly non-linear relationship between the gap conductance and the fuel center to fluid temperature difference.

[[

]]

[[

]]

Figure 5.1-4. Sensitivity of Fuel Center to Fluid Temperature Difference for 8x8 Fuel

[[

]]

Figure 5.1-5. Sensitivity of Fuel Center to Fluid Temperature Difference for 9x9 Fuel

C3CX Gap Conductance, H

[[

]]

C3DX Direct Moderator Heating, M

The direct moderator heating (DMH) is the energy released into the moderator as the fast neutrons are slowed down. [[

]] The uncertainty in the direct moderator heating is given by the uncertainty in the moderator density, which is determined by the uncertainty in the void fraction (C2AX), and by the uncertainty in the cross section, which is primarily determined by the variation with exposure. The direct moderator heating has been determined based on detailed Monte Carlo calculations with MCNP01A [3]. The DMH model implemented in TRACG accounts for the dependency on moderator density and there is no bias in predicting the mean total amount of direct moderator heating when the default inputs are used. The variation in the direct moderator heating with exposure is not explicitly modeled in TRACG, since, together with all other uncertainties, it results in less than [[]] uncertainty in the total amount of DMH. The TRACG model also accurately accounts for how direct moderator heating is distributed in the active channel (in-channel) and in the bypass and water rods (out-channel). This is confirmed by the fact that the uncertainties of the individual components compared to the MCNP predictions are only slightly larger than the uncertainty for the total.

A [[]] uncertainty is applied to the total amount of direct moderator heating in order to bound the overall uncertainty in both the amount and the distribution of the direct moderator heating. It is appropriate to consider this uncertainty to be normally distributed as indicated in Reference 3:

C8 Multiple Channel Effect, H

The flow distribution between parallel flow paths such as the fuel channels in the core is controlled by the hydraulic characteristics of the channels. The flow in each individual channel is controlled by the pressure drop components such as static head (given by the void fraction), friction and accelerational pressure drop. Therefore, the uncertainty in the flow in the individual channels and the parallel channel effects are covered by the uncertainty in the interfacial shear and the friction factors. The uncertainty in the interfacial shear is defined in Item C2AX and the uncertainty in friction factors is defined in Item C24.

In addition to the uncertainty in void fraction and friction, the channel pressure drop is dependent on the channel power level and axial distribution. The modeling of the core is derived from the code qualification studies in Reference 2. [[

]]

C10 Void Distribution, H

The uncertainty in the void fraction distribution is included through an uncertainty in the interfacial shear. The uncertainty in interfacial shear is defined in Item C2AX.

C11 Channel – Bypass Leakage Flow, M

The channel leakage flow is based on full-scale measurements for conditions covering the range of expected reactor conditions [22]. [[

]]

C12 Natural Circulation Flows, H

Natural circulation is controlled by a balance between buoyancy and friction. Therefore, the uncertainty in this phenomenon is covered by the uncertainty in interfacial shear (which determines the void fractions) and the uncertainty in the friction factors and form losses. The uncertainty in interfacial shear is defined in Items C2AX, E2 and F1, and the uncertainty in frictional losses is defined in Items A11, C24 and I3.

C23 Water Rod Hydraulics, M

The flow through the water rods is controlled by a calibrated horizontal orifice in the rod. There is a small uncertainty in the loss coefficient. [[

]]

C24 Core Pressure Drop, H

The core pressure drop is composed of static head given by the void fraction, accelerational pressure drop and friction. The uncertainty in the core pressure drop is therefore covered by the uncertainty in the interfacial shear and friction. The uncertainty in interfacial shear is defined in Item C2AX.

TRACG uses the GE design correlation for the wall friction, [[

]] is based on extensive comparisons to rod bundle pressure drop data [1] from BWR bundles. For single-phase flow in smooth pipes TRACG predicts the pressure drop with an accuracy of [[

]] For two-phase flow, the majority of the comparisons with the [[correlation have been made for rod bundle data. Data for GE14

10x10 fuel shows a [[]] Based on this data, it is judged that [[

]] is adequate for all other applications. The components of the flow losses in the fuel bundle and the uncertainty associated with each component are discussed in the following paragraphs.

The side entry orifice and lower tie plate frictional pressure drop is based on full-scale measurements for conditions covering typical reactor operating conditions. The inlet orifice is a sharp-edged orifice with a well-defined flow coefficient. The inlet region upstream of the lower tie plate has turning losses and a flow expansion at the inlet. The lower tie plate accounts for approximately one third of the total pressure drop. Reference 1 shows that the typical scatter in the loss coefficient for the lower tie plate is of the order of [[]]. Data from GE's single-phase pressure drop test facility show that the uncertainty for the combined pressure drop for the side entry orifice and the lower tie plate pressure drop is approximately [[]], when the entire uncertainty is assigned to the lower tie plate. The exact values for the biases and uncertainties for the 9x9 and 10x10 side entry orifices and lower tie plates are given in Table 5.1-1.

Table 5.1-1:

Bias and Uncertainty in Pressure Drop for 9x9 and 10x10 SEO and Lower Tie Plates

[[]]			

]]

[[

]]

The spacer frictional pressure drop is based on full-scale measurements for conditions covering the range of expected reactor conditions. For 9x9 and 10x10 fuel spacers the uncertainty in the pressure drop for the spacers is determined from full-scale ATLAS data and varies from [[]], depending on bundle type. The average uncertainty for all fuel designs is of the order of [[]]. The bias and uncertainty for current fuel products are given in Table 5.1-2.

Table 5.1-2:

Bias and Uncertainty in Pressure Drop for 9x9 and 10x10 Spacers

[[]]					

]]

The upper tie plate frictional pressure drop is based on full-scale measurements for conditions covering the range of expected reactor conditions. For 9x9 and 10x10 fuel upper tie plates, the uncertainty in the pressure drop is [[]] [51]. The bias and uncertainty for current fuel products are given in Table 5.1-3.

**Table 5.1-3:
Bias and Uncertainty in Pressure Drop for 9x9 and 10x10 Upper Tie Plates**

[[

]]

Qualification of TRACG against full-scale bundle pressure drop data from the ATLAS facility for an 8x8 bundle with ferrule spacers [2] has shown that TRACG predicts the bundle pressure drop with a bias of [[]] and a standard deviation of [[]]. These comparisons for total pressure drop are consistent with the above uncertainties for the side entry orifice, lower tie plate, spacers and upper tie plate.

For stability analysis, it is important to vary not only the total pressure drop, but also the single phase and two-phase components separately. Based on the preceding discussion, the following approach will be adopted.

[[]].

E2 Downcomer Void Profile / Two-Phase Level, H

The downcomer void fraction is determined by the interfacial drag coefficient, C_i . An appropriate uncertainty range for C_i was obtained for large hydraulic diameter regions as discussed below under F1. The downcomer two-phase level is an initial condition depending on the plant operating state. The uncertainty in this parameter is discussed in Section 6.

F1 Chimney and Upper Plenum Void Profile, H

The chimney void distribution is controlled by the interfacial drag coefficient, C_i . An appropriate uncertainty range for C_i was obtained on the basis of TRACG predictions of void fraction data from separate-effects tests by [[]].

These data are characterized by their applicability to the prediction of void fraction in regions with relatively large hydraulic diameter. Accordingly, they will be used as the basis for defining the uncertainty in interfacial drag in all regions of the reactor except the core and bypass. A statistical summary of the comparisons of TRACG predictions with measurements from these four data sets, combined as a single set of deviations, is shown in Figure 5.1-6. [[]]

]].

[[

Figure 5.1-7 [[

]]. The results are shown in

]].

[[

]]

Figure 5.1-6. Void Fraction Deviations for Tests Applicable to Regions with Large Hydraulic Diameter

[[

]]

Figure 5.1-7 Sensitivity of TRACG Prediction of Average Void Fraction in EBWR Test Facility to PIRT Multiplier on Interfacial Drag Coefficient

[[

]]

Figure 5.1-8 Probability Distribution for Multiplier on Interfacial Drag Coefficient

[[

]].

F6 Interaction between Chimney Cells H

No additional model uncertainties need to be considered for this phenomenon, as it covered by the core, bypass and chimney interfacial and wall shear models, namely C24, B14, F1. [[

]].

I1 Separator Carryunder, M

Separator carryunder affects the core inlet subcooling and hence the decay ratio for stability calculations. Carryunder is calculated by the TRACG separator model. Typical values of carryunder at normal operation are of the order of [[]]. An uncertainty of [[]].(absolute) bounds the differences between TRACG and separator data and will be used as an estimate of the 1σ uncertainty in the model.

I3 Separator Pressure Drop, H

The loss correlations for the separator pressure drop in TRACG are best fit to two and three stage separator pressure drop data [2]. 95% of the data falls within [[]] of the correlation, which has been implemented into TRACG. 95% corresponds to the 2σ level and therefore 6% is a good approximation for the 1σ uncertainty in separator pressure drop.

5.2 EFFECTS OF NODALIZATION

The nodalization strategy for the various reactor components was developed from the qualification of TRACG against test data for these components. The same consistent nodalization strategy was then applied for full-scale plant calculations. The adequacy of the nodalizations has been demonstrated and supported by sensitivity studies. Standard nodalizations for modeling of BWR reactor vessels and other components have been presented in the *TRACG Qualification Report* [2]

The nodalization for stability involves some refinements in the axial nodalization of the channel component near the boiling boundary and in the channel grouping [2]. This is discussed in more detail below. Also, the ESBWR geometry with the partitioned chimney requires special consideration. [[

]].

5.2.1 VESSEL NODALIZATION FOR ESBWR STABILITY ANALYSIS

Figure 5.2-1 shows the axial and radial nodalization of the ESBWR vessel. The axial levels and radial rings are the same as used previously for AOO analysis for the ESBWR [24], [[

]].

5.2.2 DETAILED NODALIZATION SCHEME FOR THE CHANNEL COMPONENT

[[

]]

5.2.3 CHANNEL GROUPING FOR STABILITY APPLICATIONS

Individual fuel bundles in the core may be modeled in TRACG as individual channels or may be grouped together into a single TRACG channel component. Because of current code limitations within TRACG on the number of components allowed, it is not possible to model every fuel bundle as a single TRACG channel. Consequently, it is necessary to group or combine individual fuel bundles into thermal hydraulic groups. [[

]]

The channels are grouped based on (a) hydraulic considerations to separate hydrodynamic characteristics and (b) neutron kinetics considerations to separate dynamic power sensitivity characteristics.

The channel grouping accounts for additional TRACG capability in the areas of limiting channel response, peripheral channel grouping, and vessel modeling detail. [[

]]

Figure 5.2-4 shows the typical grouping of channel components for stability analysis. [[

]].

[[

]].

**Table 5.2-1:
Void Distribution at the Top of the Bypass Region**

[[

]]

[[

]]

Figure 5.2-1: Axial and radial nodalization for ESBWR Stability Analysis

[[

]]

Figure 5.2-2: Channel Nodalization Studies from Reference 2

[[

]]

Figure 5.2-3: R- θ Nodalization for ESBWR Stability Analysis

[[

]]

Figure 5.2-4: Channel Grouping for ESBWR Stability Analysis

5.3 EFFECTS OF SCALE

Effects of scale have been specifically addressed as part of the model development as well as the qualification. In the TRACG model description report [1], the ranges of applicability of the basic models and correlations are stated and shown to cover the scale and operating range of BWRs [Table 6.0-1 of Reference 1]. This is a *necessary* condition for the validity of TRACG calculations for the full-scale BWR.

The qualification of TRACG [2] covers separate-effects tests, full and reduced scale component performance tests, scaled integral system effects tests, and full-scale BWR plant tests. Accurate predictions of data at various scales (up to a sufficiently large scale) constitute a *sufficient* condition for the validity of TRACG calculations for full-scale plants. In general, the qualification results show that both data from scaled test facilities as well as full-scale plant data are well predicted, and that there is no apparent effect of scale in the TRACG calculations.

The conclusion that there is no effect of scale in the TRACG calculations is substantiated in this section.

5.3.1 FULL SCALE TEST COVERAGE

Table 4.2-2 shows the coverage of the Medium and High ranked PIRTs for stability by test data. A number of ESBWR components have been tested at full scale. [[

]].

5.3.2 OPERATING PLANT DATA

Tests performed at BWR plants validate a number of phenomena that are highly ranked for stability. [[

]].

The most relevant and important plant data are the stability measurements that have been made at various BWRs [2]. Data have been obtained for both core wide and regional stability at various plants. [[

]]. The applicability of these data for the ESBWR has been evaluated by comparing the range of important parameters in the plant data with the corresponding ranges for the ESBWR. This comparison is shown in Table 5.3-1.

[[

]]

The void coefficient for ESBWR is at the lower end of the range of operating BWR cores. This results in favorable stability characteristics.

The power to flow ratio (which approximates the average exit quality) for the ESBWR is compared with operating plants in Figure 5.3-1. A line of constant power to flow ratio corresponding to the ESBWR rated conditions is denoted by the dashed line from the origin. The operating plant comparisons are for ABWR and Clinton, at uprated power. The extended operating domain is also shown for both plants. For Clinton, this is the MELLLA+ domain. [[

]].

The radial peaking for the ESBWR core is similar to that for operating plant cores. Thus, the comments for average power-to-flow ratio apply to the hot bundle power to flow ratio.

[[

]]

The ratio of single phase to two-phase pressure drop in the ESBWR core is similar to, but more favorable than, that for operating BWRs.

In summary, TRACG has been validated over a range of plant stability data and no additional uncertainty is needed to account for scale-up effects.

**Table 5.3-1:
Range of Key Stability Parameters - ESBWR vs. Operating Plant Data**

[[

]]

[[

]]

Figure 5.3-1: Comparison of Power and Flow per Bundle for ESBWR vs. Operating BWRs

[[

]]

Figure 5.3-2: Variation in Harmonic Sub-criticality vs. Core Size

5.4 SENSITIVITY ANALYSIS

Sensitivity studies have been performed, varying each highly ranked model parameter from -1σ to $+1\sigma$. These results are shown in Section 8. These studies serve to identify the parameters that have the largest impact on the calculated safety parameters (decay ratios).

6.0 APPLICATION UNCERTAINTIES AND BIASES

Code inputs can be divided into four broad categories: (1) geometry inputs, (2) model selection inputs, (3) initial condition inputs, and (4) plant parameters. For each type of input, it is necessary to specify the value for the input. If the calculated result is sensitive to the input value, then it is also necessary to quantify the uncertainty in the input.

The geometry inputs specify lengths, areas and volumes. Uncertainties in these quantities are due to measurement uncertainties and manufacturing tolerances. These uncertainties usually have a much smaller impact on the results than do uncertainties associated with the modeling simplifications.

Individual geometric inputs are the building blocks for the spatial nodalization. The spatial nodalization includes modeling simplifications such as the lumping together of individual elements into a single model component. For example, several similar fuel channels are lumped together and simulated as one fuel channel group. An assessment of these kinds of simplifications, along with the sensitivities to spatial nodalization, is included in the TRACG Qualification LTR [2].

Inputs are used to select the features of the model that apply for the intended application. Once established, these inputs are fully specified in the procedure for the application and do not change.

A plant parameter is defined as a plant-specific quantity such as a protection system scram characteristic, etc. Plant parameters influence the characteristics of the transient response and have essentially no impact on steady-state operation.

Initial conditions are those conditions that define a steady-state operating condition. Initial conditions may vary due to the allowable operating range or due to uncertainty in the measurement at a given operating condition. The plant Technical Specifications and Operating Procedures provide the means by which controls are instituted and the allowable initial conditions are defined. At a given operating condition, the plant measurement system has inaccuracies that also must be accounted for as an uncertainty.

6.1 KEY INITIAL CONDITIONS AND PLANT PARAMETERS

Table 6.1-1 lists the key plant initial conditions that are high ranked for the stability application. There are no plant parameters that are relevant to the stability analysis. The second column describes how the initial conditions are controlled during operation. The uncertainty is specified in Column 3. The 'Comments' column indicates the "PIRT" parameters that are varied for the TRACG analysis. These are special inputs that allow coefficients in TRACG correlations to be varied for the purpose of uncertainty analysis.

]]

Table 6.1-1 Notes

[[

II

7.0 COMBINATION OF UNCERTAINTIES

A proven Monte Carlo technique is used to combine the individual biases and uncertainties into an overall bias and uncertainty. The Monte Carlo sample is developed by performing random perturbations of model and plant parameters over their individual uncertainty ranges. Using the histogram generated by the Monte Carlo sampling technique, a probability density function is generated for code output of the primary safety criteria parameters. The determination of decay ratio with TRACG is a two-step process. The Monte Carlo trials produce a distribution of plant initial conditions. The decay ratio for each initial condition is then obtained by examining the response to a pressure or flow impulse function. The probability distribution function of decay ratios thus includes the variability in the initial conditions as well as the transient response.

In order to determine the total uncertainty in predictions with a computer code, it is necessary to combine the uncertainties due to model uncertainties (CSAU Step 9), scaling uncertainties (CSAU step 10), and plant condition or state uncertainties (CSAU Step 11). Various methods have been used to combine the effects of uncertainties in safety analysis. This section briefly summarizes different methods for combining uncertainties. All these approaches are within the framework of the CSAU methodology, since the CSAU methodology does not prescribe the approach to use. The method for combining uncertainties that is used for application to ESBWR stability analyses is the same approach that has been successfully used and approved by the NRC for the analyses of AOO transient scenarios [3].

7.1 TRADITIONAL BOUNDING ANALYSIS

A commonly used approach in traditional conservative analysis is to combine the uncertainties linearly, by taking bounding models for the phenomena and by setting plant parameters to limits expected to produce the most limiting plant response. Separate calculations may be required to obtain bounding results for different response parameters, because it may not be possible to define a single 'worst case' that will result in all key response or output parameters being calculated at their upper bounds. In any case, an advantage of this approach is that it requires no more than one computer run for each output parameter of interest. The most significant disadvantages with this method are that it is very conservative, in extreme cases can give unrealistic results; and no statistical quantification of the margins to design limits is possible. This bounding approach has historically been used for stability analysis.

7.2 STATISTICAL TREATMENT OF OVERALL CALCULATIONAL UNCERTAINTY

An improved approach employs realistic plant calculations for the evaluation of the primary safety criteria using realistic models and nominal input for the plant parameters. An uncertainty is then added on to the calculated primary safety parameters to account for modeling uncertainty, uncertainty in plant operation and state, and other effects such as effect of scale on the calculations. A statistical approach is used to determine the added uncertainty on top of the nominal calculation. Realistic models and input are used for all processes and inputs, and the design calculation accounts for uncertainties in all major models and plant parameters.

7.3 COMPARISON OF APPROACHES FOR COMBINING UNCERTAINTIES

Several options exist to perform the statistical combination of the uncertainties. Neither the CSAU methodology report [8] nor NRC Regulatory Guide 1.157 [9] specifies how this should be done. Some possible options are summarized in Table 7.3-1.

These options are discussed and compared in the following paragraphs. Justification for use of the Monte Carlo method follows.

**Table 7.3-1:
Methods for Combining Uncertainty**

Method	Description
Propagation of Errors	Uncertainties in the calculated safety parameters to individual phenomena are evaluated from single perturbations and the overall uncertainty is determined as the square root of the sum of the square of the individual uncertainties.
Response Surface Technique	Response surface for the safety parameter is generated from parameter perturbations. Statistical upper bound value determined from Monte Carlo Method using response surface.
Order Statistics (OS) Method - Single Bounding Value	Monte Carlo Method using random perturbations of all important parameters. Statistical upper bound determined from most limiting perturbation (for first order statistics).
[[]]	[[]]

7.3.1 PROPAGATION OF ERRORS

In the Propagation of Errors method, the uncertainties are combined by taking the square root of the sum of the squares (SRSS) of the individual uncertainties. In this approach, the effects of individual phenomena on key response parameters are determined, and then combined using SRSS. For this approach, a relatively small number of computer runs is required. The number of runs required is directly related to the number of input parameters for which uncertainty ranges have been established. This approach is justifiable if the effects on the calculated responses of the phenomena whose uncertainties are being accounted for are independent of each other. For complex processes requiring complex code calculations, independence rarely exists and is difficult to demonstrate. A secondary requirement for this approach is that all input and output parameters can be modeled by a normal distribution.

7.3.2 RESPONSE SURFACE TECHNIQUE

In this method, individual model and plant parameters are perturbed and the sensitivity of the primary safety parameter to these perturbations is determined. The process begins by examining each model and plant parameter uncertainty. Using test data and expert knowledge, each parameter is assigned a probability density function (i.e., normal, log normal, exponential, uniform, etc.). The probability density function (PDF) describes the method by which the uncertainty would vary from the expected value. The range for each PDF is determined from the standard deviation, if known, or by the maximum and minimum value of the parameter. As an example, the uncertainty in fuel conductivity is distributed normally with a nominal (mean) value of 0 % and a standard deviation of 13%. According to conventional response surface techniques, a large number of transient simulations per each event scenario would be needed due to the large number of parameters to be varied. At least two cases would be required (in addition to the nominal calculations) for each important plant and model parameter to quantify the responses to $\pm\sigma$ perturbations. Additional cases would be needed to quantify $\pm 2\sigma$ and $\pm 3\sigma$ perturbations if the output responses did not vary linearly with the input perturbations. Furthermore, many cases would have to be made, where several parameters are perturbed simultaneously to account for covariances. A response surface would be determined from all the cases, and Monte Carlo analysis would be used to determine the 95% fractile. This method is advantageous when few parameters are involved, but is impractical when a large number of parameters are involved due to the prohibitively large number of perturbations needed to account for non-linearities and covariances.

In the PIRTs in Section 3, over 20 high and medium ranked phenomena are identified that would need to be treated statistically. Assuming one input parameter per phenomena and ignoring other uncertainties associated with initial conditions and plant parameters, it is possible to estimate how many calculations are required. To run the base case, the $\pm 1\sigma$, $\pm 2\sigma$, and $\pm 3\sigma$ perturbations would require over 120 transient simulations per event scenario. Similarly, an even larger number of calculations would be needed to evaluate covariances. However, an important advantage is that single parameter perturbations provide useful insight by identifying the most sensitive parameters.

7.3.3 ORDER STATISTICS (OS) METHOD – SINGLE BOUNDING VALUE

The Monte Carlo method that has been used in Germany by Gesellschaft für Anlagen-und Reaktorsicherheit (GRS) [32] and for the application of TRACG to AOOs by GE [3] requires only a modest number of calculations, and automatically includes the effects of interactions between perturbations to different parameters. In the OS method, Monte Carlo trials are used to vary all uncertain model and plant parameters randomly and simultaneously, each according to its uncertainty and assumed probability density function (PDF), and then a method based on the order statistics of the output values is used to derive upper tolerance bounds (one-sided, upper tolerance limits OSUTLs).

Monte Carlo sampling of each parameter according to its assigned PDF yields the value of that parameter to be used for a particular trial. Given such a trial set of input parameters, the calculation process determines the corresponding output parameter of interest. Therefore, while the void coefficient might be set at a -1.5σ value, interfacial shear might be set to a value of $+2.0\sigma$, each according to its own probability model. In this manner, the effects of interactions between all model parameters are captured in a single calculation. Once all of the trials have been completed, the desired output parameter (e.g., decay ratio) is extracted from each of the trials and the set of parameter values is then used to construct an OSUTL for that particular output parameter. Figure 7.3-1 illustrates this process.

[[

]].

An OSUTL is a function $U = U(x_1, \dots, x_n)$ of the data x_1, \dots, x_n (which will be the values of an output parameter of interest in a set of Monte Carlo trials), defined by two numbers $0 < \alpha, \beta < 1$, so that the proportion of future values of the quantity of interest that will be less than U is $100\alpha\%$, with confidence at least $100\beta\%$ --- this is called an OSUTL with $100\alpha\%$ -content and (at least) $100\beta\%$ confidence level.

The order statistics method, originally developed by Samuel Wilks, produces OSUTLs that are valid irrespective of the probability distribution of the data, requiring only that they be a sample from a continuous PDF. [[

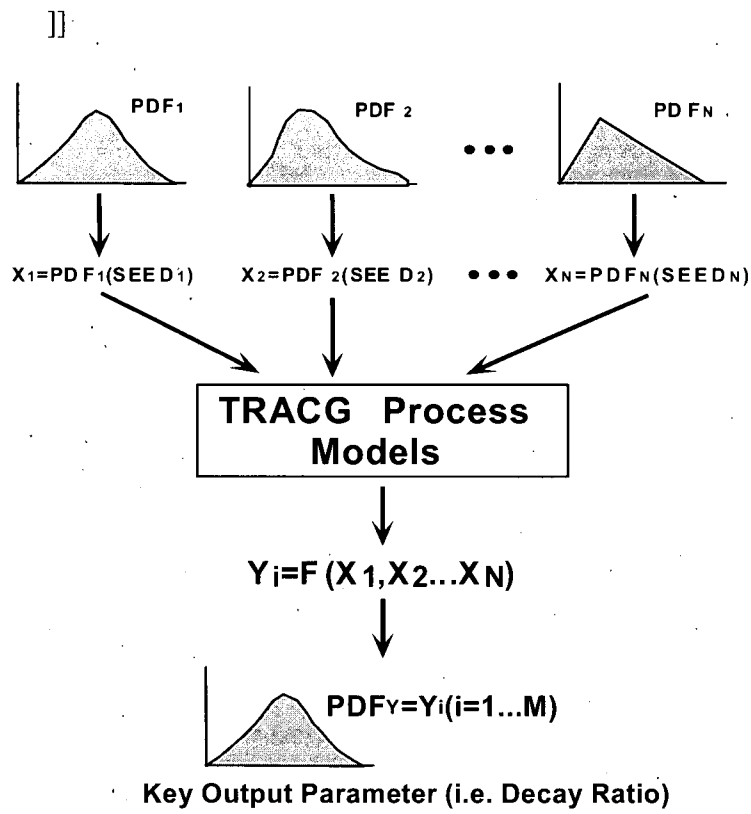


Figure 7.3-1. Schematic Process for Combining Uncertainties

7.3.4 NORMAL DISTRIBUTION ONE-SIDED UPPER TOLERANCE LIMIT

[[

]]

7.4 RECOMMENDED APPROACH FOR COMBINING UNCERTAINTIES

[[

]].

This approach to determine the total uncertainty has several advantages over other approaches as summarized in Table 7.4-1. The following expands on the discussion of these advantages:

[[

▪

]].

- A separate response surface does not have to be developed for each output parameter of interest.
- It allows for different specifications of the distributions of the uncertainties: for example, some can be specified as having a uniform distribution and some can be specified with a normal distribution. (This advantage is not unique to this method: Monte-Carlo sampling with a response surface will also allow this.)

[[

]]

Table 7.4-1
Comparisons of Methods for Combining Uncertainties

Method for Combining Uncertainties	Advantages	Disadvantages
Propagation of Errors	Relatively small number computer runs, when the number of input variables is small. The number of cases is linearly related to the number of input parameter uncertainties considered.	Approximate, because it involves linearization. Necessary to demonstrate independence of effects of individual uncertainties on responses, or else must include covariances explicitly.
Response Surface	Very precise statistical characterization of results can be achieved with a large number of Monte Carlo Trials using response surface. Different distributions can be specified for each input uncertainty. Independence of the effect of individual input parameters on response is not necessary.	Number of computer runs depends on the response surface model and increases exponentially with the number of input parameter uncertainties considered. A separate response surface must be fitted for each output variable of interest. Interactions between input parameters have to be established and considered in the development of the response surface.
[[]].
[[]].

7.5 IMPLEMENTATION OF STATISTICAL METHODOLOGY

The purpose of this section is to describe the process by which the statistical results will be used to (1) determine decay ratios for channel stability and core wide stability, and (2) establish that these safety parameters have acceptable margins to design limits.

[[

]].

7.5.1 CONFORMANCE WITH DESIGN LIMITS

The method described in Section 7.4 is applied in the following process. The number of trials may be increased to increase the confidence level for the statistical analysis.

- Identify all High and Medium ranked parameters uncertainties from Section 5 for the stability type to be analyzed. These parameters will be utilized in the statistical analysis.

[[

]]

8.0 DEMONSTRATION ANALYSES

This section presents sample results to demonstrate the application methodology for ESBWR stability analysis. Calculations made on a nominal best-estimate basis are termed "Baseline Analysis" results. These calculations are made for channel and core decay ratios. Nominal regional decay ratios are also calculated. The purpose of the regional decay ratio calculations is to provide confidence in the approach of using the channel and core-wide decay ratio map for licensing analysis.

Sensitivity studies are performed to examine the effects of the High and Medium ranked parameters on the channel and core-wide decay ratios. Uncertainties are statistically combined for the channel and core-wide decay ratios with the Monte Carlo technique discussed in Section 7. These values are compared against the design limits at the 2σ confidence level.

8.1 BASELINE ANALYSIS

The ESBWR plant has 1132 bundles and a rated thermal power of 4500 MWt. The vessel modeling is illustrated in Figure 8.1-1 and Figure 8.1-2. The plant has an equilibrium core of GE14 10x10 fuel. Figure 8.1-2 also shows the average bundle power in the various core sectors. The bundles in Ring 3 are grouped into two groups, with the bundles with inlet orificing corresponding to the peripheral region having a much lower average power level. Figure 8.1-3 illustrates the TRACG core map showing the thermal hydraulic channel groups. The number of channels in each thermal hydraulic group and the peaking factors for each group are shown in Table 8.1-1. Channel groups were created based on core position, chimney position, orifice geometry, and peaking factor. [[

]]

A sensitivity study was performed by further subdividing the larger groups based on channel power differences. The results (reported in Section 8.1.2.2) showed very little sensitivity and confirm that the chosen grouping is adequate for representing the ESBWR core for stability analysis.

Analysis was conducted at various points in the cycle: Beginning of Cycle (BOC), Middle of Cycle (MOC) near the peak reactivity state, and End of Cycle (EOC). Figure 8.1-4 shows the core average axial power profiles at these exposures. [[

]]

[[

]]

A baseline analysis was performed for the ESBWR at rated conditions, which are the most limiting from the perspective of stability due to the highest power/flow ratio. In addition, Anticipated Operational Occurrences (AOOs) that could lead to more severe conditions of power and flow were also examined. Figure 8.1-7 shows the natural circulation operating curve for the ESBWR. Two transients can lead to more limiting states for stability. A Loss-of-Feedwater (LOFW) event will lead to a drop in the level until a scram occurs on low level (Level 3). The lowest level and correspondingly, the lowest core flow are reached just prior to scram. The power/flow trajectory for this transient is shown in Figure 8.1-7. The end point is determined by the Level 3 scram, and leads to a more severe power/flow ratio than at rated conditions. A Loss-of-Feedwater Heater (LOFWH) transient results in an increase in power due to the reactivity addition by the colder feedwater. The event is terminated by a scram on high thermal power. The trajectory for this transient is also shown in Figure 8.1-7. The highest power/flow ratio is reached just prior to the scram.

8.1.1 CHANNEL STABILITY RESULTS

Channel stability analysis was performed by perturbing the flow to the high power channels while keeping the power constant. The calculation process is as follows:

[[

]]

8.1.1.1 SUPER BUNDLE STABILITY

[[

]]

8.1.2 CORE WIDE STABILITY RESULTS

Core stability was evaluated at BOC, MOC and EOC conditions. The calculations were made with the 3-D kinetics model interacting with the thermal hydraulics parameters. The calculation sequence is as follows:

[[

]]

8.1.2.1 SENSITIVITY TO METHOD OF PERTURBATION

[[

]]

8.1.2.2 SENSITIVITY TO CHANNEL GROUPING

[[

]]

8.1.2.3 SENSITIVITY TO TIME STEP SIZE

Stability studies with TRACG are performed using the explicit integration technique in the core. The time step size is then set by a Courant number of 1 in the limiting cell. Typically, this cell is in the heated portion of the active channel. In the calculations performed in the previous section it was found that the Courant number was set by the velocities in the first, small cell of the water rod. In order to eliminate a possible bias due to a smaller time step size, the small cell at the inlet of the water rod was removed, so that the Courant number limit was in the channel. The results showed negligible differences in the decay ratio due to this change in time step size for both channel and core wide stability.

8.1.3 REGIONAL STABILITY RESULTS

[[

]]

**Table 8.1-2:
Higher Harmonic Mode Sub-criticality at Different Exposures**

[[

]]

**Table 8.1-3:
Initial Conditions for Channel and Core Stability Analysis**

[[

]]

[[

]]

Figure 8.1-1. TRACG ESBWR Vessel R-Z Modeling

[[

]]

Figure 8.1-2: R- θ Nodalization of ESBWR Core Region showing Average Power (MW) in Each Region

[[

]]

Figure 8.1-3: TRACG Channel Grouping for ESBWR Core

[[

]]

Figure 8.1-4: Core Average Axial Power Shape at Different Exposures

[[

]]

Figure 8.1-5: Flux Distribution for First Azimuthal Harmonic with Axis of Symmetry

[[

]]

Figure 8.1-6: Flux Distribution for Second Azimuthal Harmonic with Axis of Symmetry

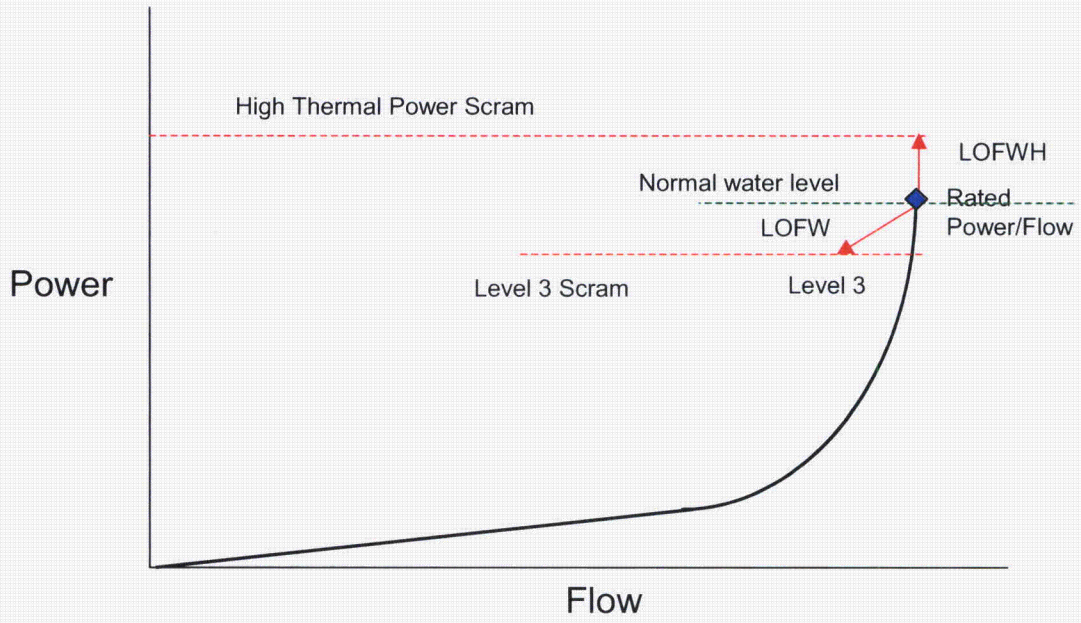


Figure 8.1-7: ESBWR Natural Circulation Operation with Limiting Conditions for Stability Analysis

[[

]]

Figure 8.1-8: Hot Bundle Flow Response to Transient Inlet Flow Perturbation

[[

]]

Figure 8.1-9: Hot Super Bundle Flow Response to Transient Inlet Flow Perturbation

[[

]]

Figure 8.1-10: Core Power Response to Transient Turbine Inlet Pressure Perturbation

[[

]]

Figure 8.1-11: Sensitivity to Perturbation Size

[[

]]

Figure 8.1-12: Power Distribution by Channel in Large Sectors in Ring 1

[[

]]

Figure 8.1-13: Power Distribution by Channel in Large Sectors in Ring 2

[[

]]

Figure 8.1-14: Finer Channel Grouping by Power Level

[[

]]

Figure 8.1-15: Sensitivity to Detailed Channel Grouping

[[

]]

Figure 8.1-16: Power Distribution for First Harmonic

[[

]]

Figure 8.1-17: Core Map showing Products of Fundamental and First Harmonic Powers
(Regions with highest absolute values are shown in dark brown)

[[

]]

Figure 8.1-18: Channel Grouping for Regional Stability Calculation (darker colored regions have higher absolute peaking)

[[

]]

Figure 8.1-19: Channel Power Responses to Out-of-Phase Flow Perturbation

[[

]]

Figure 8.1-20: Symmetrically Located Channel Power Responses to Out-of-Phase Flow Perturbation

8.2 SENSITIVITIES TO HIGH AND MEDIUM RANKED PARAMETERS

Sensitivity studies were performed for the High and Medium ranked PIRT parameters from Table 4.2-2. The parameters were ranged to their $\pm 1\sigma$ levels for the normally distributed parameters, and to the ends of their expected range for the others. [[

]]

8.2.1 CHANNEL DECAY RATIO

[[

]]

Table 8.2-1 shows the sensitivity study results. The physical parameter varied is shown in the first column with (H) in parentheses if it was ranked High. The "PIRT Multiplier" in TRACG is shown in the second column; the suffix M denotes a reduction in the multiplier (relative to the nominal value of 1) and the suffix P denotes an increase. (The feedwater enthalpy is changed via input). The range of variation is shown in the next column. The sensitivity in channel decay ratio is shown in the last column. [[

]]

8.2.2 CORE DECAY RATIO

[[

]]

Table 8.2-2 shows the sensitivity study results for the core decay ratio. The columns in the table are the same in Table 8.2-1. The additional parameters included are the void coefficient and the fuel conductivity. [[

]]

8.3 STATISTICAL ANALYSIS OF ESBWR STABILITY

Monte Carlo analyses were performed to assess the uncertainty in the calculation of the core and channel decay ratios associated with the model and application uncertainties (Sections 5 and 6). The probability distributions obtained from the Monte Carlo trials are used to estimate the One-Sided Upper Tolerance Limits (OSUTL) that bound 95% of the content with 95% confidence as discussed in Section 7.

8.3.1 CHANNEL DECAY RATIO STATISTICAL ANALYSIS

[[

]]

8.3.2 CORE WIDE DECAY RATIO STATISTICAL ANALYSIS

[[

]]

8.3.3 REGIONAL DECAY RATIO STATISTICAL ANALYSIS

[[

]]

8.3.3.1 SENSITIVITY TO TIME STEP SIZE

Stability studies with TRACG are performed using the explicit integration technique in the core. The time step size is then set by a Courant number of 1 in the limiting cell. Typically, this cell is in the heated portion of the active channel. In the calculations performed in the previous section it was found that the Courant number was set by the velocities in the first, small cell of the water rod. In order to eliminate a possible bias due to a smaller time step size, the small cell at the inlet of the water rod was removed, so that the Courant number limit was set in the channel. A calculation was performed for the limiting Monte Carlo trial. The results showed an increase in the decay ratio of 0.03 due to this change in time step size. This difference in decay ratio will be applied as a bias to all the regional decay ratio calculation results.

8.3.4 COMPARISON WITH DESIGN LIMITS

In Section 2.2, design requirements were established for the channel, core and regional decay ratio. Figure 8.3-10 shows the stability map with the design criteria. [[

]]

[[

]]

Figure 8.3-1: Monte Carlo Trials for Channel Decay Ratio

[[

]]

Figure 8.3-2: Monte Carlo Results for Channel Flow

[[

]]

Figure 8.3-3: Monte Carlo Results for Channel Decay Ratio

[[

]]

Figure 8.3-4: Monte Carlo Trials for Core Decay Ratio

[[

]]

Figure 8.3-5: Correlation between Core Decay Ratio and Power/Flow Ratio

[[

]]

Figure 8.3-6: Monte Carlo Results for Core Flow

[[

]]

Figure 8.3-7: Monte Carlo Results for Core Decay Ratio

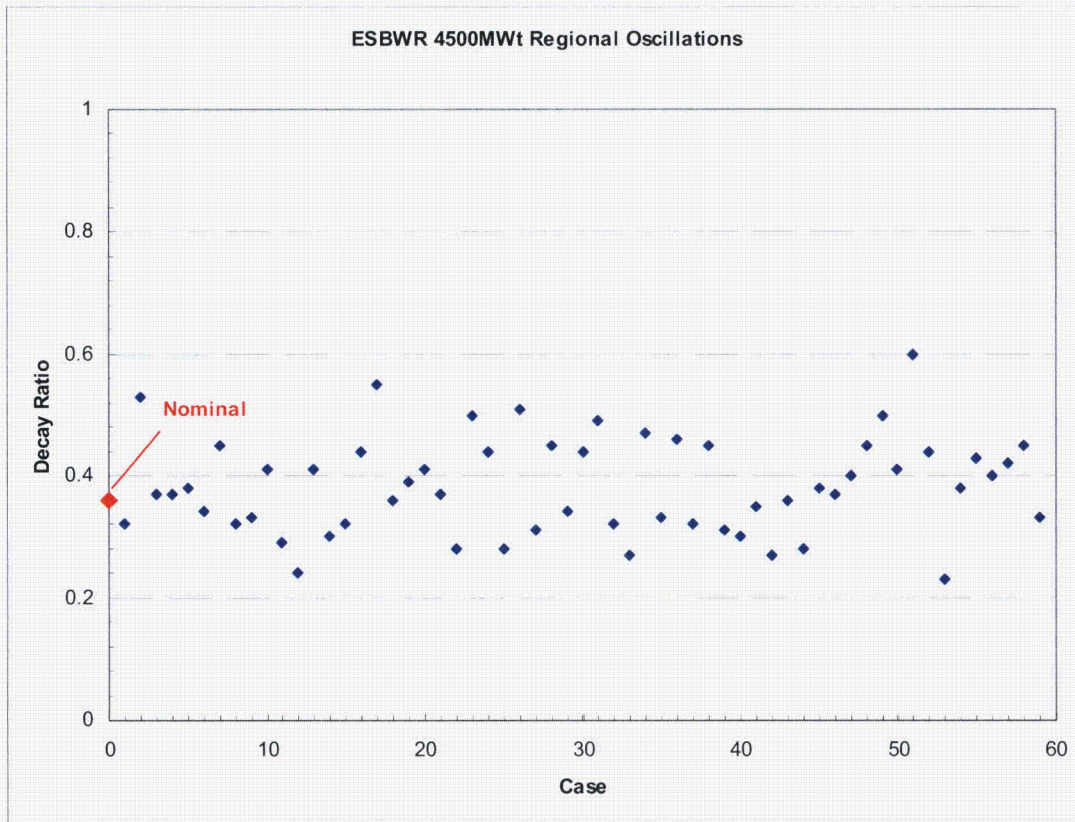
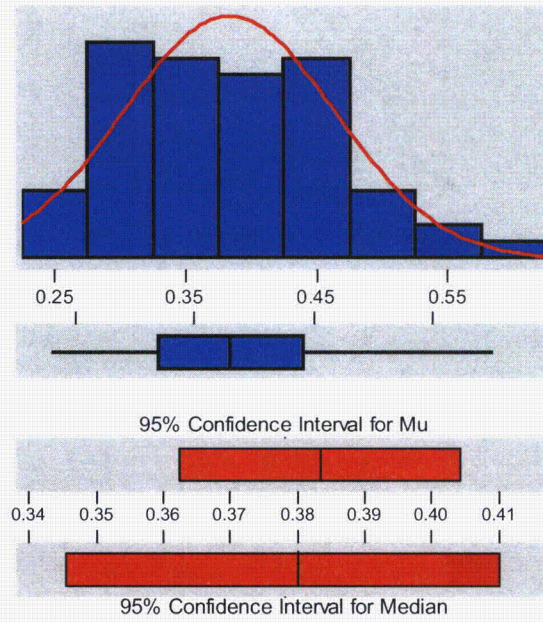


Figure 8.3-8: Monte Carlo Trials for Regional Decay Ratio

Descriptive Statistics



Variable: Decay Ratio

Anderson-Darling Normality Test

A-Squared: 0.343
 P-Value: 0.480

Mean 0.383390
 StDev 0.080593
 Variance 6.50E-03
 Skewness 0.353561
 Kurtosis -2.5E-01
 N 59

Minimum 0.230000
 1st Quartile 0.320000
 Median 0.380000
 3rd Quartile 0.440000
 Maximum 0.600000

95% Confidence Interval for Mu
 0.362387 0.404392

95% Confidence Interval for Sigma
 0.068225 0.098481

95% Confidence Interval for Median
 0.345388 0.410000

Figure 8.3-9: Monte Carlo Results for Regional Decay Ratio

[[

]]

Figure 8.3-10: Decay Ratio Results Compared to Design Criteria

8.4 STABILITY FOLLOWING ANTICIPATED OPERATIONAL OCCURRENCES (AOOS)

The rated power and flow conditions are the limiting conditions for stability for the ESBWR during normal operation. However, following an AOO the power/flow conditions could be more severe than at rated. Two AOOs were identified in Section 2.2: Loss-of Feedwater Heater (LOFWH), which results in increased power; and Loss of Feedwater Flow (LOFW), which results in a lower flow. The trajectories of the transients in the power – flow map are shown in Figure 8.4-1. The curve A-A corresponds to operation with a reduced level in the downcomer. The lower level leads to a reduction in flow. Different points on A – A correspond to changes in control reactivity or changes in core inlet subcooling.

LOFWH is a slow transient, in which the power increases slowly as the feedwater temperature drops. If no action is taken by the operator, the power would increase until a high thermal power scram occurs at 115% of rated power. [[

]]

Channel stability was also analyzed at this pre-scram power level. Figure 8.4-4 shows the response of the channel inlet flow following an instantaneous perturbation of [[

]] The decay ratio was calculated to be [[]] at rated conditions.

Analysis of the LOFW transient turned out to be more complex. The transient is rapid and unless the feedwater flow is restored, will scram in a few seconds on a trip at L3. In this period, the flow, power and subcooling are dropping and pressure is responding to the pressure controller. Rather than imposing a pressure perturbation on top of the transient response to evaluate the decay ratio, the following approach was adopted. [[

]] This operating point is more severe than the rated

condition as the flow is reduced at the same power level. It provides a conservative evaluation of the LOFW transient, as the power is higher than would occur during a LOFW.

Results of core stability analysis for the reduced level case are shown in Figure 8.4-5. The core decay ratio was evaluated to be [[]]. The hot channel stability was also evaluated by perturbing the inlet velocity. The resulting transient response is shown in Figure 8.4-6. The hot channel decay ratio increased from [[]] at rated conditions to [[]] for the reduced level case.

The results from these studies show that adequate margin is maintained to the stability design criteria even for these more severe operating states.

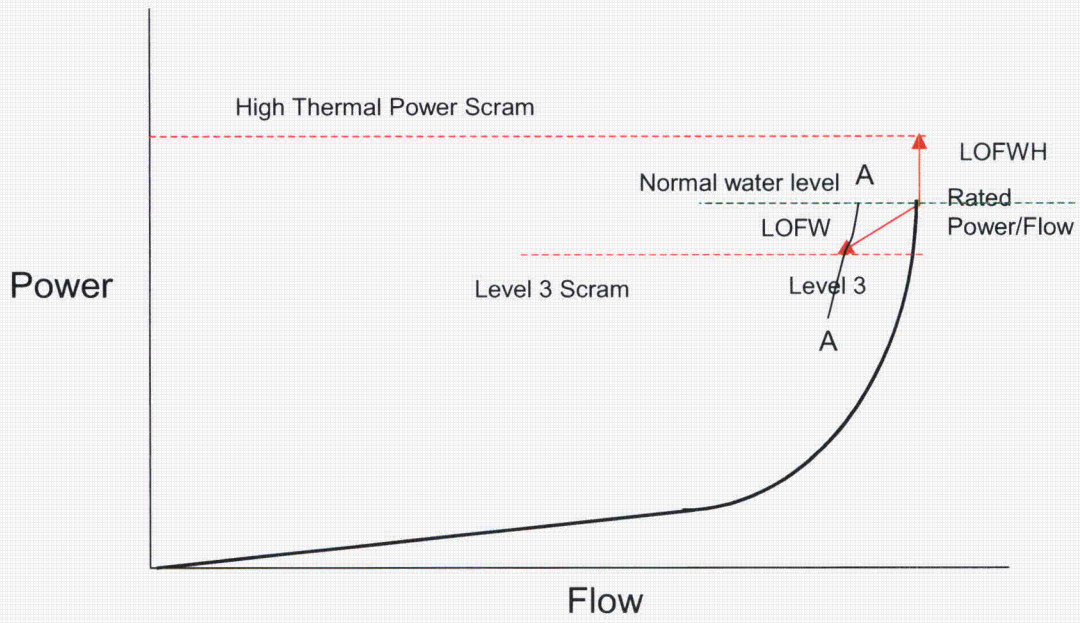


Figure 8.4-1: Stability in Expanded Operating Map

[[

]]

Figure 8.4-2: Loss of Feedwater Heater Transient

[[

]]

Figure 8.4-3: Core Power Response to Pressure Perturbation (Scram Power Level)

[[

]]

Figure 8.4-4: Hot Channel Flow Response to Inlet Flow Perturbation (Scram Power Level)

[[

]]

Figure 8.4-5: Core Power Response to Pressure Perturbation at Reduced Level

[[

]]

Figure 8.4-6: Hot Channel Response to Inlet Flow Perturbation at Reduced Level

9.0 PLANT STARTUP

In contrast to operating BWRs, the ESBWR plant starts up without recirculation pumps. At low pressure, the initiation of voiding in the core and chimney causes perceptible changes in the driving head because of the large difference between liquid and vapor densities. Consequently, startup procedures are developed to assure smooth ascension in pressure and power.

Tests in experimental natural circulation loops [26], [27], [35] have identified two mechanisms for potential flow oscillations at low pressure. First, at very low flows, a periodic "geysering" flow oscillation was found to occur due to condensation of core exit vapor in the subcooled chimney region. Condensation-induced oscillations may occur under these conditions. The condensation rate is determined by the chimney subcooling and the rate of vapor production in the core. Oscillations of this kind are unlikely given the ESBWR startup procedures, which are similar to those of the natural circulation Dodewaard reactor. Dodewaard experienced no "geysering" oscillation in its 22 refuel cycles of operation. Second, initiation of vapor production in the chimney region leads to a reduction in hydrostatic head in the chimney and a resultant core flow increase. This, in turn, could cause voids to collapse in the chimney, leading to a reduction in flow. Oscillations of this second kind (known in the literature as Type 1 instability [28], see Figure 9.1-1) had also never been seen at Dodewaard. In the final cycle of its operation, a special startup test was performed to probe the low-pressure portion of the startup trajectory. Though no oscillations were detectable on the APRMs, it was possible to infer the presence of small oscillations in core velocity from the auto correlation function of the APRM signal (Figure 9.1-2) [29]. These were small oscillations superposed on the core velocity with little, if any, reactivity impact, as the core flow is single phase in this phase of the startup transient.

In this section, the mechanism of the hydrostatic oscillations is examined and startup trajectories are analyzed with TRACG. The results show that large margins to boiling transition are maintained throughout the startup scenario.

9.1 PHENOMENA GOVERNING OSCILLATIONS DURING STARTUP

During startup, the water in the ESBWR vessel is initially heated to about 85 C by decay heat supplemented by auxiliary heaters. The ESBWR design is not finalized, but one concept for auxiliary heating is to use the Reactor Water Cleanup (RWCU)/ Shutdown Cooling (SDC) system. Following de-aeration, control rods are pulled to criticality and nuclear heatup begins at a low core power. As the water circulates through the core and downcomer by natural circulation, it is gradually heated up. The RWCU system removes a portion of the heat by draining water from the downcomer and lower plenum, cooling it in heat exchangers and returning it through the feedwater sparger. Because of the large height of the ESBWR vessel, the pressure at the water level (near the top of the separators) is lower than the core pressure by about 1 bar. Figure 9.1-3 shows a schematic of the vessel and the axial pressure profile. At low pressures corresponding to startup conditions, the pressure gradient gives rise to a significant difference in the saturation temperature between the core exit and the top of the separators. The saturation temperature profile is shown on the right side of the figure. As the circulating water is

slowly heated up, saturation temperature is first reached at the top of the separators. Vapor generation at the top of the separators results in a reduction in the density head in the separators, and the voids propagate downwards. The formation of voids also results in a larger driving head for natural circulation flow. The increase in natural circulation flow reduces the core exit temperature and leads to a collapse of the voids. This completes one cycle of the hydrostatic head oscillation. The sequence of events for one cycle is illustrated in the right hand portion of Figure 9.1-3. These oscillations persist until the inlet temperature to the core increases and a steady void fraction is established in the separators. Small oscillations in the flow rate are harmless when the flow in the core is single phase and consequently there is a very large margin to thermal limits. This type of oscillation is termed Type 1 instability in the literature.

Figure 9.1-1 is a schematic of a generalized stability map in the plane of Subcooling Number vs. Zuber Number. (The figure does not represent a quantitative stability map specifically for the ESBWR and is used primarily for illustrative purposes.) Two different boundaries are shown for core-wide (in-phase) and regional (out-of-phase) oscillations that have been covered earlier in this report. These are driven by density wave oscillations and are known as Type 2 oscillations. The region above the lower (out-of-phase) stability boundary curve is unstable; the region under the curve is stable. The Type 1 oscillations appear at the onset of voiding and occupy a narrow region next to the line that demarcates the single-phase region from the two-phase region. At normal conditions the ESBWR is very stable as shown in the figure, with significant margin to the stability boundary. During startup, the Type 1 instability region has to be crossed to get to rated pressure and power. It is best to cross the Type 1 instability region at low power before boiling starts in the core to maintain a large margin to thermal limits. Once steady voiding is established in the separators and chimney, the core power can be raised along a trajectory to full power.

The parameters that control Type 1 instability are the Zuber Number and Subcooling Number. The Froude Number is a parameter that is relevant in determining the relationship between the riser buoyancy and the circulation flow. This is important in establishing a scaling basis for tests facility design, but not for loop stability once the scaled flow characteristics are known. Another group that is important for tall columns of liquid at low system pressure is the Flashing Number. These dimensionless numbers are defined below:

$$\begin{aligned}
 N_{Zu} &= \frac{\rho_l}{\rho_{gsd}} \frac{Q}{W_c h_{fg}} \\
 N_{sub} &= \frac{\rho_l}{\rho_{gsd}} \frac{(h_{fsd} - h_{in})}{h_{fg}} \\
 N_{Fr} &= \frac{V_c^2}{gH_{dc}} \\
 N_{fl} &= \frac{\rho_l}{\rho_{gsd}} \frac{(h_{fin} - h_{fsd})}{h_{fg}}
 \end{aligned}
 \tag{9.1}$$

where

- ρ = density (kg/m³)
- V_c = core average inlet velocity (m/s)

- Q = core thermal power (kW)
 W_c = core flow (kg/s)
 h = enthalpy (kJ/kg)
 h_f = saturated liquid enthalpy (kJ/kg)
 h_{fg} = latent heat of evaporation at steam dome pressure (kJ/kg)
 H_{dc} = downcomer height (m)

sd denotes properties at the steam dome pressure and *in* denotes properties at the inlet to the core.

The significance of these quantities is discussed below with the aid of Figure 9.1-4.

The Zuber Number is a measure of the enthalpy increase in the core. As there is no increase in the enthalpy in the chimney, the Zuber number is also a measure of the total enthalpy increase in the core and chimney regions. The Flashing Number has special relevance for tall columns of liquid at low pressure. It is a measure of the enthalpy margin to flashing at the core exit (see Figure 9.1-4) when the flow just reaches saturation at the top of the chimney. The Subcooling Number is a measure of the enthalpy margin to saturation at the core inlet. At low system pressures, the definition of the Subcooling Number must be considered carefully because of the difference in pressure at different elevations. In Eq. 9.1, it is defined with respect to the saturated enthalpy at the steam dome pressure.

With the above definitions, when saturated conditions are reached at the top of the riser (Path A in Figure 9.1-4), an energy balance leads to:

$$N_{Zu} = N_{sub} \quad (9.2)$$

For Type 1 oscillations that occur when voiding begins at the top of the riser, N_{sub} is the relevant parameter to be used in the stability map of Figure 9.1-1.

For a rapid heatup rate corresponding to Path C in Figure 9.1-4, saturated conditions may be reached at the top of the core (i.e. at a pressure close to core inlet pressure) with a subcooled chimney. In the extreme case when the entire chimney is still subcooled:

$$N_{Zu} = N_{sub} + N_{fl} \quad (9.3)$$

These heatup rates can lead to condensation-induced oscillations. A large flashing number will require a correspondingly higher Zuber number (enthalpy increase in the core) to trigger such oscillations and thus provides a buffer to the occurrence of this phenomenon.

At intermediate conditions, as the void initiation location moves down into the chimney,

$$N_{sub} < N_{Zu} < (N_{sub} + N_{fl})$$

This corresponds to Path B in Figure 9.1-4.

Values of these parameters during the startup of the ESBWR are discussed further in Section 9.2.

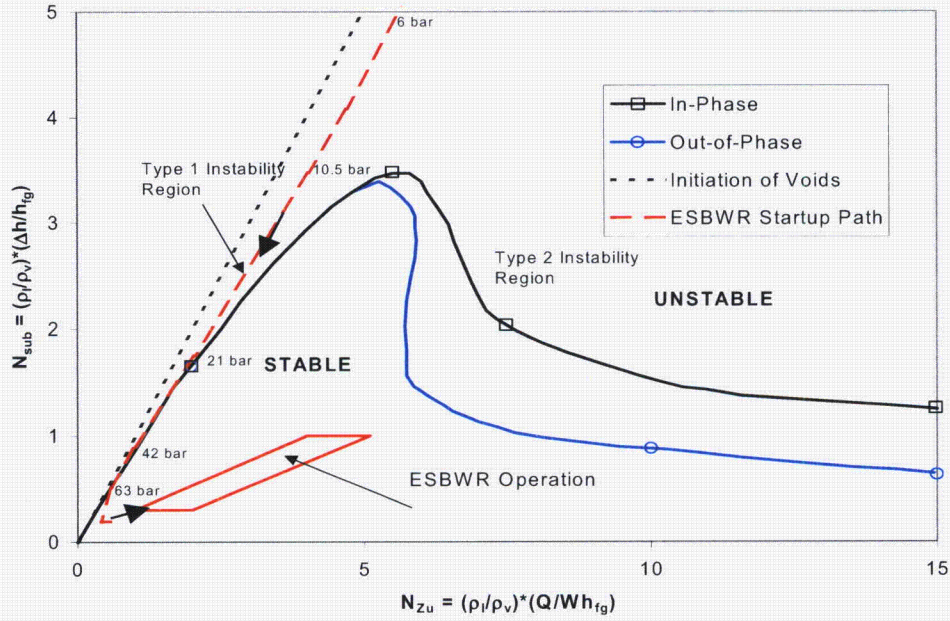


Figure 9.1-1: Generalized Stability Map showing Type 1 and Type 2 Instability [28]

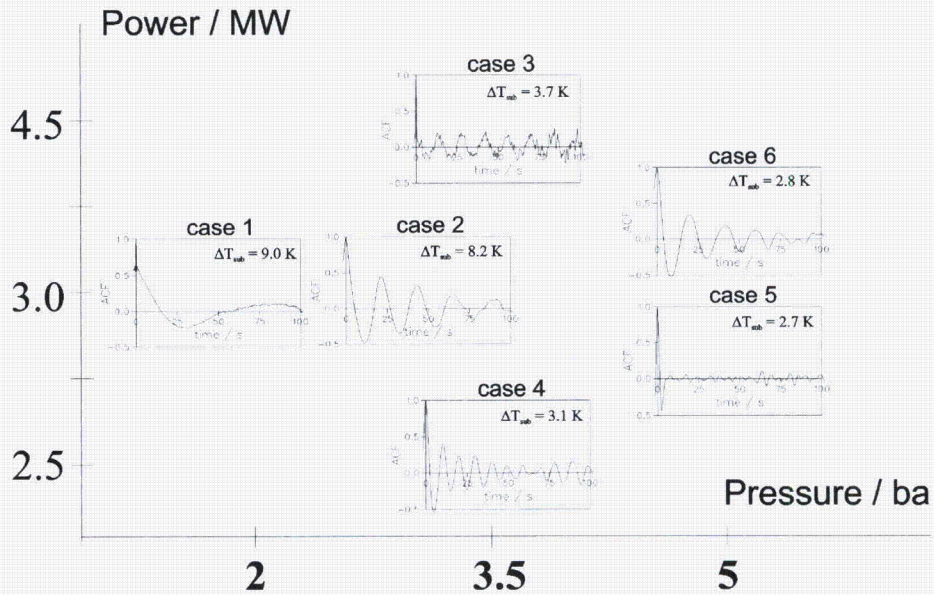


Figure 9.1-2: Indications of Periodic Behavior during Dodewaard Startup [29]

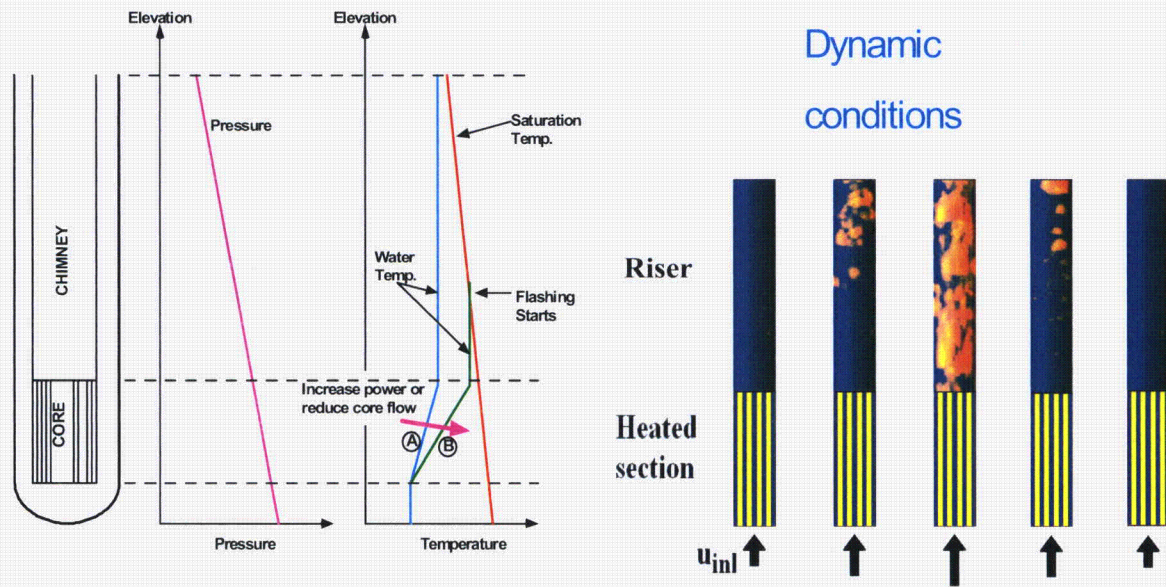


Figure 9.1-3: Thermal – Hydraulic Conditions during Startup [28]

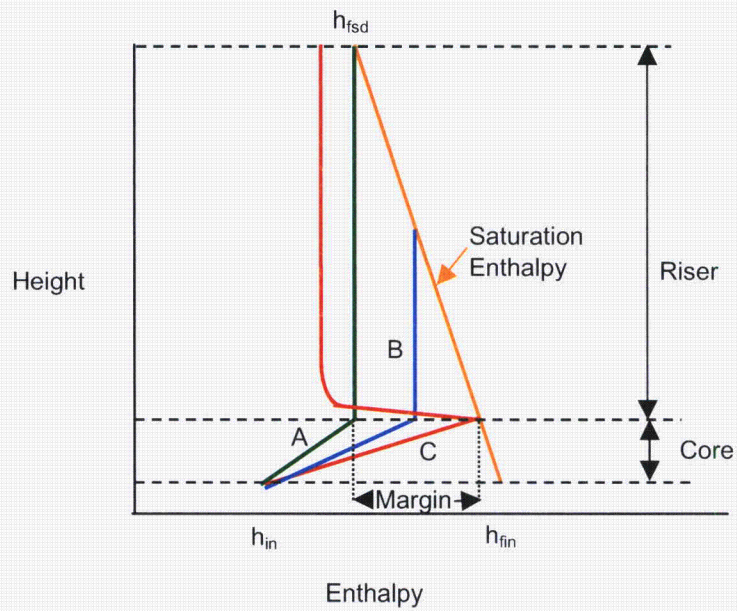


Figure 9.1-4: Enthalpy Profiles for Different Heatup Rates

9.2 APPLICABILITY OF TRACG FOR STARTUP CALCULATIONS

A PIRT was developed for density wave oscillations in Section 3. No new phenomena are introduced for the hydrostatic oscillations (Type 1 instability) that could potentially occur during ESBWR startup. The kinetics parameters are not important, as there are no reactivity feedbacks associated with these oscillations before the onset of core voiding.

The TRACG models are applicable to analyze Type 1 instabilities. At low pressure, the variations in properties with pressure along the natural circulation flow loop become important. TRACG calculates fluid properties for each node corresponding to its thermodynamic state, and therefore has the necessary capability for this purpose.

TRACG has been qualified against test data exhibiting low-pressure oscillations. TRACG Qualification for SBWR [6] includes results of comparisons with flow instability data from the CRIEPI test facility [27] (Section 6.3) and exploratory tests in the PANDA test facility (Section 6.4). The Dodewaard startup transient [29] is analyzed in Section 6.2 of the same report. No oscillations in flow were observed in the Dodewaard tests; TRACG calculated small Type 1 oscillations at the onset of void formation in the chimney. Reference 7 shows the results of comparisons between TRACG and additional CRIEPI data [30] at higher pressures of 20 and 72 bar. Table 9.2-1 shows a comparison of important non-dimensional parameters between the CRIEPI facility and the ESBWR at startup pressures. The facility was scaled to match the SBWR, and is also adequate for representing the relevant phenomena for the ESBWR. The table compares the test conditions at 2 bar with the ESBWR parameters calculated at 2 bar for the startup trajectory shown in the next section. The CRIEPI tests started at high subcooling and reduced the subcooling until Type 1 oscillations were observed. This occurred when the subcooling number and Zuber number were approximately 22. Note that the flashing number is of the order of 15 at this pressure, precluding condensation-induced oscillations ($N_{Zu} \ll N_{sub} + N_{fl}$). The ESBWR conditions at 2 bar are similar, with vapor generation at the top of the chimney and the subcooling numbers and Zuber numbers of the order of 22. Condensation-induced oscillations are precluded because of the large flashing number of 25. Table 9.2-2 shows a similar comparison with Dodewaard. The comparison is at 3 bar, which was the lowest pressure for which data were available from the startup of February 1992. The Zuber number and subcooling number are lower by a factor of 5 to 6 compared to ESBWR. The difference is largely due to the more favorable natural circulation characteristics of Dodewaard, which does not have separators. However, as expected, at 3 bar the Zuber number and subcooling numbers are of similar magnitude, indicating that the vapor generation is occurring in the chimney and not in the core. This was confirmed by the APRM readings that are consistent with single phase flow in the core. Note the magnitude of the margin to boiling in the core: the flashing number is three times the Zuber number. At 3 bar, the ESBWR also shows the Zuber number is beginning to exceed the subcooling number, indicating vapor generation at the top of the chimney. The Zuber number is significantly smaller than the sum of the subcooling and flashing numbers, demonstrating the margin to boiling in the core.

Tests showing condensation-induced oscillations have been reported by Aritomi et al. [26] and Kuran et al. [35]. The tests performed by Aritomi [26] have been analyzed and provide further evidence that TRACG can predict the phenomenon of condensation induced "geysering"

oscillations. However, these tests are not representative of the ESBWR geometry or startup process, and such oscillations are precluded for the range of heatup rates envisaged for the ESBWR.

Kuran et al. [35] also reported condensation-induced oscillations at low pressure. The tests were performed in a quarter-height facility. The paper describes four phases of plant startup. Phase II is “net vapor generation in the core” which occurs before Phase III “saturated chimney”. The ESBWR startup is designed to avoid vapor generation in the core before the chimney region is close to saturation and until the system pressure is sufficiently high (Figure 9.1-3). This avoids the condensation-induced oscillations described in the paper. Also with the quarter-height scaling, the flashing numbers will be small relative to ESBWR, making the heatup process in the test facility more prone to condensation-induced oscillations. Finally, the reactivity feedback simulation described in the paper is of much lower consequence when voids are not generated in the core at low pressures.

Table 9.2-1:
Comparison of Non-dimensional Parameters:
CRIEPI vs. ESBWR

Non-Dimensional Parameters	Typical Startup Condition (0.2 MPa)	
	ESBWR	CRIEPI
Non-dimensional downcomer cross sectional area $A_{d,e}$	1.02	1.11
Non-dimensional chimney cross sectional area A_r	2.78	2.47
Non-dimensional chimney length L_r	2.82	3.38
Ratio of vapor density to liquid density	0.0012	0.0012
Zuber Number N_{Zu}	22	21 to 25
Subcooling number N_{sub}	22	14 to 33
Flashing number N_{fl}	25	15

Table 9.2-2:
Comparison of Non-dimensional Parameters:
Dodewaard vs. ESBWR

Non-Dimensional Parameters	Typical Startup Condition (0.3 MPa)	
	ESBWR	Dodewaard
Vessel L/D	3.89	4.30
Non-dimensional chimney length L_r	2.82	1.68
Ratio of vapor density to liquid density	0.0018	0.0018
Zuber Number N_{Zu}	14	2.7
Subcooling number N_{sub}	12	2.1
Flashing number N_{fl}	13	7.6

9.3 TRACG ANALYSIS OF TYPICAL STARTUP TRAJECTORIES

9.3.1 ESBWR PLANT STARTUP

Detailed startup procedures for the ESBWR will be developed at a later stage. The startup process is expected to generally follow the established procedure from the Dodewaard plant. The Dodewaard plant started up for 22 cycles of operation without any problems related to flow or power oscillations.

Figure 9.3-1 shows the stages of the startup process. In the De-aeration Period, the reactor coolant is de-aerated by drawing a vacuum on the main condenser and reactor vessel using mechanical vacuum pumps with the steam drain lines open. The reactor coolant is heated up to between 80 and 90 C with the Reactor Water Cleanup/Shutdown Cooling System (RWCU/SDC) auxiliary heater (Figure 9.3-2) and decay heat. The reactor pressure is reduced to about 50 to 60 kPa. Following de-aeration, the Main Steam Isolation Valves (MSIVs) are closed to initiate the Startup Period. Control rods are withdrawn to criticality. Fission power is used to heat the reactor water, while maintaining the water level close to the top of the separators but well below the steam lines. Steaming at the free surface starts to pressurize the reactor vessel. The core region remains subcooled due to the large static head in the chimney and separators.

As the reactor heats up and pressurizes, the RWCU/SDC system heat exchangers are used to control the downcomer temperature, enhance coolant flow and reduce lower plenum stratification. The MSIVs are reopened at the end of the Startup Period, when the pressure reaches 6.3 MPa. Subsequently, the turbine bypass valves are used to control pressure. The RPV power is increased and preparations made to roll the turbine.

9.3.2 TRACG CALCULATIONS FOR SIMULATED STARTUP SCENARIOS

The startup transient for the ESBWR was simulated with TRACG. The TRACG calculations were performed with imposed core power, without activating the kinetics model. This is valid as long as there are no feedbacks from oscillations in the core void fraction during the startup transient. This assumption will be validated as part of the calculation. The calculation was initiated at the end of the de-aeration period with the steam dome pressure at 0.52 bar and RPV water at 82 C. The water level was maintained near the top of the separators. The MSIVs were closed to isolate the RPV. To simplify comparisons, the power level was maintained constant until the pressure reached 6.3 MPa. Subsequently, the MSIVs were opened and the power level was increased in steps to achieve rated pressure at 300 MW (6.67% of rated power).

Three heatup rates were considered. The lowest power level of 50 MW corresponds to a heatup rate of 30 C/hour and is likely to be close to the actual value for startup. The median power level of 85 MW yields a heatup rate of 55 C/hour, which is the highest allowable to comply with reactor vessel thermal stress requirements. The highest power level of 125 MW heats up the reactor vessel water at 82 C/hour which is above allowable limits, and is only included as a sensitivity study. The three power trajectories are shown in Figure 9.3-3.

Figure 9.3-4 shows the pressure response for the three cases. The circulating water heats up because of the core power. The heat exchangers in the RWCU/SDC system are enabled to

remove a part of the energy and control the core inlet subcooling. Steam generation begins at the water surface and starts to pressurize the vessel. [[

]]

Figure 9.3-5 shows the variation in core inlet subcooling as a function of time. [[

]] The core flow transient response is shown in Figure 9.3-6. [[

]]

Further insight into the core flow response is obtained by examining the core void fractions, specifically in the highest power bundles. [[

]]

Margins to thermal limits (CPR) were calculated for the three startup scenarios. The thermal margin for the high power bundles is shown in Figure 9.3-15. Large margins are maintained throughout. {3}]]

Figure 9.3-16 is the corresponding plot for the peripheral bundles. Again, large margins are maintained throughout the transient. [[

]]

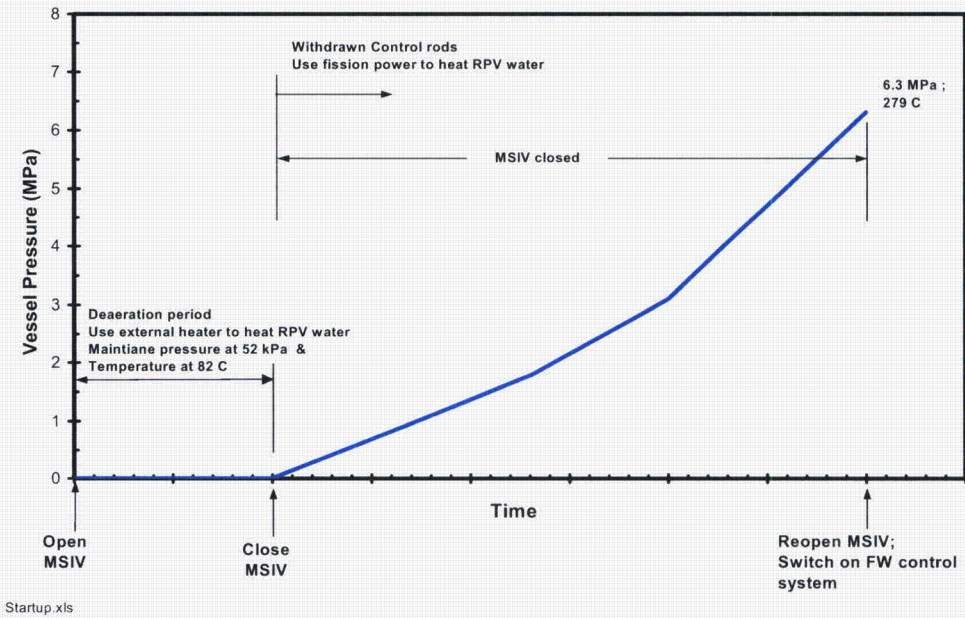


Figure 9.3-1: ESBWR Startup Trajectory

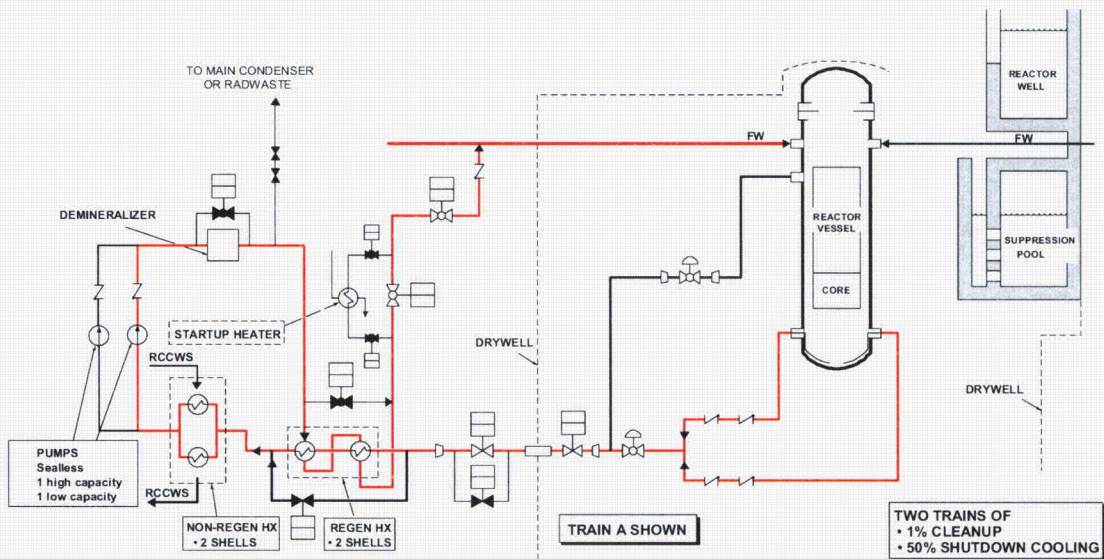


Figure 9.3-2: ESBWR Reactor Water Cleanup/Shutdown Cooling System – Schematic Diagram

[[

]]

Figure 9.3-3: TRACG Startup Simulation: Reactor Power Trajectories

[[

]]

Figure 9.3-4: TRACG Startup Simulation: Pressure Response

[[

]]

Figure 9.3-5: TRACG Startup Simulation – Core Inlet Subcooling

[[

]]

Figure 9.3-6: TRACG Startup Simulation – Core Inlet Flow

[[

]]

Figure 9.3-7: Separator Void Fraction (50 MW heatup)

[[

]]

Figure 9.3-8: Separator Void Fraction (85MW heatup)

[[

]]

Figure 9.3-9: Separator Void Fraction (125 MW heatup)

[[

]]

Figure 9.3-10: Hot Bundle Void Fraction (50 MW heatup)

[[

]]

Figure 9.3-11: Hot Bundle Void Fraction (85 MW heatup)

[[

]]

Figure 9.3-12: Hot Bundle Void Fraction (125 MW heatup)

[[

]]

Figure 9.3-13: Hot Bundle Exit Flow

[[

]]

Figure 9.3-14: Peripheral Bundle Exit Flow

[[

]]

Figure 9.3-15: Hot Bundle CPR

[[

]]

Figure 9.3-16: Peripheral Bundle CPR

9.4 SUMMARY OF ESBWR STARTUP PERFORMANCE

The TRACG simulation of ESBWR startup has demonstrated that at expected heatup rates, the startup can be accomplished without difficulty. The Type 1 instability region can be crossed with a minimum amount of flow noise. The flow noise occurred before the start of vapor generation in the core and consequently might not even be detectable on the plant power instrumentation. Thermal limits are never approached during the startup transient.

The TRACG calculations were performed without kinetics feedback. This is valid for the early part of the startup that is of interest, as there is no vapor generation in the core. TRACG calculates the condensation-induced flow oscillations observed in some experiments, but this behavior is only observed with extreme heatup rates that are well outside the range constrained by other ESBWR design considerations.

10.0 REFERENCES

- [1]. J. G. M. Andersen, et al., *TRACG Model Description*, NEDE-32176P, Revision 2, December 1999.
- [2]. J. G. M. Andersen, et al., *TRACG Qualification*, NEDE-32177P, Rev. 2, January 2000.
- [3]. J. G. M. Andersen, et al., *TRACG Application for Anticipated Operational Occurrences Transient Analysis*, NEDE-32906P-A, Revision 1, April 2003.
- [4]. GE Nuclear Energy, *General Electric Boiling Water Reactor Detect and Suppress Solution – Confirmation Density*, Licensing Topical Report NEDC-33075P, Revision 3, January 2004.
- [5]. NEDE-33147: *DSS-CD TRACG Application*, February 2004.
- [6]. J. R. Fitch, et al., *TRACG Qualification for SBWR*, NEDC-32725P, Rev.1, Vol.1 and 2, August 2002.
- [7]. J. R. Fitch, et al., *TRACG Qualification for ESBWR*, NEDC-33080P, Rev.0, August 2002.
- [8]. USNRC, *Quantifying Reactor Safety Margins: Application of Code Scaling, Applicability, and Uncertainty Evaluation Methodology to a Large-Break, Loss-of-Coolant Accident*, NUREG/CR-5249, December 1989.
- [9]. USNRC, *Best-Estimate Calculations of Emergency Core Cooling System Performance*, Regulatory Guide 1.157, May 1989.
- [10]. *ESBWR Design Description*, NEDC-33048P, Revision 1, August 2003.
- [11]. J. G. M. Andersen, C. L. Heck and J. C. Shaug, *TRACG04 User's Manual*, GE-NE-0000-0009-7162 (UM-0136), Rev. 0.
- [12]. J. S. Post and A. K. Chung, *ODYSY Application for Stability Licensing Calculations*, NEDC-32992P-A, July 2001.
- [13]. GE Nuclear Energy, *BWR Owners' Group Long-Term Stability Solutions Licensing Methodology*, NEDO-31960-A, November 1995.

- [14]. GE Nuclear Energy, *Steady State Nuclear Methods*, Licensing Topical Report NEDE-30130P-A, April 1985.
- [15]. GE Nuclear Energy, *Qualification of the One-Dimensional Core Transient Model for Boiling Water Reactors*, Licensing Topical Report NEDE-24154P-A, August 1988.
- [16]. *COLPS03A User's Manual*, UM-0133, Revision 0.
- [17]. GE Nuclear Energy, *BWR Owners' Group Long-Term Stability Solutions Licensing Methodology*, NEDO-31960-A, Supplement 1, November 1995.
- [18]. GE Nuclear Energy, *BWR Owners' Group Reactor Stability Detect and Suppress Solutions Licensing Basis Methodology for Reload Applications*, NEDO-32465-A, August 1996.
- [19]. O. Nylund, et al., *Hydrodynamic and Heat Transfer Measurements on a Full-Scale Simulated 36 Rod BHWWR Fuel Element with Non-Uniform Axial and Radial Heat Flux Distribution*, FRIGG-4, ASEA-ATOM Proprietary Report, December 1970.
- [20]. P. Saha and N. Zuber, *Point of Net Vapor Generation and Vapor Void Fraction in Subcooled Boiling*, Proc. 5th International. Heat and Mass Transfer Conference., Tokyo, Japan, 1974.
- [21]. S. O. Akerlund, et al., The GESTR-LOCA and SAFER Models for the Evaluation of the Loss-of-Coolant Accident, Vol.1, *GESTR-LOCA – A Model for the Prediction of Fuel Rod Thermal Performance*, NEDE-23785-1-PA, June 1984.
- [22]. *Supplemental Information for Plant Modifications to Eliminate Significant In-Core Vibrations*, NEDE-21156, January 1976
- [23]. L. A. Carmichael and R. O. Niemi, *Transient and Stability Tests at Peach Bottom Atomic Power Station Unit 2 at End of Cycle 2*, EPRI-NP-564, June 1978.
- [24]. B. S. Shiralkar and Y. K. Cheung, *TRACG Application to ESBWR*, NEDC-33083P, November 2002.
- [25]. J. March-Leuba and E. D. Blakeman, *A Mechanism for Out-of-Phase Instabilities in Boiling Water Reactors*, Nucl. Sci. Eng., Vol. 107, p. 173, 1991.

- [26]. M. Aritomi, J. H. Chiang, M. Mori, *Fundamental Studies on Safety-Related Thermal-Hydraulics of Natural Circulation Boiling Parallel Channel Flow System under Startup Conditions (Mechanism of Geysering in Parallel Channels)*, Nuclear Safety, Vol. 33, No.2, pp. 170-182, 1992.
- [27]. F. Inada, Y. Yasuo, *The Boiling Flow Instability of a Natural Circulation BWR with a Chimney at Low Pressure Startup*, Proc. International Conference on the Design and Safety of Advanced Nuclear Power Plants (ANP '92), Tokyo, Japan, Paper 25.3, October 25-29, 1992.
- [28]. T.H.J.J. van der Hagen, Personal communication, 2004.
- [29]. T.H.J.J. van der Hagen, F.J. van der Kaa, J. Karuza, W.H.M. Nissen, A.J.C. Stekelenburg, J.A.A. Wouters, *Startup of the Dodewaard Natural Circulation Boiling Water Reactor*, GKN Report 92-017/FY/R, 1992.
- [30]. M. Furuya et al., *Two-Phase Flow Instability in a Boiling Natural Circulation Loop at Relatively High System Pressure*, Proc. 8th International Meeting on Nuclear Reactor Thermal-Hydraulics, Vol. 3, pp. 1778-1784, Kyoto, Japan, 1997.
- [31]. F. T. Bolger and M. A. Holmes, *TRACG Application for ATWS Overpressure Transient Analysis*, NEDE-32906P, Supplement 1-A, November 2003.
- [32]. H. Glaeser and R. Pochard, *Review on Uncertainty Methods for Thermal Hydraulic Computer Codes*, International Conference on New Trends in Nuclear System Thermohydraulics Proceedings, Volume I, pp. 447-455, Pisa, Italy, 1994.
- [33]. H. A. David, Order Statistics (2nd edition), John Wiley & Sons, New York, 1969.
- [34]. D. C. Montgomery, Introduction to Statistical Quality Control, John Wiley and Sons, Inc., 1996.
- [35]. S. Kuran, M. Ishii, X. Sun, L. Cheng, Y. Xu, H. Yoon, S.T. Revankar, *Nuclear Coupled Flow Instability Study for Natural Circulation BWR Startup Transient*, Paper N6P002, 6th International Conference on Nuclear Thermal Hydraulics, Operation and Safety (NUTHOS-6), Nara, Japan, October 2004,

MFN 08-016

Enclosure 3

Affidavit

GE Hitachi Nuclear Energy

AFFIDAVIT

I, **James C. Kinsey**, state as follows:

- (1) I am the Vice President, ESBWR Licensing, GE Hitachi Nuclear Energy ("GEH"), have been delegated the function of reviewing the information described in paragraph (2) which is sought to be withheld, and have been authorized to apply for its withholding.
- (2) The information sought to be withheld is contained in Enclosure 1 of GEH letter MFN 08-016, Mr. James C. Kinsey to U.S. Nuclear Regulatory Commission, entitled *Transmittal of Accepted Version of Licensing Topical Report NEDE-33083P-A, Supplement 1, Revision 1, "TRACG Application for ESBWR Stability Analysis," January 2008*, dated January 28, 2008. The GEH proprietary information in Enclosure 1, which is entitled *Licensing Topical Report NEDE-33083P-A, Supplement 1, Revision 1, "TRACG Application for ESBWR Stability Analysis," January 2008 - GEH Proprietary Information*, is delineated by dark red font, double underline, and enclosed within double brackets. [[This sentence is an example.^{3}]] Figures and large equation objects are enclosed in double brackets before and after the object. The superscript notation ^{3} refers to Paragraph (3) of this affidavit, which provides the basis for the proprietary determination. Note that the GEH proprietary information in the NRC's Final Safety Evaluation, which is enclosed in NEDE- 33083P-A, Supplement 1, Revision 1, is identified by a single underline inside double square brackets with slightly different red font. [[This sentence is an example.]] A non-proprietary version of this information is provided in Enclosure 2, *Licensing Topical Report NEDO-33083-A, Supplement 1, Revision 1, "TRACG Application for ESBWR Stability Analysis," January 2008 - Non-Proprietary Version*.
- (3) In making this application for withholding of proprietary information of which it is the owner, GEH relies upon the exemption from disclosure set forth in the Freedom of Information Act ("FOIA"), 5 USC Sec. 552(b)(4), and the Trade Secrets Act, 18 USC Sec. 1905, and NRC regulations 10 CFR 9.17(a)(4), and 2.390(a)(4) for "trade secrets" (Exemption 4). The material for which exemption from disclosure is here sought also qualify under the narrower definition of "trade secret," within the meanings assigned to those terms for purposes of FOIA Exemption 4 in, respectively, Critical Mass Energy Project v. Nuclear Regulatory Commission, 975F2d871 (DC Cir. 1992), and Public Citizen Health Research Group v. FDA, 704F2d1280 (DC Cir. 1983).
- (4) Some examples of categories of information which fit into the definition of proprietary information are:
 - a. Information that discloses a process, method, or apparatus, including supporting data and analyses, where prevention of its use by GEH competitors without license from GEH constitutes a competitive economic advantage over other companies;

- b. Information which, if used by a competitor, would reduce his expenditure of resources or improve his competitive position in the design, manufacture, shipment, installation, assurance of quality, or licensing of a similar product;
- c. Information which reveals aspects of past, present, or future GEH customer-funded development plans and programs, resulting in potential products to GEH;
- d. Information which discloses patentable subject matter for which it may be desirable to obtain patent protection.

The information sought to be withheld is considered to be proprietary for the reasons set forth in paragraphs (4)a., and (4)b, above.

- (5) To address 10 CFR 2.390(b)(4), the information sought to be withheld is being submitted to NRC in confidence. The information is of a sort customarily held in confidence by GEH, and is in fact so held. The information sought to be withheld has, to the best of my knowledge and belief, consistently been held in confidence by GEH, no public disclosure has been made, and it is not available in public sources. All disclosures to third parties including any required transmittals to NRC, have been made, or must be made, pursuant to regulatory provisions or proprietary agreements which provide for maintenance of the information in confidence. Its initial designation as proprietary information, and the subsequent steps taken to prevent its unauthorized disclosure, are as set forth in paragraphs (6) and (7) following.
- (6) Initial approval of proprietary treatment of a document is made by the manager of the originating component, the person most likely to be acquainted with the value and sensitivity of the information in relation to industry knowledge, or subject to the terms under which it was licensed to GEH. Access to such documents within GEH is limited on a "need to know" basis.
- (7) The procedure for approval of external release of such a document typically requires review by the staff manager, project manager, principal scientist or other equivalent authority, by the manager of the cognizant marketing function (or his delegate), and by the Legal Operation, for technical content, competitive effect, and determination of the accuracy of the proprietary designation. Disclosures outside GEH are limited to regulatory bodies, customers, and potential customers, and their agents, suppliers, and licensees, and others with a legitimate need for the information, and then only in accordance with appropriate regulatory provisions or proprietary agreements.
- (8) The information identified in paragraph (2), above, is classified as proprietary because it contains the results of analytical models, methods and processes, including computer codes, which GEH has developed, and applied to perform stability evaluations using the detection and suppression capability of the confirmation density algorithm for the BWR. GEH has developed this TRACG code over many years and at a substantial cost. The reporting, evaluation and interpretations of the results, as they relate to the detection and suppression capability of the confirmation density algorithm for the BWR, was achieved at a significant cost to GEH.

The development of the evaluation process along with the interpretation and application of the analytical results is derived from the extensive experience database that constitutes a major GEH asset.

- (9) Public disclosure of the information sought to be withheld is likely to cause substantial harm to GEH's competitive position and foreclose or reduce the availability of profit-making opportunities. The information is part of GEH's comprehensive BWR safety and technology base, and its commercial value extends beyond the original development cost. The value of the technology base goes beyond the extensive physical database and analytical methodology and includes development of the expertise to determine and apply the appropriate evaluation process. In addition, the technology base includes the value derived from providing analyses done with NRC-approved methods.

The research, development, engineering, analytical and NRC review costs comprise a substantial investment of time and money by GEH.

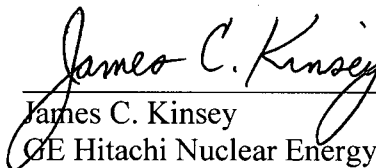
The precise value of the expertise to devise an evaluation process and apply the correct analytical methodology is difficult to quantify, but it clearly is substantial.

GEH's competitive advantage will be lost if its competitors are able to use the results of the GEH experience to normalize or verify their own process or if they are able to claim an equivalent understanding by demonstrating that they can arrive at the same or similar conclusions.

The value of this information to GEH would be lost if the information were disclosed to the public. Making such information available to competitors without their having been required to undertake a similar expenditure of resources would unfairly provide competitors with a windfall, and deprive GEH of the opportunity to exercise its competitive advantage to seek an adequate return on its large investment in developing these very valuable analytical tools.

I declare under penalty of perjury that the foregoing affidavit and the matters stated therein are true and correct to the best of my knowledge, information, and belief.

Executed on this 28th day of January 2008.


James C. Kinsey
GE Hitachi Nuclear Energy